

1-1-2010

Low Energy Search For Physics Beyond The Standard Model

Andriy Badin
Wayne State University

Follow this and additional works at: http://digitalcommons.wayne.edu/oa_dissertations



Part of the [Elementary Particles and Fields and String Theory Commons](#)

Recommended Citation

Badin, Andriy, "Low Energy Search For Physics Beyond The Standard Model" (2010). *Wayne State University Dissertations*. Paper 2.

This Open Access Dissertation is brought to you for free and open access by DigitalCommons@WayneState. It has been accepted for inclusion in Wayne State University Dissertations by an authorized administrator of DigitalCommons@WayneState.

**LOW ENERGY SEARCH FOR PHYSICS BEYOND THE STANDARD
MODEL**

by

ANDRIY BADIN

DISSERTATION

Submitted to the Graduate School

of Wayne State University,

Detroit, Michigan

in partial fulfillment of the requirements

for the degree of

DOCTOR OF PHILOSOPHY

2010

MAJOR: PHYSICS

Approved by:

Advisor

Date

DEDICATION

To my family. To my friends. To my teachers.

ACKNOWLEDGMENTS

This work would not be possible without a continuous input, guidance and support of my advisor, Dr. Alexey Petrov. His mentoring was invaluable for me from the moment when I started my Ph.D studies. Furthermore, his ideas and experience served as a ground for the projects investigated in this work, and ultimately lead to a number of publications and presentations on these projects that appeared at various conferences and journals

I am grateful to Dr. Sean Gavin for his ability to explain physics in informal matter. He really opened my eyes regarding teaching methods.

I appreciate all the help and feedback provided by the members of theoretical particle physics groups, both former and current. Particularly, I thank Dr. Fabrizio Gabbiani and Gagik Yeghiyan for their input and help during my years here. I appreciate all the proofreading of my papers and organizational help provided by Dr. Andrew Blechmann as well as his continuous availability and ability to answer any questions I have had.

I am grateful to Dr. Robert Harr and Dr. Leonid Makar-Limanov for serving on my dissertation committee. I also thank the helpful administration and staff at the Department of Physics and Astronomy including De Cowen, Doris King, LaSahara Montgomery and Wynell Pitts.

I am thankful to the Department of Physics and Astronomy, Department of Energy, and Dr. Alexey Petrov for providing continuous financial support during the course of my studies at Wayne State University.

Table of Contents

Dedication	ii
Acknowledgments	iii
List of figures	vii
1 Introduction	1
2 Theoretical aspects of the Standard Model	5
2.1 Symmetry	5
2.2 Gauge bosons, leptons and their interactions	6
2.3 Higgs mechanism. Mass generation	10
2.4 Quark mixing and the CKM matrix	14
3 Different approaches to the problem of Dark Matter	19
3.1 MOND	20
3.2 Baryonic Dark Matter	21
3.3 Non-baryonic Dark Matter	22
3.3.1 Hot and Warm Dark Matter	22
3.3.2 Cold Dark Matter	23
4 Lifetime difference in B_s mixing	29
4.1 Introduction	29
4.2 Formalism	32

4.3	Subleading $1/m_b^n$ corrections	35
4.3.1	$1/m_b$ corrections	36
4.3.2	$1/m_b^2$ corrections	38
4.3.3	Discussion	42
4.4	New Physics contributions to lifetime difference	44
4.4.1	Multi-Higgs model	48
4.4.2	Left-Right Symmetric Models	50
4.5	Conclusions	52
5	Dark Matter production in heavy meson decays	54
5.1	Introduction	54
5.2	Formalism and the Standard Model background	57
5.3	Heavy meson decaying into pair of bosons and pair of bosons + photon . . .	61
5.3.1	Generic effective Hamiltonian and $B \rightarrow \chi_0 \bar{\chi}_0(\gamma)$ decays	61
5.3.2	Production rates in particular models with scalar DM	65
5.4	Heavy meson decaying into pair of fermions and pair of fermions + photon(meson)	70
5.4.1	Generic effective Hamiltonian and $B_{d(s)} \rightarrow \chi_{1/2} \bar{\chi}_{1/2}(\gamma)$ decays	70
5.4.2	Production rates in particular models with fermionic DM	74
5.4.3	Majorana fermions	78
5.5	Vector Dark Matter production. Generic effective Hamiltonian and $B_q(D^0) \rightarrow \chi_1 \chi_1$ decays	81
5.6	Conclusions	83
6	Future developments	85

6.1 Delta-function potential	88
7 Conclusions	92
References	93
Abstract	106
Autobiographical Statement	107

List of Figures

1.1	Matter distribution in the universe [2]	3
2.1	The “mexican hat” potential incorporated in the theory of the spontaneous symmetry breaking	12
2.2	Schematical representation of the meson–anti-meson mixing process	17
3.1	Pink represents matter detected by the X-ray telescope, while blue represents the way matter should be distributed in order to explain light propagation from background galaxies[27].	21
3.2	Positron excess in the PAMELA data. Solid line - GALPROP simulation[32]	24
3.3	Sommerfeld enhancement of annihilation rate	25
4.1	Calculation of kinetic $1/m_b$ and $1/m_b^2$ corrections. The operators of Eqs. (4.26) and (4.30) are obtained by expanding the diagrams in powers of light quark momentum.	36
4.2	$1/m_b^2$ -corrections from gluonic operators.	38
4.3	Histogram of the distribution of $\Delta\Gamma_s$ values obtained by random variation of parameters of Eqs. (4.24, 4.26, 4.30, 4.33) contributing to B_s -lifetime difference $\Delta\Gamma_s$ following the prescription outline in the text.	43
4.4	Dependence of y_{ChH} on the mass of the Higgs boson. Solid line: $\tan\beta = 20$; dashed line: $\tan\beta = 10$; dotted line: $\tan\beta = 5$; dash-dotted line: $\tan\beta = 3$	50
4.5	Contributions to $\Delta\Gamma_s/\Gamma_s$ in the Left-Right Symmetric Models.	52

5.1	$\mathcal{B}(B_d \rightarrow SS)$ as a function of $x = m_S/M_{B_d}$. Values of λ and M_h were fixed at 1 and 120 GeV respectively	67
5.2	(a) allowed values of the DM-Higgs coupling λ as a function of $x = m_S/M_{B_d}$ (below the curves) for the Higgs masses of 110 GeV (red), 120 GeV (green), and 150 GeV (blue). (b) Allowed values of the Higgs mass in GeV (above the curves) for $\lambda = 0.1$ (red), 1 (green), and 5 (blue) as a function of $x = m_S/M_{B_d}$	67
5.3	(a) $\mathcal{B}(B_d \rightarrow \nu\nu)$ as a function of $x = m_\nu/M_{B_d}$ evaluated at $g' = 1$, $k = 1$ and $M_{Z'} = 1 TeV$; (b) Allowed values of the $M_{Z'}$ mass in GeV (above the curves) for $g_1 k = 1$ (black), 0.1 (red), and 10 (green) as a function of $x = m_\nu/M_{B_d}$. Solid lines represent the constraints from the 2-body decay, and the dashed ones – from the 3 body (radiative) decay. The constraints on the mass of Z' are very loose.	76
5.4	(a) $\mathcal{B}(B_d \rightarrow \nu_R \bar{\nu}_R)$ as a function of $x = m_{\nu_R}/M_{B_d}$ evaluated at $M_{W_R} = 1 TeV$, (b) Allowed values of the M_{W_R} mass in GeV (above the curves) as a function of $x = m_{\nu_R}/M_{B_d}$. Solid lines represent the constraints from the 2-body, and the dashed ones – from the 3 body (radiative) decay. As one can see, the constraints on the mass of W_R are very loose.	78
5.5	(a) $\mathcal{B}(B_d \rightarrow \chi\bar{\chi})$ as a function of $x = m_\chi/M_{B_d}$. The following numerical values were used: $\kappa = (\lambda_d \lambda_u v_u \mu)/(\lambda_u^2 v_u^2 + \mu^2) = 1$, $\tan \beta = 10$, $M_h = 102 GeV$ (b) Allowed values of the κ (above the curves) for the values of $\tan \beta = 1$ (red), 10 (green), 100 (blue), and 1000 (purple) while mass of Higgs boson was fixed at $M_h = 120 GeV$ as a function of $x = m_\chi/M_{B_d}$	81
6.1	Generic DM-SM interaction vertexes	86
6.2	Dark Matter-SM resonance production	86

Chapter 1

Introduction

The Standard Model (SM) of particle physics is an outstanding result of theoretical and experimental efforts of the past 60 years (if we date modern particle physics from 1947 when the pion was discovered). It is a consistent theory that describes experimental phenomena in the energy range of up to several hundred GeV. The Standard Model is a field-theoretic description of strong and electroweak interactions at these energies. However, it is not a closed theory. SM requires nineteen parameters as an input: three charged lepton masses, six quark masses, three gauge coupling constants, three quark mixing angles, one complex phase, mass of the Higgs boson, Higgs boson quartic coupling constant and the QCD vacuum angle. Numerical values of these parameters are neither explained nor predicted by the Standard Model. Their presence might be a result of more fundamental theory that reduces to the SM at the low energies.

The Standard Model includes two different types of particles: matter constituents (quarks and leptons) and force carriers (gauge bosons). Properties of these particles are listed in Tables 1.1 and 1.2 [1]. I do not include the Higgs boson here since it is yet to be found. In SM quarks and leptons are arranged in three generations (families). Particles from different generations display similar properties. There is an obvious mass pattern, i.e. particles in a higher generation are heavier than the ones belonging to a lower generation. As it was mentioned before, such behavior can not be explained within the Standard Model paradigm.

In addition to the mass hierarchy, there are other conceptual problems that Standard

Table 1.1: Standard Model constituents [1]

	charged lepton	lepton neutrino	up-type quark	down-type quark
	e	ν_e	u	d
mass, GeV/c^2	0.511×10^{-3}	$< 2 \times 10^{-9}$	$1.5 - 3 \times 10^{-3}$	$3.5 - 6 \times 10^{-3}$
charge, e	-1	0	$2/3$	$-1/3$
	μ	ν_μ	c	s
mass, GeV/c^2	105.7×10^{-3}	$< 2 \times 10^{-9}$	1.27	0.104
charge, e	-1	0	$2/3$	$-1/3$
	τ	ν_τ	t	b
mass, GeV/c^2	1.777	$< 2 \times 10^{-9}$	171.2	4.20
charge, e	-1	0	$2/3$	$-1/3$

Table 1.2: Gauge Bosons

	γ	\mathbf{W}^\pm	\mathbf{Z}^0	\mathbf{g}
force	e/m	weak	weak	strong
mass, GeV/c^2	0	80.4	91.2	0
charge, e	0	± 1	0	0

Model can not explain. Two of them are related to the topic of my research: gravity and dark matter. SM successfully incorporates three fundamental interactions: electromagnetic, weak and strong. It also predicts an experimentally confirmed unification of electromagnetic and weak forces, so called electroweak interaction. As one can see, gravitational interaction is not a part of the Standard Model.

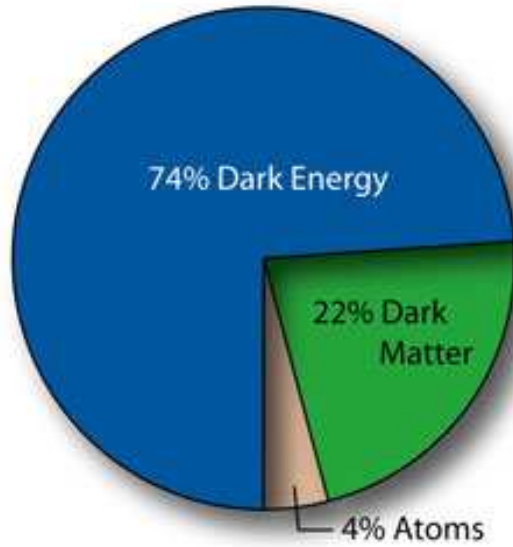


Figure 1.1: Matter distribution in the universe [2]

Dark Matter (DM) and Dark Energy (DE) are other mysteries that can not be explained by the Standard Model. It was concluded based on WMAP data, that DM and DE can make up to 95% of observed universe [2] (Fig.1.1).

Clearly, the above-mentioned puzzles motivate search for the physics beyond the Standard Model, or, as it is often called, the New Physics (NP). There are continuous experimental efforts directed at the detection of New Physics: Large Hadron Collider (LHC) and experiments hosted there (CMS, ATLAS, ALICE, LHCb etc [3]), continuing studies at the Tevatron (CDF and D0 experiments [4]), and a number of Dark Matter search experiments

(CDMS [5], DAMA [6], Xenon100 [7] to name some of them). Obviously, it is not an easy task to detect NP signals, otherwise it would have been done already. The abovementioned experiments provide us with large amount of experimental data and require theoretical explanation and understanding of observed signals. It is not an easy task as well.

The “Light” NP particles can be directly detected as decay products, while the ”heavy” ones provide an indirect input through loop diagrams (for example NP particles in the loop diagrams will affect heavy meson mixing). The best ”places” to look for the New Physics are processes which are either not well explained by the Standard Model (often it is computationally challenging to make the SM prediction) or are hard to study experimentally (missing energy decays, neutrino physics). In this sense decays of heavy mesons are the best places to search for new physics. In the Standard Model they usually occur via loop diagrams and are sensitive to the New Physics particles that can run in the loop. Also heavy mesons decays allow one to scan the relatively large mass region of potential New Physics decay products.

In this thesis we considered two of such processes. One mixing between B_s - \overline{B}_s mesons which occurs only at the loop level diagrams in the SM and thus is hard to compute to the desired degree of accuracy. As it was mentioned before, this process is sensitive to heavy NP particles. Another process considered here is a set of missing energy decays of heavy mesons. It provides an opportunity to either detect light Dark Matter in such decays or to rule out the possibility of light DM depending on the result of experimental studies. More detailed introduction to these problems is provided at the beginning of appropriate chapters.

Chapter 2

Theoretical aspects of the Standard Model

2.1 Symmetry

The Standard Model is a gauge field theory based on the $SU(3)_C \otimes SU(2)_L \otimes U(1)_Y$ symmetry groups. $SU(3)_C$ is a symmetry of strong interaction (QCD). It is unbroken, in other words it is exact symmetry of the theory, and it is confined, i.e. it is present only at certain distances between interacting particles. However, $SU(2)_L \otimes U(1)_Y$ is spontaneously broken down to $U(1)_{em}$ under the Higgs mechanism [9].

Index L in the notation of $SU(2)$ group stands for "Left" since only left-handed fermions play role in weak interaction. The fermion mass term $\bar{\psi}\psi$ mixes left- and right-handed fields:

$$\bar{\psi}\psi = \bar{\psi}_R\psi_L + \bar{\psi}_L\psi_R \quad (2.1)$$

while electromagnetic (vector) and weak (V-A) currents do not mix those components. Only left-handed fields contribute to the electro-weak currents:

$$\begin{aligned} \bar{\psi}\gamma^\mu\psi &= \bar{\psi}_R\gamma^\mu\psi_R + \bar{\psi}_L\gamma^\mu\psi_L; \\ \bar{\psi}\gamma^\mu(1 - \gamma_5)\psi &= 2\bar{\psi}\gamma^\mu P_L\psi = 2\bar{\psi}\gamma^\mu P_L^2\psi = 2\bar{\psi}P_R\gamma^\mu P_L\psi = 2\bar{\psi}_L\gamma^\mu\psi_L \end{aligned}$$

$U(1)_Y$ is associated with hypercharge Y which can be related to the third component of the weak isospin I_3 and electric charge Q through Gell-Mann–Nishijima formula:

$$Q = T_3 + Y/2 \quad (2.2)$$

Such a theory combining $SU(2)_L \otimes U(1)_Y$ requires four gauge bosons: a triplet (W_1, W_2, W_3) and a singlet B . Triplet field is associated with $SU(2)$ generators, while singlet is related to $U(1)$. Physical gauge bosons (Table.1.1) that are observed in an experiment are admixtures of those fields. Charged bosons W^\pm are linear combinations of $W_{1,2}$, while photon and Z^0 are a mixture of W_3 and B . W^\pm and Z^0 bosons gain masses via spontaneous symmetry breaking and Higgs mechanism, which will be discussed below.

2.2 Gauge bosons, leptons and their interactions

Let us introduce gauge fields and their strength tensors:

$$\begin{aligned} SU(2)_L &\rightarrow W_\mu^1, W_\mu^2, W_\mu^3, \\ U(1)_Y &\rightarrow B_\mu, \\ W_{\mu\nu}^i &\equiv \partial_\mu W_\nu^i - \partial_\nu W_\mu^i + g\epsilon^{ijk}W_\mu^j W_\nu^k, \\ B_{\mu\nu} &\equiv \partial_\mu B_\nu - \partial_\nu B_\mu, \\ \mathcal{L}_{gauge} &= -\frac{1}{4}W_{\mu\nu}^i W^{i\ \mu\nu} - \frac{1}{4}B_{\mu\nu}B^{\mu\nu}. \end{aligned} \quad (2.3)$$

Let us consider the leptonic part of the Standard Model lagrangian. Its kinetic part can be written in the following way:

$$\mathcal{L}_{lepton} = \bar{R}i\partial R + \bar{L}i\partial L. \quad (2.4)$$

where $R = l_R$ is a right-handed singlet and $L = \begin{pmatrix} l_L \\ \nu_L \end{pmatrix}$ is a left-handed doublet. There are no mass terms for fermions since it mixes left- and right-handed components, thus breaking gauge invariance. It will be introduced via the Higgs mechanism later in the chapter. To introduce the interaction between fermions and bosons, and to make the lagrangian in Eq.2.4 gauge-invariant we need to introduce covariant derivatives [10]:

$$\begin{aligned}
L &: \partial_\mu + i\frac{g}{2}\tau^i W_\mu^i + i\frac{g'}{2}Y B_\mu \\
R &: \partial_\mu + i\frac{g'}{2}Y B_\mu \\
\mathcal{L}_{lepton}^{interaction} &= \bar{L}i\gamma^\mu \left(i\frac{g}{2}\tau^i W_\mu^i + i\frac{g'}{2}Y B_\mu \right) L \\
&+ \bar{R}i\gamma^\mu \left(i\frac{g'}{2}Y B_\mu \right) R.
\end{aligned} \tag{2.5}$$

Here g and g' are coupling constants associated with groups $SU(2)_L$ and $U(1)_Y$ respectively; $Y_{L_i} = -1$ and $Y_{R_i} = -2$.

Picking up the "left" and the "right" parts of Eq.(2.5) and writing it explicitly one can obtain the following SM currents:

$$\mathcal{L}_{lepton}^L = -g\bar{L}\gamma^\mu \left(\frac{\tau^1}{2}W_\mu^1 + \frac{\tau^2}{2}W_\mu^2 \right) L - g\bar{L}\gamma^\mu \frac{\tau^3}{2}W_\mu^3 L - \frac{g'}{2}Y\bar{L}\gamma^\mu B_\mu L \tag{2.6}$$

$$\equiv \mathcal{L}_{lepton}^{L(\pm)} + \mathcal{L}_{lepton}^{L(0)} \text{ where}$$

$$\mathcal{L}_{lepton}^{L(\pm)} = -g\bar{L}\gamma^\mu \left(\frac{\tau^1}{2}W_\mu^1 + \frac{\tau^2}{2}W_\mu^2 \right) L$$

$$\mathcal{L}_{lepton}^{L(0)} = -g\bar{L}\gamma^\mu \frac{\tau^3}{2}W_\mu^3 L - \frac{g'}{2}Y\bar{L}\gamma^\mu B_\mu L \tag{2.7}$$

$$\mathcal{L}_{lepton}^{R(0)} = -\frac{g'}{2}Y\bar{R}\gamma^\mu B_\mu R. \tag{2.8}$$

Superscripts (\pm) and (0) denote charged and neutral current respectively. Let us consider

these currents separately.

Using an explicit representation of the Pauli matrices, $\mathcal{L}_{lepton}^{L(\pm)}$ can be written as follows:

$$\mathcal{L}_{lepton}^{L(\pm)} = -g\bar{L}\gamma^\mu \begin{pmatrix} 0 & W^1 - iW^2 \\ W^1 + iW^2 & 0 \end{pmatrix} L \quad (2.9)$$

It is convenient to redefine $W^{1,2}$ in such a way that new fields match the observed charged fields W^\pm :

$$\begin{aligned} W^\pm &= \frac{1}{\sqrt{2}} (W^1 \mp iW^2) \\ \mathcal{L}_{lepton}^{L(\pm)} &= -\frac{g}{2\sqrt{2}} [\bar{\nu}\gamma^\mu(1 - \gamma_5)lW_\mu^+ + \bar{l}\gamma^\mu(1 - \gamma_5)\nu W_\mu^-] \end{aligned} \quad (2.10)$$

The coupling constant g can be related to the strength of the effective four-fermion Fermi interaction:

$$\frac{g}{2\sqrt{2}} = G_W = \left(\frac{G_F M_W^2}{\sqrt{2}} \right)^{1/2} \quad (2.11)$$

Now let us consider the neutral part of the lepton lagrangian that mixes right- and left-handed fields.

$$\begin{aligned} \mathcal{L}^{L+R(0)} &= -g\bar{L}\gamma^\mu \frac{\tau^3}{2} W_\mu^3 L - \frac{g'}{2} (\bar{L}\gamma^\mu Y_L + \bar{R}\gamma^\mu Y_R) B_\mu \equiv \\ &\equiv -gJ_3^\mu W_\mu^3 - \frac{g'}{2} J_Y^\mu B_\mu \end{aligned} \quad (2.12)$$

Currents J_3^μ and J_Y^μ are defined as follows:

$$\begin{aligned} J_3^\mu &= \frac{1}{2} (\bar{\nu}_L \gamma^\mu \nu_L - \bar{l}_L \gamma^\mu l_L) \\ J_Y^\mu &= -(\bar{\nu}_L \gamma^\mu \nu_L + \bar{l}_L \gamma^\mu l_L + 2\bar{l}_R \gamma^\mu l_R) \end{aligned}$$

It is clear that they obey Gell-Mann–Nishijima relation:

$$J_{em} = J_3 + \frac{1}{2}J_Y$$

One can rotate neutral fields W_3^μ and B^μ to the new fields A^μ and Z^μ :

$$\begin{pmatrix} A^\mu \\ Z^\mu \end{pmatrix} = \begin{pmatrix} \cos \theta_W & \sin \theta_W \\ -\sin \theta_W & \cos \theta_W \end{pmatrix} \begin{pmatrix} B^\mu \\ W_3^\mu \end{pmatrix} \quad (2.13)$$

where θ_W is called the Weinberg weak mixing angle. There is the following relation between $SU(2)_L$ and $U(1)_Y$ coupling constants:

$$\sin \theta_W = \frac{g'}{\sqrt{g^2 + g'^2}}, \quad \cos \theta_W = \frac{g}{\sqrt{g^2 + g'^2}}$$

Re-writing lagrangian in terms of the new fields one can immediately notice that there is a well-defined relation between electric charge, coupling constants, and the Weinberg angle. Another important result is presence of the weak interaction that does not change charge. Strength of this interaction can be predicted by the Standard Model:

$$\begin{aligned} \mathcal{L}^{L+R}{}^{(0)} &= -g \sin \theta_W (\bar{l} \gamma^\mu l) A_\mu - \frac{g}{2 \cos \theta_W} \sum_{\psi_i = \nu, l} (\bar{\psi}_i \gamma^\mu (g_V^i - g_A^i \gamma_5) \psi_i) Z_\mu \\ e &= g \sin \theta_W = g' \cos \theta_W \\ g_V^i &= T_3^i - 2Q_i \sin^2 \theta_W, \quad g_A^i = T_3^i \end{aligned} \quad (2.14)$$

The result of Eq.(2.14) is extremely important since at the time it was obtained, there was no experimental evidence for the weak neutral current.

2.3 Higgs mechanism. Mass generation

*If the Higgs boson didn't exist,
we should have to invent
something very much like it*
C. Quigg [8]

At this point theory contains four massless gauge fields – A_μ , Z_μ , W_μ^\pm ; and two massless fermions – l , ν . The next step in the theory building is to add scalar fields in order to break symmetry and to generate weak bosons masses while keeping photon massless. In order to give masses to the gauge bosons we need to apply the so-called Higgs mechanism. Formal introduction to this mechanism is provided in the next several paragraphs. Obtained results will be generalized for the Standard Model later in the text.

Goldstone's theorem states that when an exact continuous global symmetry is spontaneously broken, the theory contains one massless scalar particle for each broken generator of the original symmetry group. However there is no experimental evidence for existence of such particles. In the mid-1960's several authors independently pointed out the way to solve this puzzle – the so called Higgs mechanism [11]. It also has a nice bonus - in the Higgs mechanism the gauge bosons become massive. In order to see how this mechanism works let us consider the charged self- interacting scalar field (Eq. (2.15)).

$$\begin{aligned}\mathcal{L} &= \partial_\mu \phi^* \partial^\mu \phi - V(\phi, \phi^*) \\ V(\phi, \phi^*) &= \mu^2 \phi^* \phi + \lambda(\phi^* \phi)^2\end{aligned}\tag{2.15}$$

Note that lagrangian (Eq.(2.15)) is invariant under the global phase transformation $\phi \rightarrow$

$\exp(-i\theta)\phi$. When we re-write it in terms of two real scalar fields it becomes invariant under $SO(2)$ transformations:

$$\begin{aligned}\phi &= \frac{\phi_1 + i\phi_2}{\sqrt{2}} \\ \mathcal{L} &= \frac{1}{2}(\partial_\mu\phi_1\partial^\mu\phi_1 + \partial_\mu\phi_2\partial^\mu\phi_2) - V(\phi_1, \phi_2) \\ \begin{pmatrix} \phi_1 \\ \phi_2 \end{pmatrix} &\longrightarrow \begin{pmatrix} \cos\theta & \sin\theta \\ -\sin\theta & \cos\theta \end{pmatrix} \begin{pmatrix} \phi_1 \\ \phi_2 \end{pmatrix}\end{aligned}\tag{2.16}$$

For $\mu^2 > 0$ the vacuum state is at $\phi_1 = \phi_2 = 0$ and for the small oscillations about the minimum,

$$\mathcal{L} = \sum_{i=1,2} = \frac{1}{2}(\partial_\mu\phi_i\partial^\mu\phi_i - \mu^2\phi_i^2),\tag{2.17}$$

which means that in this situation there are two scalar fields $\phi_{1,2}$ with mass $m^2 = \mu^2 > 0$.

In the case when $\mu^2 < 0$ we get the continuum of the vacuum states (the "mexican hat" potential, Fig.2.1). In this situation minimum of potential is at:

$$\langle|\phi|^2\rangle = \frac{\langle\phi_1\rangle^2 + \langle\phi_2\rangle^2}{2} = -\frac{\mu^2}{2\lambda} \equiv \frac{v^2}{2}\tag{2.18}$$

One can see from the Fig.2.1 that vacua are still invariant under $SO(2)$ symmetry. However, once we pick out the particular vacuum state, the symmetry is broken. This phenomenon is called spontaneous symmetry breaking. For example, we can pick the following vacuum configuration $\phi_1 = v$ and $\phi_2 = 0$. The new fields can be redefined as perturbations around the vacuum state:

$$\phi'_1 = \phi_1 - v \quad \text{and} \quad \phi'_2 = \phi_2\tag{2.19}$$

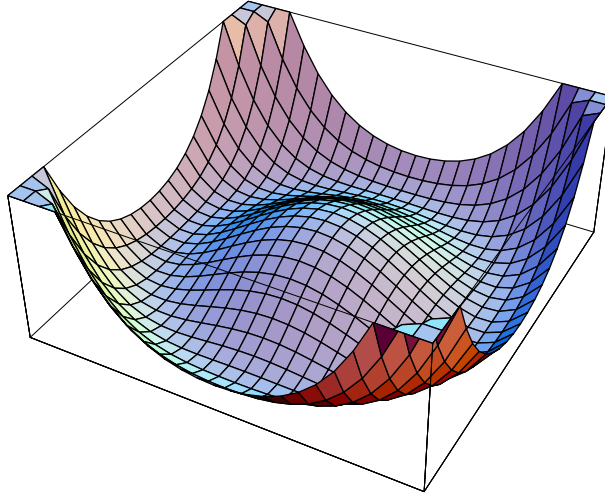


Figure 2.1: The “mexican hat” potential incorporated in the theory of the spontaneous symmetry breaking

in terms of new fields, lagrangian transforms to the following form:

$$\mathcal{L} = \frac{1}{2}\partial_\mu\phi'_1\partial^\mu\phi'_1 - \frac{1}{2}(-2\mu^2)\phi_1'^2 + \frac{1}{2}\partial_\mu\phi'_2\partial^\mu\phi'_2 + \dots \quad (2.20)$$

where ellipsis denotes interaction terms which are irrelevant for the mass generation discussion. Clearly, the new lagrangian describes interactions of two scalar fields, one of them is massless and another one is massive.

In order to apply the Higgs mechanism and to generate W^\pm and Z^0 masses let us introduce the scalar doublet and its lagrangian:

$$\begin{aligned} \Phi &\equiv \begin{pmatrix} \phi^+ \\ \phi^0 \end{pmatrix} \\ \mathcal{L} &= D_\mu\Phi^\dagger D^\mu\Phi - \mu^2\Phi^\dagger\Phi - \lambda(\Phi^\dagger\Phi)^2 \\ D_\mu &= \partial_\mu + ig\frac{\tau^i}{2}W_\mu^i + i\frac{g'}{2}YB_\mu \end{aligned} \quad (2.21)$$

We choose the vacuum expectation value of the Higgs boson in the following form:

$$\langle \Phi \rangle_0 = \begin{pmatrix} 0 \\ v/\sqrt{2} \end{pmatrix}, \text{ where } v = \sqrt{-\frac{\mu^2}{\lambda}} \quad (2.22)$$

Such a choice of the vacuum expectation value breaks $SU(2)_L \otimes U(1)_Y$ symmetry down to $U(1)_{em}$ giving mass to the W^\pm and Z^0 bosons and leaving photon massless. The Higgs doublet can be parametrized in the following form:

$$\Phi = \frac{v + H}{\sqrt{2}} \begin{pmatrix} 0 \\ 1 \end{pmatrix}. \quad (2.23)$$

After substitution of Eq.2.23 into Eq.2.21 and redefinition of gauge boson fields according to Eq.2.10 one obtains the following result:

$$D^\mu \Phi D_\mu \Phi \rightarrow \frac{1}{2} \partial_\mu H \partial^\mu H + \frac{g^2}{4} (v + H)^2 \left(W_\mu^+ W^{-\mu} + \frac{1}{2 \cos^2 \theta_W} Z^\mu Z_\mu \right) \quad (2.24)$$

Comparing the latter term with the mass term for W^\pm and Z^0 bosons one can identify:

$$\begin{aligned} M_W &= \frac{gv}{2} \\ M_Z &= \frac{1}{\cos \theta_W} \frac{gv}{2} = \frac{M_W}{\cos \theta_W} \end{aligned} \quad (2.25)$$

The approach can be generalized for the case of non-Abelian theory. Lepton and quark masses are obtained from Yukawa interaction of leptons (quarks) with Higgs boson (see Section 2.4). It is necessary to stress that the Higgs mechanism explains how particles get masses in the SM framework, but it does not predict their numerical values. Thus

particles masses need to be introduced as input parameters of the model as mentioned in the Chapter.1. We will not go into more details about mass generation in the Standard Model since it is not the main topic of dissertation. Interested reader can find plenty of information on this matter in almost any particle physics textbook [12].

We would like to point out that Higgs boson is the missing piece of the Standard Model and it is yet to be discovered. There are various extensions to the basic Higgs mechanism: extended Higgs sector (for example [13] and [14]), composite Higgs boson [15, 16], etc. All of them employ the same idea of symmetry breaking but have different particle content. Only experimental confirmation can determine which theory is correct.

2.4 Quark mixing and the CKM matrix

The electroweak sector of the Standard Model is a $SU(2)_L \otimes U(1)_Y$ gauge theory. The left-handed quarks are $SU(2)_L$ doublets, while the right-handed quarks are singlets. If $SU(2)_L \otimes U(1)_Y$ was an exact symmetry of the theory, then quarks would be massless and there would be no difference between mass and interaction eigenstates. As it was discussed in the previous section, interaction between Higgs boson and quarks breaks symmetry and generates quark masses. Let us consider in detail how it is realized and why it leads to quark mixing.

$$\mathcal{L}_{quark-Higgs} = - \sum_{i,j=1}^3 U_{ij} \bar{R}_{U_i} \tilde{\Phi}^\dagger L_j + D_{ij} \bar{R}_{D_i} \Phi^\dagger L_j + h.c \quad (2.26)$$

$$\tilde{\Phi} = i\sigma_2 \Phi^* = \begin{pmatrix} \phi^{0*} \\ -\phi^- \end{pmatrix}. \quad (2.27)$$

Here $\tilde{\Phi}$ is the conjugated Higgs doublet; $U_{i,j}$, R_{U_i} and $D_{i,j}$, R_{D_i} are Yukawa matrices and right-handed singlets for up- and down-type quarks respectively. From the vacuum expectation values of Higgs doublets Φ and $\tilde{\Phi}$ we obtain the mass matrices for up- and down-type quarks:

$$\mathcal{M}_{ij}^{U(D)} = \frac{v}{\sqrt{2}} U(D)_{ij} \quad (2.28)$$

These matrices are non-diagonal, thus the weak eigenstates q' are a superposition of the mass eigenstates q . Each of matrices $U(D)_{ij}$ can be diagonalized using unitary transformation. However, they can not be diagonalized *simultaneously*.

$$\begin{aligned} \begin{pmatrix} u' \\ c' \\ t' \end{pmatrix}_{L,R} &= F_{L,R}^{(U)} \begin{pmatrix} u \\ c \\ t \end{pmatrix}_{L,R}, \quad \begin{pmatrix} d' \\ s' \\ b' \end{pmatrix}_{L,R} = F_{L,R}^{(D)} \begin{pmatrix} d \\ s \\ b \end{pmatrix}_{L,R} \\ F_R^{(U)-1} \mathcal{M}^U F_L^{(U)} &= \begin{pmatrix} m_u & 0 & 0 \\ 0 & m_c & 0 \\ 0 & 0 & m_t \end{pmatrix} \\ F_R^{(D)-1} \mathcal{M}^D F_L^{(D)} &= \begin{pmatrix} m_d & 0 & 0 \\ 0 & m_s & 0 \\ 0 & 0 & m_b \end{pmatrix} \end{aligned} \quad (2.29)$$

For the weak charged V-A current it results in the following:

$$\overline{(u' \ c' \ t')}_L \gamma_\mu \begin{pmatrix} d' \\ s' \\ b' \end{pmatrix}_L = \overline{(u \ c \ t)}_L (F_L^{(U)\dagger} F_L^{(D)}) \gamma_\mu \begin{pmatrix} d \\ s \\ b \end{pmatrix}_L \quad (2.30)$$

with generation mixing between mass eigenstates encoded in the matrix V :

$$V \equiv F_L^{(U)\dagger} F_L^{(D)} \quad (2.31)$$

On the other hand, neutral current of quarks does not produce generation mixing:

$$\overline{(u' \ c' \ t')}_L \gamma_\mu \begin{pmatrix} u' \\ c' \\ t' \end{pmatrix}_L = \overline{(u \ c \ t)}_L (F_L^{(U)\dagger} F_L^{(U)}) \gamma_\mu \begin{pmatrix} u \\ c \\ t \end{pmatrix}_L, \quad (2.32)$$

where $F_L^{(U)\dagger} F_L^{(U)} = 1$ because of unitarity

Thus there are no flavor changing neutral currents in the Standard Model at tree level. However such currents can be realized in loop diagrams.

V_{ij} is Cabibbo-Kobayashi-Maskawa (CKM) matrix [17]. In general the N generations quark mixing matrix is described by $(N - 1)^2$ parameters which include $N(N - 1)/2$ Euler-type angles and $(N - 1)(N - 2)/2$ complex phases. The latter relationship is especially interesting since it shows that in case of two quark generations the Cabibbo matrix is real, while for three generations it contains irreducible complex phase. This phase is required to provide description of CP violation within the Standard Model framework.

There are various parameterizations of the CKM matrix. One of them is the Wolfenstein parametrization [18]. It is based on the expansion of each element as a power series of small

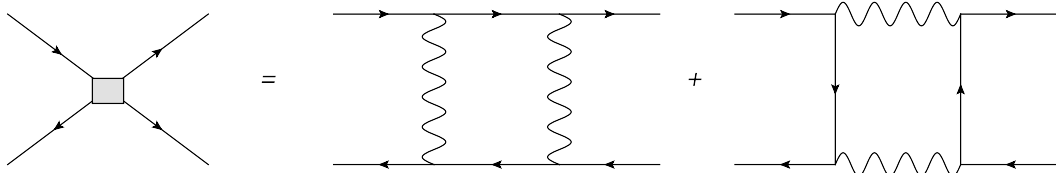


Figure 2.2: Schematic representation of the meson–anti-meson mixing process

parameter $\lambda = |V_{us}| = 0.22$:

$$V = \begin{pmatrix} 1 - \frac{\lambda^2}{2} & \lambda & A\lambda^3(\rho - i\eta) \\ -\lambda & 1 - \frac{\lambda^2}{2} & A\lambda^2 \\ A\lambda^3(1 - \rho - i\eta) & -A\lambda^2 & 1 \end{pmatrix} + O(\lambda^4) \quad (2.33)$$

This parametrization is very convenient for phenomenological applications since it allows estimation of the relative size of various effects almost immediately (for example CKM favored versus CKM suppressed decay rates).

There is a fascinating phenomenological observation arising from quark mixing. It is mixing of a meson and an anti-meson. Schematically this effect can be described in the following way. Meson contains quark q_1 and anti-quark \bar{q}_2 . Due to quark mixing, it can experience the following transitions: $q_1 \rightarrow q_i \rightarrow q_2$ and $\bar{q}_2 \rightarrow \bar{q}_i \rightarrow \bar{q}_1$ thus resulting in transition from meson to anti-meson (schematically this process is presented on Fig.2.2). Since, as it was mentioned before, weak eigenstates do not coincide with mass eigenstates, the meson detected in an experiment (mass eigenstate) will be a mixture of meson and anti-meson interaction eigenstates. This was first observed in $K^0 - \bar{K}^0$ system [19], later in the B_d [20] system and the most recent observations detected mixing in the D^0 [21] and B_s [22, 23] systems. These neutral mesons (K^0 , B_d , D^0 and B_s) are the only hadrons that mix with their own anti-particles.

Meson-antimeson mixing serves as an indispensable way of placing constraints on various models of New Physics (NP). This is usually ascribed to the fact that this process only occurs at the one-loop level in the Standard Model (SM) of electroweak interactions. This makes it sensitive to the effects of possible NP particles in the loops or even to new tree-level interactions that can possibly contribute to the flavor-changing $\Delta Q = 2$ interactions. Technical details of the meson-antimeson calculations are provided in Chapter 4. We considered several examples of the New Physics signals in the B_s mixing and placed constraints on some models of the physics beyond the Standard Model.

However, New Physics is not necessarily heavy (i.e. with mass of the NP particles at the electroweak scale or above). One of the examples of the physical phenomena that is not described within the Standard Model and still can be relatively light is Dark Matter (DM). In the next chapter we provide an introduction to the Dark Matter subject and briefly discuss several theoretical approaches to the problem of DM.

Chapter 3

Different approaches to the problem of Dark Matter

As briefly mentioned in the Chapter1, the Dark Matter (DM) and Dark Energy are not described in the Standard Model. It means that, despite the huge success of the Standard Model in description of elementary particle phenomenology, we still do not know what 95% of the Universe is made off (see Fig.1.1). First experimental evidence for the dark matter dates back to the 1937 [24] when Swiss astronomer Fritz Zwicky noticed discrepancy between predicted and observed values of orbital velocities of galaxies in clusters. In order to solve this puzzle he postulated the existence of the "missing mass". There were a lot of efforts directed to understanding the nature of the Dark Matter and it's properties. Many models were proposed, however there is no confirmed experimental detection of DM at microscopic (particle) level as opposed to the macroscopic (galactic) scale.

The most popular solutions of the Dark Matter puzzle can be classified in the following way. On one hand, in order to explain the rotational curves of galaxies one can modify gravity. Such an approach is called MOND – MOdified Newtonian Dynamics. On the other hand, one can introduce various sources of the "missing mass", which would provide the same results. The latter set of ideas can be separated into two additional subsets – baryonic and non-baryonic DM. All of them are briefly discussed below.

3.1 MOND

The MOdified Newtonian Dynamics is an extremely attractive way to explain the galactic rotation curves. This approach is based on the assumption that Newtonian gravity fails at certain scales. New particle species are not introduced in such theories. The MOND paradigm was introduced by Milgrom [25]. Its basic idea is quite simple - for small accelerations ($a_c \approx 10^{-10} m s^{-2}$), Newtonian dynamics is no longer applicable to describe the behavior of a test mass, and should be modified.

$$a = \mu(a_N/a_c)a_N \tag{3.1}$$

where a_N is Newtonian acceleration due to gravity and μ is a smooth monotonic function with the requirement $\mu(1) = 1$ [26].

MOND approach works extremely well for the explanation of gravitational rotation curves requiring in principle only one input parameter - a_c . However, MOND fails to explain the mass distribution in the Bullet Cluster Fig.3.1. Another problem associated with the MOND approach is that it can not explain DAMA/LIBRA results for the annual modulation of the DM flux[6]. Yet another drawback of the MOND approach is that it does not explain PAMELA data [31]. It is necessary to mention that while these experimental results might be due to the Dark Matter, it is not necessarily so. Thus Modified Newtonian Dynamics is not completely disfavored by any current experiment searching for the Dark Matter.

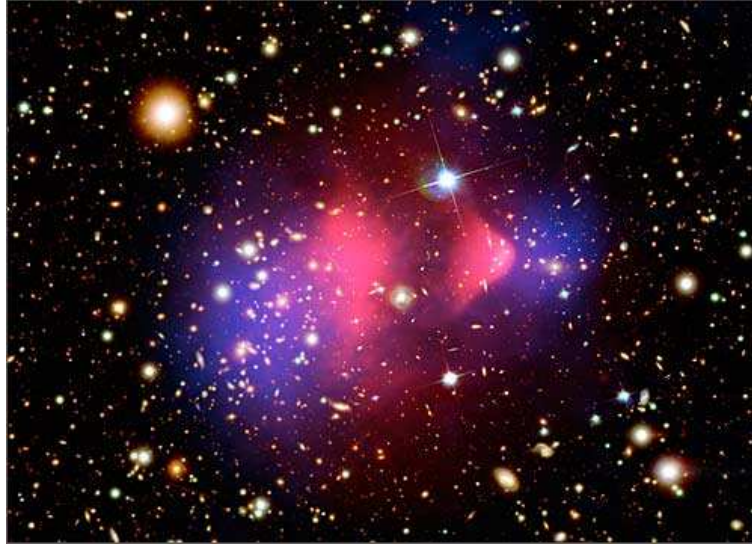


Figure 3.1: Pink represents matter detected by the X-ray telescope, while blue represents the way matter should be distributed in order to explain light propagation from background galaxies[27].

3.2 Baryonic Dark Matter

Baryonic Dark matter is a type of DM that is composed of baryons. In other words, baryonic DM is composed of ordinary matter and can not be detected by its emitted radiations. The main candidates for baryonic Dark Matter are non-luminous gas, and Massive Astrophysical Compact Halo Objects (MACHO) (MACHOs include black holes, neutron stars and brown dwarfs.). The total amount of baryonic DM can be inferred from the Big Bang nucleosynthesis and cosmic microwave background measurements. Both of the approaches show that amount of baryonic DM is much smaller than total amount of Dark Matter in the Universe [28].

3.3 Non-baryonic Dark Matter

Another way to treat the Dark Matter is to assume that there are some particles not described by the Standard Model that account for the invisible mass in the Universe. The lack of experimental information about coupling of the DM to the Standard Model particles forces us to rely on various assumptions and expectations. Naturally, in such an approach there are plenty of the Dark Matter candidates[29]. One of the ways too classify Dark Matter is based on its temperature. This way, non-baryonic DM can be divided into three subsets - hot, warm and cold Dark Matter.

3.3.1 Hot and Warm Dark Matter

Hot Dark Matter is a hypothetical model of the Dark Matter which consists of ultra-relativistic particles. Neutrinos are the first hot DM candidate we can think of. They almost do not interact with ordinary matter, are hard to detect and observe. All these reasons make us think that "missing mass" can be made up of neutrinos.

Sterile neutrinos can also serve as a warm Dark Matter particles, however this would require non-thermal resonant DM production[30].

In this situation, the first guess is not right. Hot (and warm) DM can not explain formation of individual galaxies after Big Bang. It can not explain small scale structure in the Universe and would smear out the large scale structures. Also, neutrinos are not abundant enough to reproduce the relic abundance observations. Nowadays, the hot Dark Matter is considered only as a part of mixed Dark Matter theories.

3.3.2 Cold Dark Matter

In contrast to hot Dark Matter, the concept of cold DM (CDM) can explain small scale structures in the Universe. In the cold Dark Matter theory, structure grows hierarchically (bottom-up) with small objects collapsing and merging into more massive ones. From cosmological point of view the CDM theory does not make prediction about properties of the Dark Matter, other than stating that it should be cold. The cold Dark Matter candidates are provided in theories beyond the Standard Model. Usually CDM candidates are divided in two classes - axions and WIMPs (Weakly Interacting Massive Particles). WIMPs can be further divided into supersymmetric DM and light (with mass of a few GeV) DM.

- *WIMP*

The observed relic abundance is $\Omega_{DM}h^2 \approx 10^{-1}[2]$. The relic abundance of the particle is inversely proportional to the annihilation cross-section:

$$\Omega_X \sim \frac{1}{\langle \sigma v \rangle} \sim \frac{m_X^2}{g_x^4} \quad (3.2)$$

Thus weakly interacting particles ($g_x \sim 0.5$) with mass at the weak scale ($m_X \sim 100GeV$) seem to be the perfect candidates for the Dark Matter (WIMP = Weakly Interacting Massive Particle). This coincidence is called the "*WIMP miracle*" and brought a lot of attention to the models which provide WIMP candidates. More supporting evidence for WIMP models is a positron excess in the PAMELA data[31] - Fig.3.2. As one can see, an excess of positron flux is observed at the energy scale of $\sim 100GeV$ thus suggesting that something new might be at this scale or above it.

While arguments for WIMP as a Dark Matter candidate seem to be convincing, there are several problems that should be addressed in this approach. Considering WIMP as

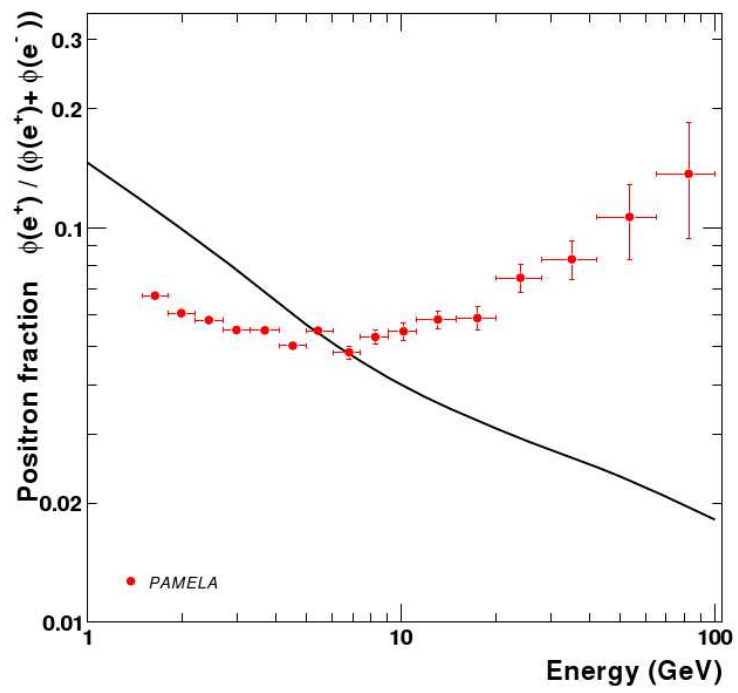


Figure 3.2: Positron excess in the PAMELA data. Solid line - GALPROP simulation[32]

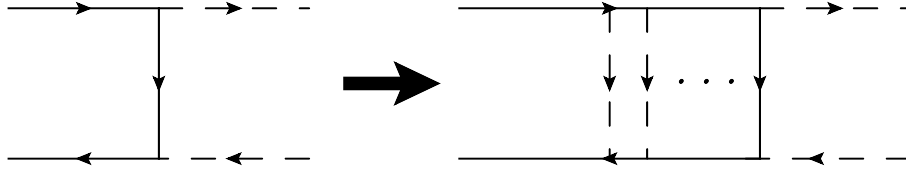


Figure 3.3: Sommerfeld enhancement of annihilation rate

a DM candidate, one can estimate positron excess and it turns out to be a factor 100 to 1000 too small to explain the PAMELA data. In principle this problem can be solved via introduction of various enhancement factors, so-called boost factors. While it is unlikely to get such an enhancement from an astrophysical source, particle physics can provide it. Annihilation cross-section can be enhanced via the so-called "Sommerfeld effect" [33]. It is a non relativistic quantum effect which arises due to the distortion of the particle wave function by the potential at the low kinetic energy. In the quantum field theory language it means multiple force carrier exchanges before annihilation (Fig.3.3). Large enhancement factors require the Dark Matter to be strongly coupled to the force carrier and/or mass of the force carrier to be small. Such a scenario induces the dark matter self-interaction which is excluded for the light force carriers by halo ellipticity [34]. Possible solutions to this problem include but are not limited to the alternative DM production mechanisms, alternative cosmology at the freeze-out, astrophysical boost in addition to the Sommerfeld enhancement [35].

Since there are no DM candidates in the Standard Model particle content, there should be more general theory that will have some. One of the most popular extension of the SM is the supersymmetry. Depending on the particular realization of the supersymmetric scenario, different particles can serve as Dark Matter - neutralino, wino, sneutrino, gravitino, axino.

Existence of fermionic Dark Matter with mass less than few GeV is forbidden under Lee-Weinber limit [36] since it would cause cosmological problems (for details see Chapter 5). However, spin $S = 0$ particles with masses as low as few MeV are not forbidden by this limit. Another motivation for light scalar DM is an experimental observation of 511 keV gamma-rays emitted from the direction of the galactic center by the INTEGRAL space telescope [37]. Such a spectrum can be explained by Dark Matter annihilation into electron-positron pairs which later annihilate into photons.

- *Axion*

WIMP and supersymmetric DM candidates have received a lot of attention lately. However, the axion also provides a well-motivated and promising candidate for cold Dark Matter.[38]

Axions were first introduced in QCD to solve the strong-CP problem. The QCD lagrangian may be written as

$$\mathcal{L}'_{QCD} = \mathcal{L}_{QCD} + \theta \frac{g^2}{32\pi^2} G\tilde{G} \quad (3.3)$$

The first term in the Eq.3.3 is a part of the QCD lagrangian that allows us to make successful phenomenological predictions. However, the second term violates the CP symmetry. It is an experimental fact, that CP is not violated in strong interaction, or if it is, the level of violation is tiny. From constraints of the neutron dipole moment it was determined that $\theta \leq 10^{-10}$. Axion arises in the Peccei-Quinn solution for the strong CP problems [39]. The basic idea of this solutions is to introduce a $U(1)$ symmetry which is broken at a certain scale f . This way θ becomes dynamical field (the Goldstone boson of this symmetry).

The variety of astrophysical observations require the mass of axion to be $m_a \sim 10^{-4} eV$. Smaller mass would result in an unacceptably large cosmological abundance of axions. Larger masses are ruled out by combination of astrophysical observations and laboratory experiments [40]. If the mass of axion falls into this range, then it provides the relic density $\Omega_a \sim 1$ and may therefore be the halo dark matter.

It is necessary to mention, that axions can be produced and detected in the accelerators. The only way to detect axions is to use experiments that are specifically designed for the axion dark matter detection.[41].

To summarize everything that was said about Dark Matter in this chapter we would like to say that the only thing we know for sure about DM is the fact that it exists. Modified gravity cannot explain all of the astrophysical puzzles, for example, the Bullet cluster mentioned earlier. If we strongly believe in the MOND we still shall have to add invisible mass to explain experimental observations. Thus Dark Matter exists! Everything else, including different types of the Dark Matter, explanations of the various experimental data, is nothing more but the reality of the search process. We are trying to guess what the Dark Matter could be and then to determine whether initial assumption fits experimental observations. Baryonic (luminous) matter makes up $\sim 5\%$ of the mass of the Universe and the Standard Model contains six quarks, three families of leptons, four gauge bosons. Dark Matter is responsible for $\sim 25\%$ of the mass. Attempt to explain it using single particle is just the first step towards understanding of what the Dark Matter is made off. There are already some results for Dark Matter models with extended particle content [42, 43, 44].

Currently there are several experiments dedicated to the detection of the Dark Matter [5, 6, 7]. These experiments are based on the detection of recoil energy after collision of Dark Matter particle with nuclei. There is a very low sensitivity to the light DM ($m_{DM} \sim GeV$),

since in such a situation the recoil energy will be small. In Chapter 5 I considered production of the light Dark Matter in the missing energy decays of the heavy mesons. Such processes would probe the Dark Matter with mass $m_{DM} \sim GeV$ and would supplement results of the direct detection experiments. Results of Chapter 5 rely on current experimental limits for missing energy decays of B_s , B_d , D^0 mesons. Depending on further improvement of experimental data, it will allow to either detect light DM in the above-mentioned decays or to completely disfavor the Light Dark Matter paradigm.

Chapter 4

Lifetime difference in B_s mixing

4.1 Introduction

As briefly mentioned in Chapters 1 and 2, mixing processes are sensitive to the New Physics particles that can be contributing to the loop diagrams. Mixing allows us to indirectly probe the heavy New Physics degrees of freedom using the low energy data from the meson-antimeson mixing. Results of this chapter are based on work done in collaboration with Alexey A. Petrov and Fabrizio Gabbiani [45].

We set up the relevant formalism and argue for the need to compute $1/m_b^2$ corrections to leading and next-to-leading effects in Sect. 4.2. In Sect. 4.3 we discuss the impact of $1/m_b^2$ corrections to the lifetime difference of B_s mesons and assess the convergence of the $1/m_b$ expansion. We also present the complete SM results for $\Delta\Gamma_s$ including $1/m_b^2$ corrections. We then discuss the possible effects from $\Delta B = 1$ New Physics contributions in Sect. 4.4. Finally, we present our conclusions on this subject in Sect. 4.5.

Flavor-changing interactions induce non-diagonal terms in the meson-antimeson mass matrix that describes the dynamics of those states. Diagonalizing this matrix gives two mass eigenstates that are superpositions of flavor eigenstates. In the B_s system mass eigenstates,

denoted as “heavy” $|B_H\rangle$ and “light” $|B_L\rangle$,

$$\begin{aligned} |B_H\rangle &= p|B_s\rangle + q|\bar{B}_s\rangle, \\ |B_L\rangle &= p|B_s\rangle - q|\bar{B}_s\rangle, \end{aligned} \tag{4.1}$$

were predicted to have a rather significant mass and width differences,

$$\Delta M_{B_s} = M_H - M_L, \quad \Delta\Gamma_{B_s} = \Gamma_L - \Gamma_H, \tag{4.2}$$

where $M_{H,L}$ and $\Gamma_{H,L}$ denote mass and width of mass eigenstates. Since in the Standard Model the mass difference is dominated by the top quark contributions, it is computable with great accuracy. Thus one might expect that possible NP contributions can be easily isolated. Unfortunately, a recent observation of mass difference of mass eigenstates in B_s mixing by CDF [22] and D0 [23],

$$\begin{aligned} \Delta M_{B_s} &= 17.77 \pm 0.10 \pm 0.07 \text{ ps}^{-1} \quad (\text{CDF}), \\ 17 \text{ ps}^{-1} &< \Delta M_{B_s} < 21 \text{ ps}^{-1} \quad (\text{D0}), \end{aligned} \tag{4.3}$$

put the hopes of spectacular NP effects in B_s system rest. In fact, analyses of mixing in the strange, charm and beauty quark systems all yielded positive signals, yet all of those signals seem to be explained quite well by the SM interactions. Yet, some contribution from New Physics particles is still possible, so even the energy scales above those directly accessible at the Tevatron or LHC can be probed with B_s mixing, provided that QCD sum rule [46] or lattice QCD [47, 48, 49, 50] calculations supply the relevant hadronic parameters with sufficient accuracy.

In addition to the mass difference ΔM_s , a number of experimental collaborations reported the observation of a lifetime difference $\Delta\Gamma_s$ in the B_s system. Combining recent result from D0 [51] with earlier measurements from CDF [52] and ALEPH [53], Particle Data Group (PDG) quotes [1]

$$\Delta\Gamma_s = 0.16^{+0.10}_{-0.13} \text{ ps}^{-1}, \quad \frac{\Delta\Gamma_s}{\Gamma_{B_s}} = 0.121^{+0.083}_{-0.090}, \quad (4.4)$$

while Heavy Flavor Averaging Group (HFAG) [54] gives

$$\Delta\Gamma_s = 0.071^{+0.053}_{-0.057} \text{ ps}^{-1}, \quad \frac{\Delta\Gamma_s}{\Gamma_{B_s}} = 0.104^{+0.076}_{-0.084}. \quad (4.5)$$

Differently from the mass difference ΔM_s , the lifetime difference $\Delta\Gamma_s$ is definitely dominated by the SM contributions, as it is generated by the on-shell intermediate states [55, 56, 57, 58]. While this might appear to make it less exciting for indirect searches for New Physics, besides “merely” providing yet another test for heavy quark expansion, it is nonetheless a useful quantity for a combined analysis of possible NP contributions to $B_s^0 - \bar{B}_s^0$ mixing [59, 60, 61, 62].

It has been argued [61] that CP-violating NP contributions to $\Delta B = 2$ amplitudes can only reduce the experimentally observed lifetime difference compared to its SM value, therefore it is important to have an accurate theoretical evaluation of $\Delta\Gamma_s$ in the SM. It is also important to note that $\Delta B = 1$ NP contributions can affect $\Delta\Gamma_s$, but do not have to follow the same pattern. Indeed, the level at which $\Delta B = 1$ NP can affect $\Delta\Gamma_s$ depends both on the particular extension of the SM, as well as on the projected accuracy of lattice calculations of hadronic parameters which drives the uncertainties on the theoretical prediction of $\Delta\Gamma_s$. So it is advantageous to evaluate the effect of NP contributions on $\Delta\Gamma_s$.

4.2 Formalism

In the limit of exact CP conservation the mass eigenstates of the $B_s^0-\bar{B}_s^0$ system are $|B_{H/L}\rangle = (|B_s\rangle \pm |\bar{B}_s\rangle)/\sqrt{2}$, with the convention $CP|B_s\rangle = -|\bar{B}_s\rangle$. The width difference between mass eigenstates is then given by [55]

$$\Delta\Gamma_{B_s} \equiv \Gamma_L - \Gamma_H = -2\Gamma_{12} = -2\Gamma_{21}, \quad (4.6)$$

where Γ_{ij} are the elements of the decay-width matrix, $i, j = 1, 2$ ($|1\rangle = |B_s\rangle$, $|2\rangle = |\bar{B}_s\rangle$).

We use the optical theorem to relate the off-diagonal elements of the decay-width matrix Γ entering the neutral B -meson oscillations to the imaginary part of the forward matrix element of the transition operator \mathcal{T} :

$$\Gamma_{21}(B_s) = \frac{1}{2M_{B_s}} \langle \bar{B}_s | \mathcal{T} | B_s \rangle, \quad \mathcal{T} = \text{Im } i \int d^4x T \{ H_{\text{eff}}(x) H_{\text{eff}}(0) \}. \quad (4.7)$$

Here H_{eff} is the low energy effective weak Hamiltonian mediating bottom-quark decays. The component that is relevant for Γ_{21} reads explicitly

$$\mathcal{H}_{\text{eff}} = \frac{G_F}{\sqrt{2}} V_{cb}^* V_{cs} \left(\sum_{r=1}^6 C_r Q_r + C_8 Q_8 \right), \quad (4.8)$$

defining the operators

$$Q_1 = (\bar{b}_i c_j)_{V-A} (\bar{c}_j s_i)_{V-A}, \quad Q_2 = (\bar{b}_i c_i)_{V-A} (\bar{c}_j s_j)_{V-A}, \quad (4.9)$$

$$Q_3 = (\bar{b}_i s_i)_{V-A} (\bar{q}_j q_j)_{V-A}, \quad Q_4 = (\bar{b}_i s_j)_{V-A} (\bar{q}_j q_i)_{V-A}, \quad (4.10)$$

$$Q_5 = (\bar{b}_i s_i)_{V-A} (\bar{q}_j q_j)_{V+A}, \quad Q_6 = (\bar{b}_i s_j)_{V-A} (\bar{q}_j q_i)_{V+A}, \quad (4.11)$$

$$Q_8 = \frac{g}{8\pi^2} m_b \bar{b}_i \sigma^{\mu\nu} (1 - \gamma_5) T_{ij}^a s_j G_{\mu\nu}^a. \quad (4.12)$$

Here i, j are color indices and a summation over $q = u, d, s, c, b$ is implied. $V \pm A$ refers to $\gamma^\mu(1 \pm \gamma_5)$ and $S - P$ (which we need below) to $(1 - \gamma_5)$. C_1, \dots, C_6 are the corresponding Wilson coefficient functions at the renormalization scale μ , which are known at next-to-leading order. We have also included the chromomagnetic operator Q_8 , contributing to \mathcal{T} at $\mathcal{O}(\alpha_s)$. Note that for a negative C_8 , as conventionally used in the literature, the Feynman rule for the quark-gluon vertex is $-ig\gamma_\mu T^a$. A detailed review and explicit expressions may be found in [63]. Cabibbo-suppressed channels have been neglected in Eq. (4.8).

In the heavy-quark limit, the energy release supplied by the b-quark is large, so the correlator in Eq. (4.7) is dominated by short-distance physics [64]. An Operator Product Expansion (OPE) can be constructed for Eq. (4.7), which results in its expansion as a series of matrix elements of local operators of increasing dimension suppressed by powers of $1/m_b$:

$$\Gamma_{21}(B_s) = \frac{1}{2M_{B_s}} \sum_k \langle B_s | \mathcal{T}_k | B_s \rangle = \sum_k \frac{C_k(\mu)}{m_b^k} \langle B_s | \mathcal{O}_k^{\Delta B=2}(\mu) | B_s \rangle. \quad (4.13)$$

In other words, the calculation of $\Gamma_{21}(B_s)$ is equivalent to computing the matching coefficients of the effective $\Delta B = 2$ Lagrangian with subsequent computation of its matrix elements. Eventually the scale dependence of the Wilson coefficients in Eq. (4.13) is bound to match the scale dependence of the computed matrix elements.

Expanding the operator product (4.7) for small $x \sim 1/m_b$, the transition operator \mathcal{T} can be written to leading order in the $1/m_b$ expansion as [55, 56]

$$\mathcal{T} = -\frac{G_F^2 m_b^2}{12\pi} (V_{cb}^* V_{cs})^2 [F(z) Q(\mu_2) + F_S(z) Q_S(\mu_2)], \quad (4.14)$$

which results in [57]

$$\begin{aligned} \Gamma_{21}(B_s) &= -\frac{G_F^2 m_b^2}{12\pi(2M_{B_s})} (V_{cb}^* V_{cs})^2 \sqrt{1-4z} \times \\ &\times \left\{ [(1-z)(2C_1 C_2 + N_c C_2^2) + (1-4z)C_1^2/2] \langle Q \rangle + \right. \\ &\left. + (1+2z)(2C_1 C_2 + N_c C_2^2 - C_1^2) \langle Q_S \rangle \right\}, \end{aligned} \quad (4.15)$$

with $z = m_c^2/m_b^2$ and the basis of $\Delta B = 2$ operators¹

$$Q = (\bar{b}_i s_i)_{V-A} (\bar{b}_j s_j)_{V-A}, \quad Q_S = (\bar{b}_i s_i)_{S-P} (\bar{b}_j s_j)_{S-P}. \quad (4.16)$$

In writing Eq. (4.14) we have used the Fierz identities and the equations of motion to eliminate the color re-arranged operators

$$\tilde{Q} = (\bar{b}_i s_j)_{V-A} (\bar{b}_j s_i)_{V-A}, \quad \tilde{Q}_S = (\bar{b}_i s_j)_{S-P} (\bar{b}_j s_i)_{S-P}, \quad (4.17)$$

always working to leading order in $1/m_b$. Note that $\langle \dots \rangle$ denote matrix elements of the above operators taken between B_s and \bar{B}_s states. The Wilson coefficients F and F_S can be extracted by computing the matrix elements between quark states of \mathcal{T} in Eq. (4.7).

The coefficients in the transition operator (4.14) at next-to-leading order, still neglecting the penguin sector, can be written as [56]:

$$F(z) = F_{11}(z)C_2^2(\mu_1) + F_{12}(z)C_1(\mu_1)C_2(\mu_1) + F_{22}(z)C_1^2(\mu_1), \quad (4.18)$$

$$F_{ij}(z) = F_{ij}^{(0)}(z) + \frac{\alpha_s(\mu_1)}{4\pi} F_{ij}^{(1)}(z), \quad (4.19)$$

¹It was recently argued that better-converging results can be obtained in a modified basis [58].

and similarly for $F_S(z)$. The leading order functions $F_{ij}^{(0)}$, $F_{S,ij}^{(0)}$ read explicitly

$$F_{11}^{(0)}(z) = 3\sqrt{1-4z}(1-z), \quad F_{S,11}^{(0)}(z) = 3\sqrt{1-4z}(1+2z), \quad (4.20)$$

$$F_{12}^{(0)}(z) = 2\sqrt{1-4z}(1-z), \quad F_{S,12}^{(0)}(z) = 2\sqrt{1-4z}(1+2z), \quad (4.21)$$

$$F_{22}^{(0)}(z) = \frac{1}{2}(1-4z)^{3/2}, \quad F_{S,22}^{(0)}(z) = -\sqrt{1-4z}(1+2z). \quad (4.22)$$

The next-to-leading order (NLO) expressions $F_{ij}^{(1)}$, $F_{S,ij}^{(1)}$ are given in Ref. [56].

The penguin correction to Eq. (4.14),

$$\mathcal{T}_p = -\frac{G_F^2 m_b^2}{12\pi} (V_{cb}^* V_{cs})^2 [P(z)Q + P_S(z)Q_S], \quad (4.23)$$

is also shown in Ref. [56].

4.3 Subleading $1/m_b^n$ corrections

Here we present the higher order corrections to $\Gamma_{21}(B_s)$ in Eq. (4.15) in the heavy-quark expansion, denoted below as $\delta_{1/m}$ and δ_{1/m^2} :

$$\begin{aligned} \Gamma_{21}(B_s) &= -\frac{G_F^2 m_b^2}{12\pi(2M_{B_s})} (V_{cb}^* V_{cs})^2 \times \\ &\times \{ [F(z) + P(z)] \langle Q \rangle + [F_S(z) + P_S(z)] \langle Q_S \rangle + \delta_{1/m} + \delta_{1/m^2} \}. \end{aligned} \quad (4.24)$$

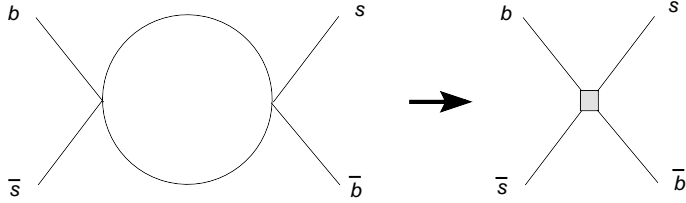


Figure 4.1: Calculation of kinetic $1/m_b$ and $1/m_b^2$ corrections. The operators of Eqs. (4.26) and (4.30) are obtained by expanding the diagrams in powers of light quark momentum.

The matrix elements for Q and Q_S are known to be [55, 56, 57]

$$\begin{aligned}
 \langle Q \rangle &\equiv \langle \bar{B}_s | Q | B_s \rangle = f_{B_s}^2 M_{B_s}^2 2 \left(1 + \frac{1}{N_c} \right) B, \\
 \langle Q_S \rangle &\equiv \langle \bar{B}_s | Q_S | B_s \rangle = -f_{B_s}^2 M_{B_s}^2 \frac{M_{B_s}^2}{(m_b + m_s)^2} \left(2 - \frac{1}{N_c} \right) B_S, \\
 \delta_{1/m} &= \langle \bar{B}_s | \mathcal{T}_{1/m} | B_s \rangle, \quad \text{and} \quad \delta_{1/m^2} = \langle \bar{B}_s | \mathcal{T}_{1/m^2} | B_s \rangle,
 \end{aligned} \tag{4.25}$$

where M_{B_s} and f_{B_s} are the mass and decay constant of the B_s meson and N_c is the number of colors. The parameters B and B_S are defined such that $B = B_S = 1$ corresponds to the factorization (or ‘vacuum insertion’) approach, which can provide a first estimate.

4.3.1 $1/m_b$ corrections

The $1/m_b$ corrections are computed, as in Ref. [55, 57, 64, 65], by expanding the forward scattering amplitude of Eq. (4.7) in the light-quark momentum and matching the result onto the operators containing derivative insertions (see Fig. 4.1). The $\delta_{1/m}$ contributions can be

written in the following form:

$$\begin{aligned} \mathcal{T}_{1/m} &= \sqrt{1-4z} \left\{ (1+2z) [C_1^2 (R_2 + 2R_4) - 2(2C_1C_2 + N_cC_2^2) (R_1 + R_2)] \right. \\ &\quad \left. - \frac{12z^2}{1-4z} [(2C_1C_2 + N_cC^2) (R_2 + 2R_3) + 2C_1^2 R_3] \right\}, \end{aligned} \quad (4.26)$$

where the operators R_i are defined as

$$\begin{aligned} R_1 &= \frac{m_s}{m_b} \bar{b}_i \gamma^\mu (1 - \gamma_5) s_i \bar{b}_j \gamma_\mu (1 + \gamma_5) s_j, \\ R_2 &= \frac{1}{m_b^2} \bar{b}_i \overleftarrow{D}_\rho \gamma^\mu (1 - \gamma_5) \overrightarrow{D}^\rho s_i \bar{b}_j \gamma_\mu (1 - \gamma_5) s_j, \\ R_3 &= \frac{1}{m_b^2} \bar{b}_i \overleftarrow{D}_\rho (1 - \gamma_5) \overrightarrow{D}^\rho s_i \bar{b}_j (1 - \gamma_5) s_j, \\ R_4 &= \frac{1}{m_b} \bar{b}_i (1 - \gamma_5) i \overrightarrow{D}_\mu s_i \bar{b}_j \gamma^\mu (1 - \gamma_5) s_j. \end{aligned} \quad (4.27)$$

Their matrix elements read [55, 57]:

$$\begin{aligned} \langle \bar{B}_s | R_1 | B_s \rangle &= \left(2 + \frac{1}{N_c} \right) \frac{m_s}{m_b} f_{B_s}^2 M_{B_s}^2 B_1^s, \\ \langle \bar{B}_s | R_2 | B_s \rangle &= \left(-1 + \frac{1}{N_c} \right) f_{B_s}^2 M_{B_s}^2 \left(\frac{M_{B_s}^2}{m_b^2} - 1 \right) B_2^s, \\ \langle \bar{B}_s | R_3 | B_s \rangle &= \left(1 + \frac{1}{2N_c} \right) f_{B_s}^2 M_{B_s}^2 \left(\frac{M_{B_s}^2}{m_b^2} - 1 \right) B_3^s, \\ \langle \bar{B}_s | R_4 | B_s \rangle &= -f_{B_s}^2 M_{B_s}^2 \left(\frac{M_{B_s}^2}{m_b^2} - 1 \right) B_4^s. \end{aligned} \quad (4.28)$$

Some of those parameters have been computed in lattice QCD [47, 48, 49, 50].² In this paper we use the results of Ref. [47].

The color-rearranged operators \tilde{R}_i that follow from the expressions for R_i by interchang-

²For estimates of these matrix elements based on QCD sum rules, see Ref. [46].

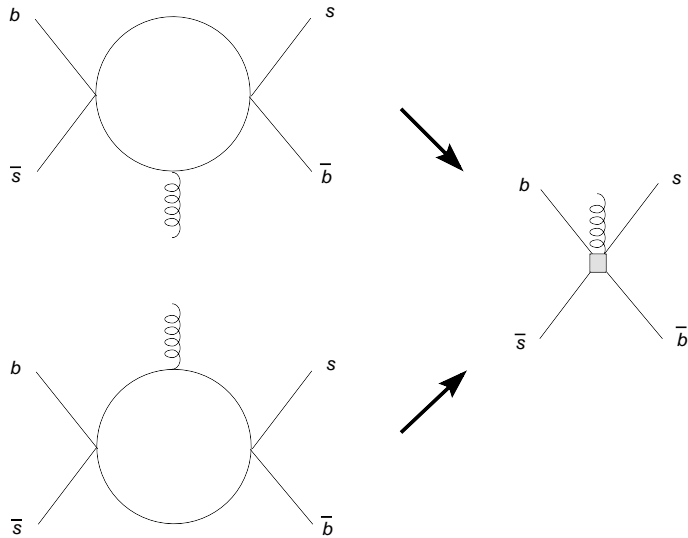


Figure 4.2: $1/m_b^2$ -corrections from gluonic operators.

ing color indexes of b_i and s_j Dirac spinors have been eliminated using Fierz identities and the equations of motion as in Eq. (4.16). Note that the above result contains *full* QCD b -fields, thus there is no immediate power counting available for these operators. The power counting becomes manifest at the level of the matrix elements.

4.3.2 $1/m_b^2$ corrections

It was shown in Refs. [55, 57] that $1/m_b$ -corrections are quite large, so it is important to assess the convergence of $1/m_b$ -expansion in the calculation of the B_s lifetime difference. In order to do so, we compute a set of δ_{1/m_b^2} corrections to leading order. As expected, at this order more operators will contribute. We will parametrize the $1/m_b^2$ corrections similarly to our parametrization of $1/m_b$ effects above and use the factorization approximation to assess their contributions to the B_s lifetime difference.

Two classes of corrections arise at this order. One class involves kinetic corrections which can be computed in a way analogous to the previous case by expanding the forward scattering

amplitudes in the powers of the light-quark momentum. A second class involves corrections arising from the interaction with background gluon fields. The complete set of corrections is the sum of those,

$$\mathcal{T}_{1/m^2} = \mathcal{T}_{1/m^2}^{kin} + \mathcal{T}_{1/m^2}^G. \quad (4.29)$$

Let us consider each class of corrections in turn. The kinetic corrections can be written as

$$\begin{aligned} \mathcal{T}_{1/m^2}^{kin} &= \sqrt{1-4z} \left[\frac{24z^2}{(1-4z)^2} (3-10z) [C_1^2 W_3 + (2C_1 C_2 + N_c C_2^2)(W_3 + W_2/2)] \right. \\ &+ \frac{12z^2}{1-4z} \frac{m_s^2}{m_b^2} [C_1^2 Q_S - (2C_1 C_2 + N_c C_2^2)(Q_S + Q/2)] \\ &+ \frac{24z^2}{1-4z} [2C_1^2 W_4 - 2(2C_1 C_2 + N_c C_2^2)(W_1 + W_2/2)] \\ &\left. - (1-2z) \frac{m_s^2}{m_b^2} (C_1^2 + 2C_1 C_2 + N_c C_2^2) Q_R \right]. \end{aligned} \quad (4.30)$$

We again retain the dependence on quark masses in the above expression, including the terms proportional to m_s . The operators in Eq. (4.30) are defined as

$$\begin{aligned} Q_R &= (\bar{b}_i s_i)_{S+P} (\bar{b}_j s_j)_{S+P}, \\ W_1 &= \frac{m_s}{m_b} \bar{b}_i \overleftarrow{D}^\alpha (1-\gamma_5) \overrightarrow{D}_{\alpha s_i} \bar{b}_j (1+\gamma_5) s_j, \\ W_2 &= \frac{1}{m_b^4} \bar{b}_i \overleftarrow{D}^\alpha \overleftarrow{D}^\beta \gamma^\mu (1-\gamma_5) \overrightarrow{D}_\alpha \overrightarrow{D}_{\beta s_i} \bar{b}_j \gamma_\mu (1-\gamma_5) s_j, \\ W_3 &= \frac{1}{m_b^4} \bar{b}_i \overleftarrow{D}^\alpha \overleftarrow{D}^\beta (1-\gamma_5) \overrightarrow{D}_\alpha \overrightarrow{D}_{\beta s_i} \bar{b}_j (1-\gamma_5) s_j, \\ W_4 &= \frac{1}{m_b^4} \bar{b}_i \overleftarrow{D}^\alpha (1-\gamma_5) i \overrightarrow{D}_\mu \overrightarrow{D}_{\alpha s_i} \bar{b}_j \gamma^\mu (1-\gamma_5) s_j, \end{aligned} \quad (4.31)$$

where, as before, we have eliminated the color-rearranged operators \widetilde{W}_i in favor of the operators W_i . The parametrization of the matrix elements of the above operators is given

below,

$$\begin{aligned}
\langle \bar{B}_s | Q_R | B_s \rangle &= - \left(2 - \frac{1}{N_c} \right) f_{B_s}^2 M_{B_s}^2 \frac{M_{B_s}^2}{(m_b + m_s)^2} \alpha_1, \\
\langle \bar{B}_s | W_1 | B_s \rangle &= \frac{m_s}{m_b} \left(1 + \frac{1}{2N_c} \right) f_{B_s}^2 M_{B_s}^2 \left(\frac{M_{B_s}^2}{m_b^2} - 1 \right) \alpha_2, \\
\langle \bar{B}_s | W_2 | B_s \rangle &= \frac{1}{2} \left(-1 + \frac{1}{N_c} \right) f_{B_s}^2 M_{B_s}^2 \left(\frac{M_{B_s}^2}{m_b^2} - 1 \right)^2 \alpha_3, \\
\langle \bar{B}_s | W_3 | B_s \rangle &= \frac{1}{2} \left(1 + \frac{1}{2N_c} \right) f_{B_s}^2 M_{B_s}^2 \left(\frac{M_{B_s}^2}{m_b^2} - 1 \right)^2 \alpha_4, \\
\langle \bar{B}_s | W_4 | B_s \rangle &= -\frac{1}{2} f_{B_s}^2 M_{B_s}^2 \left(\frac{M_{B_s}^2}{m_b^2} - 1 \right)^2 \alpha_5.
\end{aligned} \tag{4.32}$$

Note that in factorization approximation all the bag parameters α_i should be set to 1. In addition to the set of kinetic corrections considered above, the effects of the interactions of the intermediate quarks with background gluon fields should also be included at this order. The contribution of those operators can be computed from the diagram of Fig. 4.2, resulting in

$$\begin{aligned}
\mathcal{T}_{1/m^2}^G &= - \frac{G_F^2 (V_{cb}^* V_{cs})^2}{4\pi\sqrt{1-4z}} \left\{ C_1^2 [(1-4z)P_1 - (1-4z)P_2 + 4zP_3 - 4zP_4] \right. \\
&\quad \left. + 4 C_1 C_2 z [P_5 + P_6 - P_7 - P_8] \right\}.
\end{aligned} \tag{4.33}$$

The local four-quark operators in the above formulas are shown in Eq. (4.34):

$$\begin{aligned}
P_1 &= \bar{b}_i \gamma^\mu (1 - \gamma_5) s_i \bar{b}_k \gamma^\nu (1 - \gamma_5) t_{kl}^a \tilde{G}_{\mu\nu}^a s_l, \\
P_2 &= \bar{b}_k \gamma^\mu (1 - \gamma_5) t_{kl}^a \tilde{G}_{\mu\nu}^a s_l \bar{b}_i \gamma^\nu (1 - \gamma_5) s_i, \\
P_3 &= \frac{1}{m_b^2} \bar{b}_i \overleftarrow{D}^\mu \overleftarrow{D}^\alpha \gamma^\alpha (1 - \gamma_5) s_i \bar{b}_k \gamma_\nu (1 - \gamma_5) t_{kl}^a \tilde{G}_{\mu\nu}^a s_l, \\
P_4 &= \frac{1}{m_b^2} \bar{b}_k \overleftarrow{D}^\nu \overleftarrow{D}^\alpha \gamma^\mu (1 - \gamma_5) t_{kl}^a \tilde{G}_{\mu\nu}^a s_l \bar{b}_i \gamma_\alpha (1 - \gamma_5) s_i, \\
P_5 &= \frac{1}{m_b^2} \bar{b}_k \overleftarrow{D}^\nu \overleftarrow{D}^\alpha \gamma^\mu (1 - \gamma_5) s_i t_{kl}^a \tilde{G}_{\mu\nu}^a \bar{b}_i \gamma_\alpha (1 - \gamma_5) s_l, \\
P_6 &= \frac{1}{m_b^2} \bar{b}_i \overleftarrow{D}^\nu \overleftarrow{D}^\alpha \gamma^\mu (1 - \gamma_5) s_k t_{kl}^a \tilde{G}_{\mu\nu}^a \bar{b}_l \gamma_\alpha (1 - \gamma_5) s_i, \\
P_7 &= \frac{1}{m_b^2} \bar{b}_k \overleftarrow{D}^\mu \overleftarrow{D}^\alpha \gamma^\alpha (1 - \gamma_5) s_i t_{kl}^a \tilde{G}_{\mu\nu}^a \bar{b}_i \gamma_\nu (1 - \gamma_5) s_l, \\
P_8 &= \frac{1}{m_b^2} \bar{b}_i \overleftarrow{D}^\mu \overleftarrow{D}^\alpha \gamma^\alpha (1 - \gamma_5) s_k t_{kl}^a \tilde{G}_{\mu\nu}^a \bar{b}_l \gamma_\nu (1 - \gamma_5) s_i.
\end{aligned} \tag{4.34}$$

Analogously to the previous section, and following Ref. [65], we parametrize the matrix elements in Eq. (4.34) as

$$\langle \bar{B}_s | P_i | B_s \rangle = \frac{1}{4} f_{B_s}^2 M_{B_s}^2 \left(\frac{M_{B_s}^2}{m_b^2} - 1 \right)^2 \beta_i. \tag{4.35}$$

We set $\beta_i = 1 \text{ GeV}^2$ to obtain a numerical estimate of this effect. It is clear that no precise prediction is possible with so many operators contributing to the lifetime difference. This, of course, is expected, as the number of contributing operators always increases significantly with each order in OPE. We can nonetheless evaluate the contribution of both $1/m_b$ and $1/m_b^2$ by randomly varying the parameters describing the matrix elements by $\pm 30\%$ around their “factorized” values. This way we obtain the interval of predictions of $\Delta\Gamma_s$ and estimate the uncertainty of our result.

4.3.3 Discussion

Now we discuss the phenomenological implications of the results presented in the previous sections. As usual in OPE-based calculations next-order corrections bring new unknown coefficients. In our numerical results we assume the value of the b -quark pole mass to be $m_b = 4.8 \pm 0.2$ GeV and $f_{B_s} = 230 \pm 25$ MeV. It might be advantageous to see what effects higher-order $1/m_b^2$ corrections have on the value of $\Delta\Gamma_s$. In order to see that we fix all perturbative parameters at the middle of their allowed ranges and show the dependence of $\Delta\Gamma_s$ on non-perturbative parameters defined in Eqs. (4.28), (4.32), and (4.35):

$$\begin{aligned}
\Delta\Gamma_s = & \left[0.0005B + 0.1732B_s + 0.0024B_1 - 0.0237B_2 - 0.0024B_3 - 0.0436B_4 \right. \\
& + 2 \times 10^{-5}\alpha_1 + 4 \times 10^{-5}\alpha_2 + 4 \times 10^{-5}\alpha_3 + 0.0009\alpha_4 - 0.0007\alpha_5 \\
& + 0.0002\beta_1 - 0.0002\beta_2 + 6 \times 10^{-5}\beta_3 - 6 \times 10^{-5}\beta_4 - 1 \times 10^{-5}\beta_5 \\
& \left. - 1 \times 10^{-5}\beta_6 + 1 \times 10^{-5}\beta_7 + 1 \times 10^{-5}\beta_8 \right] \quad (\text{ps}^{-1}).
\end{aligned} \tag{4.36}$$

As one can see, $1/m_b^2$ corrections provide rather minor overall impact on the calculation of $\Delta\Gamma_s$. In particular, contributions of gluonic operators are essentially negligible.

To obtain the complete Standard Model estimate of $\Delta\Gamma_s$, we fix the perturbative scale in our calculations to $\mu = m_b$ and vary the values of parameters of the matrix elements. Following the technique used in [65] we adopt the statistical approach for presenting our results and generate 100000-point probability distributions of the lifetime, obtained by randomly varying our parameters within a $\pm 30\%$ interval around their ‘‘factorization’’ values. The decay constant f_{B_s} and the b -quark pole mass m_b are taken to vary within a 1σ interval as indicated above. The results are presented in Fig. 4.3. This figure represents the main result of this paper [66].

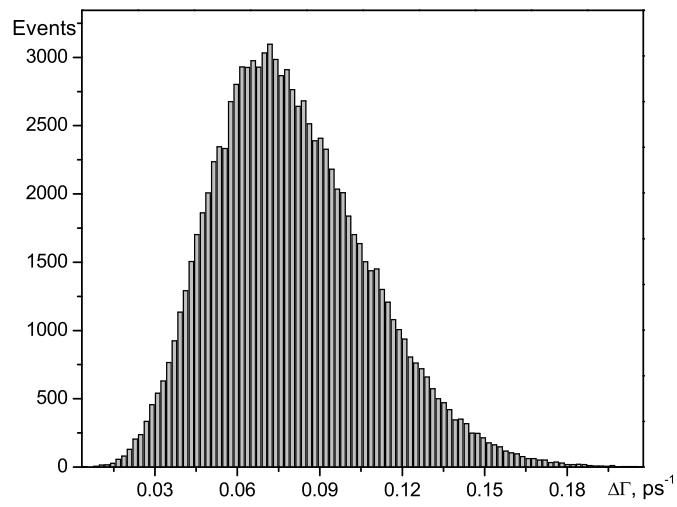


Figure 4.3: Histogram of the distribution of $\Delta\Gamma_s$ values obtained by random variation of parameters of Eqs. (4.24, 4.26, 4.30, 4.33) contributing to B_s -lifetime difference $\Delta\Gamma_s$ following the prescription outline in the text.

There is no theoretically-consistent way to translate the histogram of Figure 4.3 into numerical predictions for $\Delta\Gamma_s$. As a useful estimate we give a numerical prediction by estimating the width of the distribution Fig. 4.3 at the middle of its height and position of the maximum of the curve as the most probable value. We caution that predictions obtained this way should be treated with care, as it is not expected that the theoretical predictions are distributed according to the Gaussian distribution. Nevertheless, following the procedure described above one obtains

$$\Delta\Gamma_s = 0.072^{+0.034}_{-0.030} \text{ ps}^{-1}, \quad \frac{\Delta\Gamma_s}{\Gamma_{B_s}} = 0.104 \pm 0.049, \quad (4.37)$$

where we added the experimental error from the determination of Γ_s and theoretical error from our calculation of $\Delta\Gamma_s$ in quadrature.

4.4 New Physics contributions to lifetime difference

In the previous section we have shown that $1/m_b^2$ -corrections to the lifetime difference of the light and heavy eigenstates in the B_s system are quite small, which makes the prediction of $\Delta\Gamma_s$ quite reliable ³. Additionally improving the accuracy of the lattice or QCD sum rule determinations of non-perturbative “bag parameters” in Eq. (4.36) would make this prediction even more solid.

In this respect, it might be interesting to consider the effects of New Physics on the lifetime difference in B_s system. Why would it be worthwhile to perform this exercise, especially since it is known that $\Delta\Gamma_s$ is dominated by the on-shell, real intermediate states? Wouldn't $\Delta B = 1$ New Physics amplitudes that can potentially affect $\Delta\Gamma_s$ already show up

³As was argued in Ref. [58], perturbative scale dependence can be further reduced by switching to a different basis of leading-order operators.

in the experimental studies of exclusive B_s decays? This is indeed so. However, it might be difficult to separate New Physics effects from the dominant (but somewhat uncertain) Standard Model contributions, as theoretical control over soft QCD effects is harder to achieve in the calculations of exclusive decays despite recent significant advances in this area [67].

It was recently pointed out that NP contributions can dominate lifetime difference in $D^0 - \bar{D}^0$ system in the flavor $SU(3)$ limit [68]. In that system this effect can be traced to the fact that the SM contribution vanishes in that limit. While similar effect does not occur in B_s mixing, good theoretical control over non-perturbative uncertainties in the calculation of $\Delta\Gamma_s$ makes calculations of NP contributions worthwhile. In B_s -system one can show that

$$\begin{aligned}\Delta M_s &= 2|M_{12}|, \\ \Delta\Gamma_s &= \frac{4\text{Re}(M_{12}\Gamma_{12}^*)}{\Delta M_s}.\end{aligned}\tag{4.38}$$

In the Standard Model the phase difference between the mixing amplitude and the dominant decay amplitudes is $\arg(-V_{cb}^*V_{cs}/V_{tb}^*V_{ts})$, *i.e.* essentially zero. If NP contribution has a CP-violating phase that exceeds that of the Standard Model, one can write, denoting $2\xi = \arg(M_{12}\Gamma_{12}^*)$,

$$\Delta\Gamma_s = 2|\Gamma_{12}|\cos 2\xi.\tag{4.39}$$

Since in the Standard Model Γ_{12} is dominated by the $b \rightarrow c\bar{c}s$ transition, its phase is negligible. Then, as was pointed out in [61, 62], CP-violating contributions to M_{12} must *reduce* the lifetime difference in B_s -system,

$$\Delta\Gamma_s = \Delta\Gamma_s^{SM}\cos 2\xi,\tag{4.40}$$

where 2ξ is a CP-violating phase of M_{12} , which is assumed to be dominated by some $\Delta B = 2$ New Physics.

Contrary to CP-violating $\Delta B = 2$ NP contributions to M_{12} , any $\Delta B = 1$ NP amplitudes can interfere with the Standard Model ones both constructively and destructively, depending on the model. Since no spectacular NP phases have been observed in B_s mixing, it appears that M_{12} is dominated by the Standard Model CP-conserving contribution. In that case, the phase $\arg(M_{12}\Gamma_{12}^*) = \arg(\Gamma_{12}^*) = 2\xi'$ is dominated by the phase of New Physics contribution to Γ_{12}^* . In that case

$$\Delta\Gamma_s = \Delta\Gamma_s^{SM} + \Delta\Gamma_s^{NP} \cos 2\xi', \quad (4.41)$$

where $\Delta\Gamma_s^{NP}$ is a contribution resulting from the interference of the SM and NP $\Delta B = 1$ operators, which can either enhance or suppress $\Delta\Gamma_s$ compared to the Standard Model contribution. We shall compute $\Delta\Gamma_s^{NP}$ by first employing the generic set of effective operators, and then specifying to particular extensions of the SM. We shall concentrate on CP-conserving contributions.

Using the completeness relation the NP contribution to the $B_s^0\text{-}\bar{B}_s^0$ lifetime difference becomes

$$\left. \frac{\Delta\Gamma_s}{\Gamma_{B_s}} \right|_{NP} = \frac{1}{M_{B_s}\Gamma_{B_s}} \langle \bar{B}_s | \text{Im } \mathcal{T} | B_s \rangle, \quad (4.42)$$

where $\mathcal{T} = i \int d^4x T(\mathcal{H}_{SM}^{\Delta B=1}(x) \mathcal{H}_{NP}^{\Delta B=1}(0))$.

We represent the generic NP $\Delta B = 1$ Hamiltonian $\mathcal{H}_{NP}^{\Delta B=1}$ as

$$\mathcal{H}_{NP}^{\Delta B=1} = \sum_{q,q'} D_{qq'} [\bar{\mathcal{C}}_1(\mu)Q_1 + \bar{\mathcal{C}}_2(\mu)Q_2], \quad (4.43)$$

$$Q_1 = \bar{b}_i \bar{\Gamma}_1 q'_i \bar{q}_j \Gamma_2 s_j, \quad Q_2 = \bar{b}_i \bar{\Gamma}_1 q'_j \bar{q}_j \Gamma_2 s_i,$$

where the spin matrices $\bar{\Gamma}_{1,2}$ can have an arbitrary Dirac structure, $D_{qq'}$ are some New Physics-generated coefficient functions [68], and $\bar{\mathcal{C}}_{1,2}(\mu)$ are Wilson coefficients evaluated at the energy scale μ . This gives us the following contribution to the lifetime difference:

$$\Delta\Gamma_s^{NP} = -\frac{8G_F\sqrt{2}}{M_{B_s}} \sum_{qq'} D_{qq'} V_{qb}^* V_{q's} (K_1 \delta_{ij} \delta_{kl} + K_2 \delta_{kj} \delta_{il}) \sum_{m=1}^5 I_j(x, x') \langle \bar{B}_s | O_m^{ijkl} | B_s \rangle. \quad (4.44)$$

Here i, j, k, l are the color indices, and $\{K_\alpha\}$ are combinations of Wilson coefficients with the number of colors $N_c = 3$,

$$K_1 = (\mathcal{C}_2 \bar{\mathcal{C}}_2 N_c + (\mathcal{C}_2 \bar{\mathcal{C}}_1 + \bar{\mathcal{C}}_2 \mathcal{C}_1)), \quad K_2 = \mathcal{C}_1 \bar{\mathcal{C}}_1 \quad (4.45)$$

/ The operators O_m^{ijkl} are the following:

$$\begin{aligned} O_1^{ijkl} &= (\bar{b}_i \Gamma^\nu \gamma^\rho \Gamma_2 s_l) (\bar{b}_k \Gamma_1 \gamma_\rho \Gamma_\nu s_j) \\ O_2^{ijkl} &= (\bar{b}_i \Gamma^\nu \not{p} \Gamma_2 s_l) (\bar{b}_k \Gamma_1 \not{p} \Gamma_\nu s_j) \\ O_3^{ijkl} &= (\bar{b}_i \Gamma^\nu \Gamma_2 s_l) (\bar{b}_k \Gamma_1 \not{p} \Gamma_\nu s_j), \\ O_4^{ijkl} &= (\bar{b}_i \Gamma^\nu \not{p} \Gamma_2 s_l) (\bar{b}_k \Gamma_1 \Gamma_\nu s_j) \\ O_5^{ijkl} &= (\bar{b}_i \Gamma^\nu \Gamma_2 s_l) (\bar{b}_k \Gamma_1 \Gamma_\nu s_j), \end{aligned} \quad (4.46)$$

where \not{p} is the b -quark momentum operator. Defining $z_q \equiv m_q^2/m_b^2$ and $z_{q'} \equiv m_{q'}^2/m_b^2$ the

coefficients $I_j(z_q, z_{q'})$ can be written as follows:

$$\begin{aligned}
I_1(z_q, z_{q'}) &= -\frac{k^* m_b}{48\pi} [1 - 2(z_q + z_{q'}) + (z_q - z_{q'})^2], \\
I_2(z_q, z_{q'}) &= -\frac{k^*}{24m_b\pi} [1 + (z_q + z_{q'}) - 2(z_q - z_{q'})^2], \\
I_3(z_q, z_{q'}) &= \frac{k^*}{8\pi} \sqrt{z_q} [1 + z_{q'} - z_q], \\
I_4(z_q, z_{q'}) &= -\frac{k^*}{8\pi} \sqrt{z_{q'}} [1 - z_{q'} + z_q], \\
I_5(z_q, z_{q'}) &= \frac{k^* m_b}{4\pi} \sqrt{z_q z_{q'}},
\end{aligned} \tag{4.47}$$

where $k^* = (m_b/2) [1 - 2(z_q + z_{q'}) + (z_q - z_{q'})^2]^{1/2}$. This is the most general formula for the New Physics contribution to the lifetime difference in B_s mesons. We now look into two particular examples extensions of the Standard Model, multi-doublet Higgs models and Left-Right Symmetric Models, that can contribute to $\Delta\Gamma_s$.

4.4.1 Multi-Higgs model

One of possible realizations of New Physics is a multi-Higgs doublet model [69]. Many of SM extensions, particularly the supersymmetric ones, require extended Higgs sector in order to break additional symmetries of NP down to $SU(2)_L \times U(1)$ of the Standard Model. These constructions contain charged Higgs bosons as parts of the extended Higgs sector. These models provide new flavor-changing interactions mediated by charged Higgs bosons, which lead to rich low-energy phenomenology [70, 71]. In the low-energy limit, charged Higgs exchange leads to the following four-fermion interaction [72],

$$\mathcal{H}_{ChH}^{\Delta B=1} = -\frac{\sqrt{2}G_F}{M_H^2} \bar{b}_i \bar{\Gamma}_1 q'_i \bar{q}_j \bar{\Gamma}_2 s_j, \tag{4.48}$$

where $\bar{\Gamma}_i$, $i = 1, 2$, are

$$\begin{aligned}\bar{\Gamma}_1 &= m_b V_{cb}^* \cot \beta P_L - m_c V_{cb}^* \tan \beta P_R, \\ \bar{\Gamma}_2 &= m_s V_{cs} \cot \beta P_R - m_c V_{cs} \tan \beta P_L,\end{aligned}\tag{4.49}$$

and $P_{L,R} = (1 \mp \gamma_2)/2$. Inserting Eq.(4.48) into Eq. (4.44) leads to a contribution to the lifetime difference $(\Delta\Gamma_s/\Gamma_s)_{ChH}$ from three operators with various coefficients,

$$\begin{aligned}\frac{\Delta\Gamma_s}{\Gamma_{B_s}} \Big|_{ChH} &= \frac{16G_F^2 m_b^2 (V_{cb}^* V_{cs})^2}{M_B \Gamma_{B_s} M_H^2} \times \\ &\times [\langle Q_1 \rangle (4K_2 \sqrt{z_s} I_1 \cot^2 \beta + 2(\cot^2 \beta m_b^2 \sqrt{z_s} I_2 - m_b \sqrt{z_c} I_4)(K_2 - K_1)) \\ &+ \langle Q_2 \rangle (-2K_1 \sqrt{z_s} I_1 \cot^2 \beta + (\cot^2 \beta m_b^2 \sqrt{z_s} I_2 - m_b \sqrt{z_c} I_4)(K_2 - K_1)) \\ &+ \langle Q_3 \rangle (K_1 + K_2) (z_c \tan^2 \beta I_5 - m_b \sqrt{z_c} I_3)].\end{aligned}\tag{4.50}$$

Coefficients $I_i \equiv I_i(z_c, z_s)$, K_i are defined above, and $\langle Q_i \rangle$ are

$$\begin{aligned}Q_1 &= (\bar{b}_{iL} s_{iR}) (\bar{b}_{kR} s_{kL}), & \langle Q_1 \rangle &= -\frac{1}{4} f_B^2 M_B^2 \frac{M_B^2}{(m_b + m_s)^2} \left(2 + \frac{1}{N_c} \right) \\ Q_2 &= (\bar{b}_{iR} \gamma^\nu s_{iR}) (\bar{b}_{kL} \gamma_\nu s_{kL}), & \langle Q_2 \rangle &= -\frac{1}{2} f_B^2 M_B^2 \left(1 + \frac{2}{N_c} \right), \\ Q_3 &= (\bar{b}_{iL} \gamma^\nu s_{iL}) (\bar{b}_{kL} \gamma_\nu s_{kL}), & \langle Q_3 \rangle &= \frac{1}{2} f_B^2 M_B^2 \left(1 + \frac{1}{N_c} \right).\end{aligned}\tag{4.51}$$

For values of $M_H = 85 \text{ GeV}$ and $\cot \beta = 0.05$ [1] we obtain $(\Delta\Gamma_s/\Gamma_s)_{ChH} \approx 0.006$. This is about 6% of the Standard Model value, too small to constrain the model from this observable.

The dependence of $(\Delta\Gamma_s/\Gamma_s)_{ChH}$ on the mass of the Higgs boson is shown in Fig. 4.4.

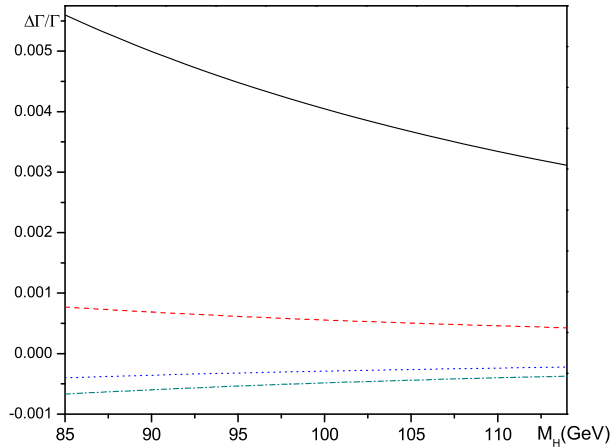


Figure 4.4: Dependence of y_{ChH} on the mass of the Higgs boson. Solid line: $\tan \beta = 20$; dashed line: $\tan \beta = 10$; dotted line: $\tan \beta = 5$; dash-dotted line: $\tan \beta = 3$.

4.4.2 Left-Right Symmetric Models

One of the puzzling features of the Standard Model is the left-handed structure of the electroweak interactions. A possible extension of the SM, a Left-Right Symmetric Model (LRSM) assumes the extended $SU(2)_L \times SU(2)_R$ symmetry of the theory, which restores parity at high energies [73]. While in the simplest realizations of LRSM the right-handed symmetry is broken at a very high scale, models can be consistently modified to yield W_R -bosons whose masses are not far above 1 TeV range [74]. In this case flavor-changing interaction from W_R -bosons can affect $\Delta\Gamma_s$ (for a similar effect in D -mixing, see [68]).

In principle, manifest left-right symmetry requires that couplings to left-handed particles be the same as the ones to the right-handed particles, *e.g.* $g_L = g_R$. This also assumes that the right-handed CKM matrix $V_{ik}^{(R)}$ should be the same as the left-handed CKM matrix V_{ik} . In this case, kaon mixing constraints exclude $M_{W_R} < 1.6$ TeV [75] (direct constraints are

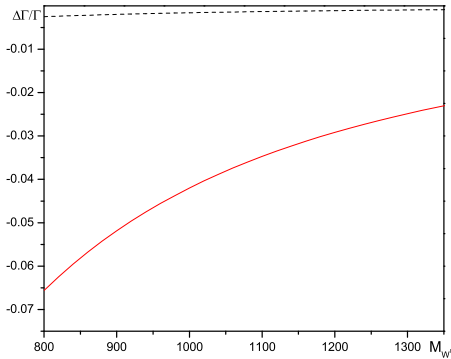
weaker by approximately a factor of two). However, $V_{ik}^{(R)}$ could also be quite different from the V_{ik} , as long as it is still unitary. In this case of non-manifest left-right symmetry the bounds on M_{W_R} are significantly weaker, $M_{W_R} > 0.3$ TeV from kaon mixing [76]. To assess the contribution from W_R to $\Delta\Gamma_s$, we equate

$$D_{qq'} = V_{cb}^{*(R)} V_{cs}^{(R)} \frac{G_F^{(R)}}{\sqrt{2}}, \quad \bar{\Gamma}_{1,2} = \gamma^\mu P_R \quad (4.52)$$

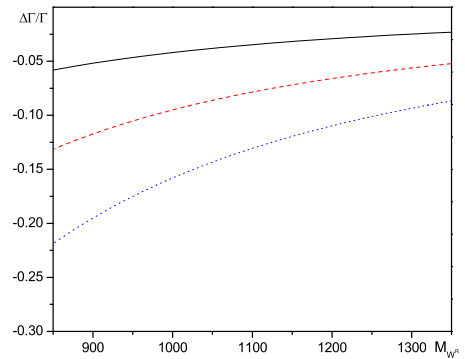
in Eq. (4.44) and evaluate the respective operators. Here $G_F^{(R)}/\sqrt{2} = g_R^2/8M_W^{(R)2}$, and we assume $g_R = \kappa g_L$. In the studies of non-manifest LRSM, we shall also assume $\kappa = 1, 1.5, 2$ [77]. At the end, LRSM gives the following contribution to the value of $\Delta\Gamma_s/\Gamma_{B_s}$:

$$\left. \frac{\Delta\Gamma_s}{\Gamma_{B_s}} \right|_{LR} = -V_{cb}^* V_{cs} V_{cb}^{*(R)} V_{cs}^{(R)} \frac{2\kappa^2 G_F^2 m_b^2 z_c \sqrt{1-4z_c}}{\pi M_B \Gamma_{B_s}} \left(\frac{M_W}{M_W^{(R)}} \right)^2 [C_1 \langle Q_2 \rangle - 2C_2 \langle Q_1 \rangle]. \quad (4.53)$$

The dependence of $(\Delta\Gamma_s/\Gamma_{B_s})_{LR}$ on the mass of the W_R boson is given in Fig. 4.5. We see that contrary to the D -meson case [68, 78], B_s -mixing could provide decent constraints on the values of $M_W^{(R)}$. For instance, in a non-manifest LRSM (with relevant $V_{ij}^{(R)} \approx 1$), $\kappa = 1$, and $M_W^{(R)} = 1$ TeV, one obtains $(\Delta\Gamma_s/\Gamma_{B_s})_{LR} \simeq -0.04$. This is a rather large contribution to $\Delta\Gamma_s$, more than a third of the absolute value of the Standard Model contribution and of the opposite sign. The LRSM contributions for $\kappa > 1$ are even larger. As expected, in the case of manifest LRSM ($V_{ij}^{(R)} = V_{ij}$) the contribution from this model is less marked, $(\Delta\Gamma_s/\Gamma_{B_s})_{LR} < 0.002$ for $M_W^{(R)} > 800$ GeV.



(a) Dependence of $\Delta\Gamma_s/\Gamma_s$ on $M_W^{(R)}$. Solid line: non-manifest LRSM ($\kappa = 1$), dashed line: manifest LRSM.



(b) Dependence of $\Delta\Gamma_s/\Gamma_s$ on $M_W^{(R)}$ in non-manifest LRSM. Solid line: $\kappa = 1$, dashed line: $\kappa = 1.5$, dotted line: $\kappa = 2$.

Figure 4.5: Contributions to $\Delta\Gamma_s/\Gamma_s$ in the Left-Right Symmetric Models.

4.5 Conclusions

We computed the subleading $1/m_b^2$ corrections to the difference in the lifetimes of B_s meson eigenstate. We showed that they can be parameterized by 13 nonperturbative parameters, which we denote α_i and β_i . We adopted the statistical approach for presenting our results and generate 100000-point probability distributions of the lifetime difference, obtained by randomly varying our parameters within a $\pm 30\%$ interval around their “factorization” values, except for the case when the parameters are known from lattice QCD. In this case they are taken to vary within a 1σ interval as indicated above.

The results are presented in Fig. (4.3). While there is no theoretically-consistent way to translate the histogram of Fig. 4.3 into numerical predictions for $\Delta\Gamma_s/\Gamma_s$, we provide an estimate by taking the width of the distribution Fig. 4.3 at the middle of its height as $1\text{-}\sigma$

variance and position of the maximum of the curve as the most probable value,

$$\Delta\Gamma_s = 0.072^{+0.034}_{-0.030} \text{ ps}^{-1}, \quad \frac{\Delta\Gamma_s}{\Gamma_{B_s}} = 0.104 \pm 0.049, \quad (4.54)$$

The effects of $1/m_b^2$ corrections to calculations of $\Delta\Gamma_s$ are shown to be small.

We also investigated $\Delta B = 1$ New Physics contributions to the width difference in the B_s system. We have shown that these contributions can both enhance or reduce the Standard Model contribution. We considered the most general four-fermion effective Hamiltonian, which can be generated by any reasonable extension of the Standard Model and derived its contribution to $\Delta\Gamma_s$. We then evaluated effects of charged Higgses and right-handed W's on the lifetime difference. While the contribution of charged Higgs was shown to be negligible in $\Delta\Gamma_s$, LRSM can be constrained with measurement of $\Delta\Gamma_s$, provided lattice or QCD sum rule community provide better estimates of non-perturbative parameters entering the SM calculation of the width difference in B_s mesons.

Mixing in the heavy meson-antimeson systems is an extremely useful way to probe the physics Beyond the Standard Model. However, it allows to probe only heavy New Physics degrees of freedom. The light New Physics (for example certain models of the Dark Matter) can be tested in the decays of the Standard Model particles. In the next chapter we consider production of the light Dark Matter in the missing energy decays of the B_s , B_d and D^0 mesons.

Chapter 5

Dark Matter production in heavy meson decays

5.1 Introduction

The presence of cold Dark Matter (DM) in our universe provides the most natural explanation for several observational puzzles, from the original measurement of the rotational curves [24] of galaxies to the observation of background objects in the Bullet Cluster [79] and spectrum features of the cosmic microwave background (CMB) fluctuations. In the conventional picture, DM accounts for the majority of mass in our Universe. However, the nature of DM is still very much a mystery, which could intimately connect astronomical observations with predictions of various elementary particle theories. Many such theories, with the notable exception of the Standard Model (SM), predict one or more stable, electrically-neutral particles in their spectrum [80]. These particles could form all or part of the non-baryonic Dark Matter in the Universe.

Different models provide different assignments for DM particles' spin and various windows for their masses and couplings to luminous matter. In the most popular models DM is a weakly interacting particle with mass set around the electroweak energy scale. This follows from the experimental measurements of the relic abundance $\Omega_{DM}h^2 \sim 0.12$ by

WMAP collaboration [81]

$$\Omega_{DM}h^2 \sim \langle \sigma_{ann}v_{rel} \rangle^{-1} \propto \frac{M^2}{g^4} \sim 0.12, \quad (5.1)$$

where M and g are the mass and the interaction strength associated with DM annihilation respectively. As one can see, a weakly-interacting massive particle (WIMP) with electroweak-scale mass naturally gives the result of Eq. (5.1). This, coupled with an observation that very light DM particles might overclose the Universe (known as the Lee-Weinberg limit [36]), seems to exclude the possibility of the light-mass solution for DM, setting $M_{DM} > 2 - 6$ GeV.

A detailed look at this argument reveals that those constraints could be easily avoided, so even MeV-scale particles can be good DM candidates. For instance, DM could be non-fermionic [82, 83], in which case the usual suppression of the DM annihilation cross-section used in setting the Lee-Weinberg limit does not hold. In addition, low energy resonances could enhance the cross-section without the need for a large coupling constant. Other solutions, which also provide low-mass candidates for DM particles, are also possible [84, 85].

There are many experiments designed to search for both direct interactions of DM with the detector and indirect evidence of DM annihilations in our galaxy or other galaxies by looking for the products such as gamma-rays, positrons and antiprotons. Those can in principle probe low-mass DM. However, direct searches, performed by experiments such as DAMA and CDMS [6], rely on the measurement of the kinematic recoil of the nuclei in DM interactions. For cold DM particles, such measurements lose sensitivity with the decreasing mass of the WIMP as recoil energy becomes smaller [86]. Indirect experiments, such as HESS [87], are specifically tuned to see large energy secondaries, only possible for weak-scale WIMPs. The backgrounds for positron and antiproton searches by HEAT and PAMELA experiments [31] could be prohibitively large at small energies.

It is well-known that the existing e^+e^- flavor factories and future super-flavor factories could provide the perfect opportunity to search for rare processes, especially the ones that require high purity of the final states. In particular, probes of rare B-decays, such as $B \rightarrow K^{(*)}\nu\bar{\nu}$, are only possible at those machines. These colliders, where $B_q(D)$ and $\bar{B}_q(\bar{D})$ are produced in charge and CP-correlated states, have an opportunity to tag the decaying heavy meson “on the other side,” which provides the charge or CP-identification of the decaying “signal” B or D meson. In fact, many CP-violating parameters have been measured at B-factories using this method [88]. It is then possible to perform a similar tag on the meson decaying to a pair of light DM particles or a pair of DM particles and a photon. The latter process might become important for some DM models as it eliminates helicity suppression of the final state¹. Moreover, compared to $B \rightarrow K + \cancel{E}$ transitions, where \cancel{E} is missing energy, a massless photon could provide better experimental opportunities for tagging without reducing the probed parameter space of the DM masses. Finally, searches for light DM in heavy meson decays could be more sensitive than direct detection and other experiments, as DM couplings to heavy quarks could be enhanced, as for example happens in Higgs portal models [89].

We compute branching ratios for the heavy meson states decaying into $\chi_s\bar{\chi}_s$ and $\chi_s\bar{\chi}_s\gamma$. Here χ_s is a DM particle of spin s , which appears as missing energy in a detector. The DM *anti-particle* $\bar{\chi}_s$ may or may not coincide with χ_s . We shall first consider model-independent interactions of DM particles of spin-0, spin-1/2, and spin-1 with quarks. In each case we write the most general effective Hamiltonian coupling DM particles to flavor-changing $b \rightarrow q$ (where $q = s(d)$) or $c \rightarrow u$ current and compute $B(D) \rightarrow \chi_s\bar{\chi}_s(\gamma)$ decay rates. We then consider popular models, already available in the literature, that can generate those processes.

¹This is similar to the situation in leptonic decays of B -mesons, where the branching ratios $\mathcal{B}(B \rightarrow \mu\nu\gamma) \approx \mathcal{B}(B \rightarrow \mu\nu)$ and $\mathcal{B}(B \rightarrow e\nu\gamma) \gg \mathcal{B}(B \rightarrow e\nu)$.

5.2 Formalism and the Standard Model background

The computation of decay rates for two-body processes $B_q(D) \rightarrow \chi_s \bar{\chi}_s$ is a straightforward task which only requires the knowledge of appropriate $B \rightarrow$ vacuum matrix elements. We use conventional parameterization for those,

$$\begin{aligned} \langle 0 | \bar{b} \gamma^\mu q | B_q \rangle &= 0, & \langle 0 | \bar{b} q | B_q \rangle &= 0, \\ \langle 0 | \bar{b} \gamma^\mu \gamma_5 q | B_q \rangle &= i f_{B_q} P^\mu, & \langle 0 | \bar{b} \gamma_5 q | B_q \rangle &= -i \frac{f_{B_q} M_{B_q}^2}{m_b + m_q}, \end{aligned} \quad (5.2)$$

where P^μ is the 4-momentum of heavy meson B_q . Similar formulas can be obtained for D -meson. In what follows we shall provide relevant derivations for B_q mesons only, but report results for both B_q and D^0 -meson decays.

Before computing the relevant DM production rates, let us study the Standard Model background for the decays with missing energy realized in transitions to $\nu \bar{\nu}$ states. The Standard Model effective Hamiltonian for $B_q(D) \rightarrow \nu \bar{\nu}(\gamma)$ reads

$$\mathcal{H}_{eff} = \frac{4G_F}{\sqrt{2}} \frac{\alpha}{2\pi \sin^2 \theta_W} \sum_{l=e,\mu,\tau} \sum_k \lambda_k X^l(x_k) (J_{Qq}^\mu) (\bar{\nu}_L^l \gamma_\mu \nu_L^l), \quad (5.3)$$

where $J_{Qq}^\mu = \bar{q}_L \gamma^\mu b_L$ for beauty, and $J_{Qq}^\mu = \bar{u}_L \gamma^\mu c_L$ for charm transitions, and we consider Dirac neutrinos. The functions $\lambda_k X^l(x_k)$ are relevant combinations of the Cabbibo-Kobayashi-Maskawa (CKM) factors and Inami-Lim functions. For $b \rightarrow q$ transitions these functions are overwhelmingly dominated by the top-quark contribution,

$$\sum_k \lambda_k X^l(x_k) = V_{tq}^* V_{tb} X(x_t), \quad \text{with } X(x_t) = \frac{x_t}{8} \left[\frac{x_t + 2}{x_t - 1} + \frac{3(x_t - 2)}{(x_t - 1)^2} \ln x_t \right] \quad (5.4)$$

and $x_t = m_t^2/M_W^2$. Perturbative QCD corrections can be taken into account by the replace-

ment [90]

$$X_0(x_t) \rightarrow \left[X_0(x_t) + \frac{\alpha_s}{4\pi} X_1(x_t) \right] \left[1 - \frac{\alpha_s}{3\pi} \left(\pi^2 - \frac{25}{4} \right) \right], \quad (5.5)$$

where $X_1(x_t)$ can be found in Ref. [90]. Such a corrections change our estimate by at most 10%, and therefore are neglected in our analysis. For $c \rightarrow u$ transitions we keep the contributions from both internal b and s -quarks, so

$$\sum_k \lambda_k X^l(x_k) = V_{cs}^* V_{us} X^l(x_s) + V_{cb}^* V_{ub} X^l(x_b), \text{ with } X^l(x_q) = \overline{D}(x_q, y_l)/2 \quad (5.6)$$

where $\overline{D}(x_q, y_l)$ is the Inami-Lim function [91] for $y_l = m_l^2/m_W^2$,

$$\begin{aligned} \overline{D}(x_q, y_l) &= \frac{1}{8} \frac{x_q y_l}{x_q - y_l} \left(\frac{y_l - 4}{y_l - 1} \right)^2 \log y_l \\ &+ \frac{1}{8} \left[\frac{x_q}{y_l - x_q} \left(\frac{x_q - 4}{x_q - 1} \right)^2 + 1 + \frac{3}{(x_q - 1)^2} \right] x_q \ln x_q \\ &+ \frac{x_q}{4} - \frac{3}{8} \left(1 + 3 \frac{1}{y_l - 1} \right) \frac{x_q}{x_q - 1} \end{aligned} \quad (5.7)$$

Given this, one can easily estimate branching ratios for $B_q(D) \rightarrow \nu \bar{\nu}$ decays. One can immediately notice that the left-handed structure of the Hamiltonian should result in helicity suppression of those transitions. Assuming for neutrino masses that $m_\nu \sim \sum_i m_{\nu_i} < 0.62$ eV [94], where m_{ν_i} is the mass of one of the neutrinos, we obtain for the branching ratio

$$\mathcal{B}(B_s \rightarrow \nu \bar{\nu}) = \frac{G_F^2 \alpha^2 f_B^2 M_B^3}{16\pi^3 \sin^4 \theta_W \Gamma_{B_s}} |V_{tb} V_{ts}^*|^2 X(x_t)^2 x_\nu^2 \simeq 3.07 \times 10^{-24} \quad (5.8)$$

where $x_\nu = m_\nu/M_{B_q}$ and $\Gamma_{B_s} = \Gamma_{B_d} = 1/\tau_B$ is the total width of the B_s meson. With $\tau_B = 1.548$ ps we obtain $\mathcal{B}(B_d \rightarrow \nu \bar{\nu}) = 1.24 \times 10^{-25}$. A similar calculation yields $\mathcal{B}(D^0 \rightarrow \nu \bar{\nu}) = 1.1 \times 10^{-30}$. Clearly such tiny rates imply that decays of heavy mesons into

neutrino-antineutrino final states in the Standard Model can be safely neglected as sources of background in the searches for DM in $B_q(D)$ -decays. This is one of the main differences between this study and studies of DM production in $B \rightarrow K^{(*)} + \cancel{E}$ transitions [82].

Helicity suppression in the final state can be overcome by adding a third particle, such as a photon, to the final state. The calculation of $B(D) \rightarrow \nu\bar{\nu}\gamma$ has been done before [95], so here we simply present an update. The branching ratio for $B(D) \rightarrow \nu\bar{\nu}\gamma$ in principle depends on several form-factors,

$$\begin{aligned}\langle\gamma(k)|\bar{b}\gamma_\mu q|B_q(k+q)\rangle &= e\epsilon_{\mu\nu\rho\sigma}\epsilon^{*\nu}q^\rho k^\sigma\frac{f_V^B(q^2)}{M_{B_q}}, \\ \langle\gamma(k)|\bar{b}\gamma_\mu\gamma_5 q|B_q(k+q)\rangle &= -ie\left[\epsilon_\mu^*(kq) - (\epsilon^*q)k_\mu\right]\frac{f_A^B(q^2)}{M_{B_q}}\end{aligned}\quad (5.9)$$

$$\langle\gamma(k)|\bar{b}\sigma_{\mu\nu}q|B_q(k+q)\rangle = \frac{e}{M_{B_q}^2}\epsilon_{\mu\nu\lambda\sigma}\left[G\epsilon^{*\lambda}k^\sigma + H\epsilon^{*\lambda}q^\sigma + N(\epsilon^*q)q^\lambda k^\sigma\right]\quad (5.10)$$

$$\begin{aligned}G &= 4g_1, & N &= \frac{-4}{q^2}(f_1 + g_1), \\ H &= \frac{-4(qk)}{q^2}(f_1 + g_1), & f_1(g_1) &= \frac{f_0(g_0)}{\left(1 - q^2/\mu_{f(g)}^2\right)^2}\end{aligned}\quad (5.11)$$

where f_0, g_0, μ_f, μ_g are known from QCD light-cone sum rules.

Matrix element $\langle\gamma(k)|\bar{b}\sigma_{\mu\nu}\gamma_5 q|B_q(k+q)\rangle$ can be obtained using identity [93]:

$$\sigma_{\mu\nu} = -\frac{i}{2}\epsilon_{\mu\nu\alpha\beta}\sigma_{\alpha\beta}\gamma_5$$

Similar formulas hold for D -decays. It is important to note that only one out of two form-

factors is independent. Indeed, as it was shown in [100, 101],

$$f_V^B(E_\gamma) = f_A^B(E_\gamma) = \frac{f_{B_q} M_{B_q}}{2E_\gamma} \left(-Q_q R_q + \frac{Q_b}{m_b} \right) + \mathcal{O} \left(\frac{\Lambda_{QCD}^2}{E_\gamma^2} \right) \equiv \frac{f_{B_q} M_{B_q}}{2E_\gamma} F_{B_q}, \quad (5.12)$$

where $R_q^{-1} \sim M_{B_q} - m_b$, and $F_{B_q} = -Q_q R_q + \frac{Q_b}{m_b} \sim \frac{M_{B_q} Q_b - m_b(Q_b + Q_q)}{m_b(M_{B_q} - m_b)}$. $Q_q = Q_b = +1/3$ are the electrical charges of q and b -quarks. Similar form factor can be obtained for the D -meson after a suitable redefinition of quark masses and charges. One-loop QCD corrections to the Eq. (5.12) can also be computed [102].

The amplitude for $B_q(D) \rightarrow \nu \bar{\nu} \gamma$ transition could be written as

$$A(B_q \rightarrow \nu \bar{\nu} \gamma) = \frac{2e C_1^{SM}(x_t)}{M_{B_q}} \bar{\nu}_L \gamma^\mu \nu_L \times \\ \left[\epsilon_{\mu\nu\rho\sigma} \epsilon^{*\nu} q^\rho k^\sigma f_V^B(q^2) + i \left[\epsilon_\mu^*(kq) - (\epsilon^* q) k_\mu \right] f_A^B(q^2) \right], \quad (5.13)$$

where $C_1^{SM}(x_t) = G_F \alpha V_{tb} V_{tq}^* X_0(x_t) / (2\sqrt{2}\pi \sin^2 \theta_W)$ and e is the electric charge. This results in the photon energy spectrum and branching ratio integrated over all photon energies,

$$\frac{d\Gamma}{dE_\gamma}(B_q \rightarrow \nu \bar{\nu} \gamma) = \frac{4f_{B_q}^2 G_F^2 \alpha^3}{3M_{B_q}} |V_{tb} V_{tq}^* X_0(x_t)|^2 \left(\frac{F_{B_q}}{4\pi^2 \sin^2 \theta_W} \right)^2 \\ \times M_{B_q}^2 E_\gamma (M_{B_q} + E_\gamma) \sqrt{\frac{M_{B_q}(1 - 4x^2) - 2E_\gamma}{M_{B_q} - 2E_\gamma}} \quad (5.14)$$

$$\mathcal{B}(B_q \rightarrow \nu \bar{\nu} \gamma) = \frac{2}{\Gamma_{B_q}} f_{B_q}^2 G_F^2 \alpha^3 M_{B_q}^5 |V_{tb} V_{tq}^* X_0(x_t)|^2 \left(\frac{F_{B_q}}{12\pi^2 \sin^2 \theta_W} \right)^2, \quad (5.15)$$

where we set $x_\nu = 0$. Numerically, $\mathcal{B}(B_s \rightarrow \nu \bar{\nu} \gamma) = \Gamma(B_s \rightarrow \nu \bar{\nu} \gamma) / \Gamma_{B_s} = 3.68 \times 10^{-8}$. Similar results for B_d and D^0 mesons are $\mathcal{B}(B_d \rightarrow \nu \bar{\nu} \gamma) = 1.96 \times 10^{-9}$ and $\mathcal{B}(D^0 \rightarrow \nu \bar{\nu} \gamma) = 3.96 \times 10^{-14}$ respectively.

It is important to notice that the approach to rare radiative transitions described above

works extremely well for SM neutrinos in the final state since $E_\gamma \gg \Lambda_{QCD}$ over most of the available phase space. It might not be the case for the DM production. In particular, for $m_{DM} \geq 2$ GeV, the photon energy is quite small and corrections to Eq. (5.12) could become significant. Therefore, our results obtained by using the formalism above should be corrected, for instance, using heavy meson chiral techniques.

One can see that while the branching ratios for the decays into $\nu\bar{\nu}\gamma$ final states are orders of magnitude larger than the corresponding decays into $\nu\bar{\nu}$ final states, they are still way beyond experimental sensitivities of currently operating detectors. Thus, we conclude that SM provides no irreducible background to studies of light DM in present experiments.

5.3 Scalar Dark Matter production

5.3.1 Generic effective Hamiltonian and $B \rightarrow \chi_0\bar{\chi}_0(\gamma)$ decays

Let us consider the generic case of a complex neutral scalar field χ_0 describing the DM and limit our discussion to effective operators of dimension no more than six. In this case, a generic effective Hamiltonian has a very simple form,

$$\mathcal{H}_{eff}^{(s)} = 2 \sum_i \frac{C_i^{(s)}}{\Lambda^2} O_i, \quad (5.16)$$

where Λ is the scale associated with the particle(s) mediating interactions between the SM and DM fields, and $C_i^{(s)}$ are the Wilson coefficients. The effective operators are

$$\begin{aligned}
O_1 &= m_b(\bar{b}_R q_L)(\chi_0^* \chi_0), \\
O_2 &= m_b(\bar{b}_L q_R)(\chi_0^* \chi_0), \\
O_3 &= (\bar{b}_L \gamma^\mu q_L)(\chi_0^* \overleftrightarrow{\partial}_\mu \chi_0), \\
O_4 &= (\bar{b}_R \gamma^\mu q_R)(\chi_0^* \overleftrightarrow{\partial}_\mu \chi_0),
\end{aligned} \tag{5.17}$$

where $\overleftrightarrow{\partial} = (\overrightarrow{\partial} - \overleftarrow{\partial})/2$. For relevant D -meson decays one should substitute $m_b \rightarrow m_c$ and $b \rightarrow q$ currents with $c \rightarrow u$ currents. Operators $O_{3,4}$ disappear for DM in the form of real scalar fields. We note that while the generic form of Eq. (5.17) implies that the mediator of interaction between DM and the SM fields is assumed to be heavy, $M_\Lambda > m_{B_q(D)}$, it is easy to account for the light mediator by substituting $C_i^{(s)}/\Lambda^2 \rightarrow \tilde{C}_i^{(s)}/(M_{B_q(D)}^2 - M_\Lambda^2)$. Clearly, a resonant enhancement of the $B(D) \rightarrow \chi_0 \chi_0$ rate is possible if for some reason the mediator's mass happens to be close to $M_{B_q(D)}$. If observed, this enhancement would be seen as anomalously large Wilson coefficients of the effective Hamiltonian of Eq. (5.17).

Let us first compute the $B(D) \rightarrow \chi_0 \chi_0$ transition rate. It follows from Eq. (5.17) that the decay branching ratio is

$$\mathcal{B}(B_q \rightarrow \chi_0 \chi_0) = \frac{(C_1^{(s)} - C_2^{(s)})^2}{4\pi M_{B_q} \Gamma_{B_q}} \left(\frac{f_{B_q} M_{B_q}^2 m_b}{\Lambda^2 (m_b + m_q)} \right)^2 \sqrt{1 - 4x_\chi^2} \tag{5.18}$$

where $x_\chi = m_\chi/M_{B_q}$ is a rescaled DM mass. Clearly, this rate is not helicity-suppressed, so it could be quite a sensitive tool to determine DM properties at e^+e^- flavor factories. The result for a corresponding D -decay can be obtained via trivial substitution of quark masses,

widths and decay constants. Computing the decay rate for various values of Dark Matter masses and comparing it with the experimental results for B_d missing energy decays [97],

$$\begin{aligned}\mathcal{B}(B_d \rightarrow \cancel{E}) &< 2.2 \times 10^{-4} \\ \mathcal{B}(B_d \rightarrow \cancel{E} + \gamma) &< 4.7 \times 10^{-5},\end{aligned}\tag{5.19}$$

we get the following constraints on coupling constants:

$$\left(\frac{C_1^{(s)} - C_2^{(s)}}{\Lambda^2}\right)^2 \leq 2.03 \times 10^{-16} \text{ GeV}^{-4} \text{ for } m_\chi = 0\tag{5.20}$$

$$\left(\frac{C_1^{(s)} - C_2^{(s)}}{\Lambda^2}\right)^2 \leq 2.07 \times 10^{-16} \text{ GeV}^{-4} \text{ for } m_\chi = 0.1 \times M_{B_d}\tag{5.21}$$

$$\left(\frac{C_1^{(s)} - C_2^{(s)}}{\Lambda^2}\right)^2 \leq 2.22 \times 10^{-16} \text{ GeV}^{-4} \text{ for } m_\chi = 0.2 \times M_{B_d}\tag{5.22}$$

$$\left(\frac{C_1^{(s)} - C_2^{(s)}}{\Lambda^2}\right)^2 \leq 2.54 \times 10^{-16} \text{ GeV}^{-4} \text{ for } m_\chi = 0.3 \times M_{B_d}\tag{5.23}$$

$$\left(\frac{C_1^{(s)} - C_2^{(s)}}{\Lambda^2}\right)^2 \leq 3.39 \times 10^{-16} \text{ GeV}^{-4} \text{ for } m_\chi = 0.4 \times M_{B_d}\tag{5.24}$$

These constraints are much stricter than those in [96].

Applying the formalism described above, distribution of the photon energy and decay

width of radiative decay $B_q(D) \rightarrow \chi_0^* \chi_0 \gamma$ can be computed,

$$\frac{d\Gamma}{dE_\gamma}(B_q \rightarrow \chi_0^* \chi_0 \gamma) = \frac{f_{B_q}^2 \alpha C_3^{(s)} C_4^{(s)}}{3\Lambda^4} \left(\frac{F_{B_q}}{4\pi}\right)^2 \frac{2M_{B_q}^2 E_\gamma (M_{B_q}(1 - 4x_\chi^2) - 2E_\gamma)^{3/2}}{\sqrt{M_{B_q} - 2E_\gamma}} \quad (5.25)$$

$$\begin{aligned} \mathcal{B}(B_q \rightarrow \chi_0^* \chi_0 \gamma) &= \frac{f_{B_q}^2 \alpha C_3^{(s)} C_4^{(s)} M_{B_q}^5}{6\Lambda^4 \Gamma_{B_q}} \left(\frac{F_{B_q}}{4\pi}\right)^2 \\ &\times \left(\frac{1}{6} \sqrt{1 - 4x_\chi^2} (1 - 16x_\chi^2 - 12x_\chi^4) - 12x_\chi^4 \log \frac{2x_\chi}{1 + \sqrt{1 - 4x_\chi^2}} \right), \end{aligned} \quad (5.26)$$

We observe that Eqs. (5.25) and (5.26) do not depend on $C_{1,2}^{(s)}$. This can be most easily seen from the fact that $B_q(D) \rightarrow \gamma$ form factors of scalar and pseudoscalar currents are zero, as follows from Eq. (5.9). Computing decay rates for various values of Dark Matter mass we are able to restrict DM properties based on experimental constraints on B_d decays with missing energy given in Eq. (5.19):

$$\begin{aligned} \frac{C_3^{(s)}}{\Lambda^2} \frac{C_4^{(s)}}{\Lambda^2} &\leq 1.55 \times 10^{-12} \text{ GeV}^{-4} \text{ for } m = 0 \\ \frac{C_3^{(s)}}{\Lambda^2} \frac{C_4^{(s)}}{\Lambda^2} &\leq 1.86 \times 10^{-12} \text{ GeV}^{-4} \text{ for } m = 0.1 \times M_{B_d} \\ \frac{C_3^{(s)}}{\Lambda^2} \frac{C_4^{(s)}}{\Lambda^2} &\leq 3.20 \times 10^{-12} \text{ GeV}^{-4} \text{ for } m = 0.2 \times M_{B_d} \\ \frac{C_3^{(s)}}{\Lambda^2} \frac{C_4^{(s)}}{\Lambda^2} &\leq 9.06 \times 10^{-12} \text{ GeV}^{-4} \text{ for } m = 0.3 \times M_{B_d} \\ \frac{C_3^{(s)}}{\Lambda^2} \frac{C_4^{(s)}}{\Lambda^2} &\leq 7.44 \times 10^{-11} \text{ GeV}^{-4} \text{ for } m = 0.4 \times M_{B_d} \end{aligned} \quad (5.27)$$

Note that Eqs. (5.25) and (5.26) depend on C_3 and C_4 , while Eq. (5.18) depends only on C_1 and C_2 . Since the models with self-conjugated DM scalar fields only contain operators O_1 and O_2 , $B_q(D) \rightarrow \chi_0 \chi_0(\gamma)$ transitions could be used to test the structure of the scalar DM sector.

5.3.2 Production rates in particular models with scalar DM

In this section we apply the techniques described above for the most general effective Hamiltonian for DM particles interacting with the SM fields to particular model implementations of scalar DM, already available in the literature. The list of models considered below is by no means exhaustive.

Minimal and next-to-minimal Scalar Dark Matter models

The simplest possible model for scalar DM involves a real scalar field $\chi_0 \equiv S$ coupled to the SM particles through the exchange of Higgs boson [82, 107]. This is also a very constrained model, where the only two new parameters are the mass parameter m_0 of the scalar DM particle S and the Higgs-scalar coupling λ . Nevertheless, it is possible to have light DM in this model even though it might require some degree of fine-tuning. The SM Lagrangian is modified by

$$\begin{aligned} -\mathcal{L}_S &= \frac{\lambda_S}{4} S^4 + \frac{m_0^2}{2} S^2 + \lambda S^2 H^\dagger H \\ &= \frac{\lambda_S}{4} S^4 + \frac{1}{2}(m_0^2 + \lambda v_{EW}^2) S^2 + \lambda v_{EW} S^2 h + \frac{\lambda}{2} S^2 h^2 \end{aligned} \quad (5.28)$$

where H is the Standard Model Higgs doublet, $v_{EW} = 246$ GeV is the Higgs vacuum expectation value and h is the corresponding physical Higgs boson. We require S to satisfy $S \rightarrow -S$ to make it a good Dark Matter candidate. The scalar DM particle can be made light by requiring cancellations between the terms defining its mass, $m^2 = m_0^2 + \lambda v_{EW}^2$.

The transition $B \rightarrow SS$ occurs in the minimal model as a one-loop process, and since mediating Higgs boson is much heavier than other particles involved in the process, it can

be integrated out. The resulting effective Hamiltonian reads

$$\mathcal{H}_{eff}^{(s)} = \frac{3\lambda g_w^2 V_{tb} V_{tq}^* x_t m_b}{64M_H^2 \pi^2} (\bar{b}_L q_R) S^2, \quad (5.29)$$

which implies that $C_{1,3,4}^{(s)} = 0$, $C_2^{(s)} = 3\lambda g_w^2 V_{tb} V_{tq}^* x_t / 128\pi^2$, and $\Lambda = M_H$. Thus, from Eq. (5.18), the branching ratio for the $B \rightarrow SS$ decay in this model is

$$\mathcal{B}(B_q \rightarrow SS) = \left[\frac{3g_w^2 V_{tb} V_{tq}^* x_t m_b}{128\pi^2} \right]^2 \frac{\sqrt{1-4x_S^2}}{16\pi M_B \Gamma_{B_q}} \left(\frac{\lambda^2}{M_H^4} \right) \left(\frac{f_{B_q} M_{B_q}^2}{m_b + m_q} \right)^2, \quad (5.30)$$

where $x_S = m_S/m_{B_q}$. Note that this rate depends not only on the mass of S but also on the parameter $\kappa = \lambda^2/M_H^4$. This parameter also drives the calculation of the relic density of S [107],

$$\sigma_{ann} v_{rel} = \frac{8v_{EW}^2 \lambda^2}{M_H^2} \times \lim_{m_{h^*} \rightarrow 2m_S} \frac{\Gamma_{h^*X}}{m_{h^*}^*}, \quad (5.31)$$

where Γ_{h^*X} is the rate for the decay $h^* \rightarrow X$ for a virtual Higgs with $M_H \sim 2m_S$. We can, therefore, fix κ from the relic density calculation. This gives for the branching ratios of B_q and D -decays,

$$\mathcal{B}(B_s \rightarrow SS) \approx (4.5 \times 10^5 \text{ GeV}^4) \times \frac{\lambda^2}{M_H^4} \sqrt{1-4x_S^2} \quad (5.32)$$

$$\mathcal{B}(B_d \rightarrow SS) \approx (1.3 \times 10^4 \text{ GeV}^4) \times \frac{\lambda^2}{M_H^4} \sqrt{1-4x_S^2} \quad (5.33)$$

$$\mathcal{B}(D^0 \rightarrow SS) \approx (2.9 \times 10^{-6} \text{ GeV}^4) \times \frac{\lambda^2}{M_H^4} \sqrt{1-4x_S^2} \quad (5.34)$$

We require the branching ratios to be smaller than the current experimental upper bound [97] for the missing energy decay given in Eq. (5.19). With this we are able to put the following

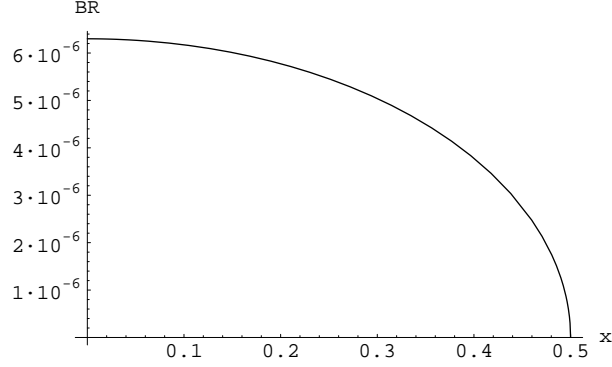


Figure 5.1: $\mathcal{B}(B_d \rightarrow SS)$ as a function of $x = m_S/M_{B_d}$. Values of λ and M_h were fixed at 1 and 120 GeV respectively

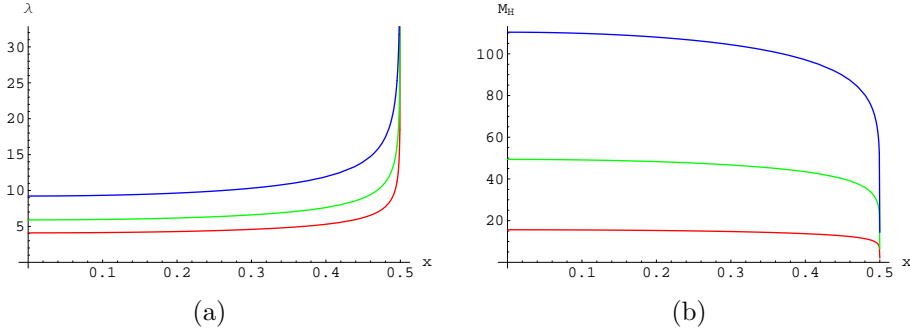


Figure 5.2: (a) allowed values of the DM-Higgs coupling λ as a function of $x = m_S/M_{B_d}$ (below the curves) for the Higgs masses of 110 GeV (red), 120 GeV (green), and 150 GeV (blue). (b) Allowed values of the Higgs mass in GeV (above the curves) for $\lambda = 0.1$ (red), 1 (green), and 5 (blue) as a function of $x = m_S/M_{B_d}$.

restriction onto the parameters of this model:

$$\left(\frac{\lambda}{M_H^2}\right)^2 \sqrt{1 - 4x_S^2} \leq 1.68 \times 10^{-7}. \quad (5.35)$$

We present the resulting branching ratios as a function of m_{χ_0} in Fig. 5.1. Comparing the above branching ratio with the available experimental data we can put constraints on the parameters of this model, which we present in Fig. 5.2. For the particular values of Dark

Matter particles mass we get

$$\begin{aligned}
\left| \frac{\lambda}{M_H^2} \right| &\leq 8.2 \times 10^{-4} \text{ GeV}^{-2} \text{ for } m_S = 0 \\
\left| \frac{\lambda}{M_H^2} \right| &\leq 8.3 \times 10^{-4} \text{ GeV}^{-2} \text{ for } m_S = 0.1 \times M_{B_q} \\
\left| \frac{\lambda}{M_H^2} \right| &\leq 8.6 \times 10^{-4} \text{ GeV}^{-2} \text{ for } m_S = 0.2 \times M_{B_q} \\
\left| \frac{\lambda}{M_H^2} \right| &\leq 9.2 \times 10^{-4} \text{ GeV}^{-2} \text{ for } m_S = 0.3 \times M_{B_q} \\
\left| \frac{\lambda}{M_H^2} \right| &\leq 1.1 \times 10^{-3} \text{ GeV}^{-2} \text{ for } m_S = 0.1 \times M_{B_q}
\end{aligned} \tag{5.36}$$

The minimal scalar model described above can be made less restricted if we introduce another mediator for DM-SM interactions, which should somewhat alleviate the fine-tuning present in the minimal model [107]. This can be done in a variety of ways. The simplest one is to introduce another Higgs-like field U ,

$$\begin{aligned}
-\mathcal{L}_{S'} &= \frac{\lambda_S}{4} S^4 + \frac{m_0^2}{2} S^2 + (\mu_1 U + \mu_2 U^2) S^2 + V(U) + \eta' U^2 H^\dagger H \\
&= \frac{m_s^2}{2} S^2 + \frac{m_u^2}{2} u^2 + \mu u S^2 + \eta v_{EW} u h + \dots,
\end{aligned} \tag{5.37}$$

where we only display mass and relevant interaction terms; ellipses stands for other terms in the Lagrangian that are irrelevant for this discussion.

Here u denotes the excitation around vacuum expectation value of U , and μ and η are parameters with values of the order of electroweak scale. As far as the studies of DM production in heavy flavor decays are concerned, extended models of this class are equivalent to the minimal model after suitable redefinition of parameters [107]. Performing such redefinitions,

we obtain

$$\begin{aligned}
\mathcal{B}(B_s \rightarrow SS) &\approx (2.1 \times 10^{-4}) \times \frac{\eta^2 \mu^2}{M_U^4} \sqrt{1 - 4x_S^2}, \\
\mathcal{B}(B_d \rightarrow SS) &\approx (6.3 \times 10^{-6}) \times \frac{\eta^2 \mu^2}{M_U^4} \sqrt{1 - 4x_S^2}, \\
\mathcal{B}(D^0 \rightarrow SS) &\approx (1.38 \times 10^{-14}) \times \frac{\eta^2 \mu^2}{M_U^4} \sqrt{1 - 4x_S^2},
\end{aligned} \tag{5.38}$$

where M_U is the mass of the Higgs-like field U of Eq. (5.37). In the results above, the mass of the Higgs boson was fixed at $M_h = 120$ GeV. Since the S -field is a real scalar field in both the minimal and the extended models, these models do not give rise to the radiative decay $B_q \rightarrow SS\gamma$.

Dark Matter with two Higgs doublets (2HDM)

In this subsection we consider a singlet scalar WIMP S that interacts with two Higgs doublets, H_u and H_d :

$$-\mathcal{L} = \frac{m_0^2}{2} S^2 + \lambda_1 S^2 (|H_d^0|^2 + |H_d^-|^2) + \lambda_2 S^2 (|H_u^0|^2 + |H_u^+|^2) + \lambda_3 S^2 (H_d^- H_u^+ - H_d^0 H_u^0). \tag{5.39}$$

We shall assume that $\lambda_1 \gg \lambda_2$, as the opposite limit gives results that are not different from the minimal scalar model considered above. The contribution of λ_3 is suppressed because of the cancellation of two diagrams, as explained in [82].

Calculating the effective Hamiltonian results in the following expressions for the Wilson coefficients,

$$C_2^{(s)} = C_1^{(s)} = \frac{\lambda_1 g_w^2 V_{tb} V_{tq}^* x_t (1 - a_t + a_t \log a_t)}{128 \pi^2 (1 - a_t)^2} \text{ and } \Lambda = M_H, \tag{5.40}$$

where $a_q = (m_q/M_H)^2$. As in the previous subsection, no decay into dark matter plus photon

is possible within the framework of this model. However, decay into a pair of dark matter particles is possible

$$\begin{aligned}
\mathcal{B}(B_s \rightarrow SS) &\approx (0.73 \times 10^2 \text{ GeV}^4) \times \lambda_1^2 \sqrt{1 - 4x_S^2} \left(\frac{a_t \log a_t - a_t + 1}{M_H^2 (1 - a_t)^2} \right)^2, \\
\mathcal{B}(B_d \rightarrow SS) &\approx (2.1 \text{ GeV}^4) \times \lambda_1^2 \sqrt{1 - 4x_S^2} \left(\frac{a_t \log a_t - a_t + 1}{M_H^2 (1 - a_t)^2} \right)^2, \\
\mathcal{B}(D^0 \rightarrow SS) &\approx (5.0 \times 10^2 \text{ GeV}^4) \times \lambda_1^2 \sqrt{1 - 4x_S^2} \left(\sum_{q=b,s,d} V_{uq} V_{cq}^* \frac{a_q \log a_q - a_q + 1}{M_H^2 (1 - a_q)^2} \right)^2.
\end{aligned} \tag{5.41}$$

Eqs. (5.41) can be used for constraining parameters of this model in $B_q \rightarrow SS$ transitions.

5.4 Fermionic Dark Matter production

5.4.1 Generic effective Hamiltonian and $B_{d(s)} \rightarrow \chi_{1/2} \overline{\chi_{1/2}}(\gamma)$ decays

Let us now consider a generic case of fermionic Dark Matter production. It is possible that the DM particles have half-integral spin; so many New Physics models, including Minimal Supersymmetric Standard Model (MSSM), have fermionic DM candidates. However, most of those models naturally assign rather large masses to their DM candidates. Nevertheless, either after some fine-tuning of the relevant parameters or after introducing a light DM-SM mediator, relatively light DM particles are still possible. Let us consider their production in the decays of heavy mesons. Once again, limiting ourselves to the operators of dimension of no more than six, a relevant effective Hamiltonian reads

$$\mathcal{H}_{eff}^f = \frac{4}{\Lambda^2} \sum_i C_i^{(f)} Q_i, \tag{5.42}$$

where C_i 's are relevant Wilson coefficients and Λ represents the mass scale relevant for DM-quark interactions (*e.g.* mediator mass). In general, there are twelve possible effective operators,

$$\begin{aligned}
Q_1 &= (\bar{b}_L \gamma_\mu s_L)(\bar{\chi}_{1/2L} \gamma^\mu \chi_{1/2L}), & Q_2 &= (\bar{b}_L \gamma_\mu s_L)\bar{\chi}_{1/2R} \gamma^\mu \chi_{1/2R}, \\
Q_3 &= (\bar{b}_R \gamma_\mu s_R)(\bar{\chi}_{1/2L} \gamma^\mu \chi_{1/2L}), & Q_4 &= (\bar{b}_R \gamma_\mu s_R)(\bar{\chi}_{1/2R} \gamma^\mu \chi_{1/2R}), \\
Q_5 &= (\bar{b}_L s_R)(\bar{\chi}_{1/2L} \chi_{1/2R}), & Q_6 &= (\bar{b}_L s_R)(\bar{\chi}_{1/2R} \chi_{1/2L}), \\
Q_7 &= (\bar{b}_R s_L)(\bar{\chi}_{1/2L} \chi_{1/2R}), & Q_8 &= (\bar{b}_R s_L)(\bar{\chi}_{1/2R} \chi_{1/2L}), \\
Q_9 &= (\bar{b}_L \sigma_{\mu\nu} s_R)(\bar{\chi}_{1/2L} \sigma^{\mu\nu} \chi_{1/2R}), & Q_{10} &= (\bar{b}_L \sigma_{\mu\nu} s_R)(\bar{\chi}_{1/2R} \sigma^{\mu\nu} \chi_{1/2L}), \\
Q_{11} &= (\bar{b}_R \sigma_{\mu\nu} s_L)(\bar{\chi}_{1/2L} \sigma^{\mu\nu} \chi_{1/2R}), & Q_{12} &= (\bar{b}_R \sigma_{\mu\nu} s_L)(\bar{\chi}_{1/2R} \sigma^{\mu\nu} \chi_{1/2L}),
\end{aligned} \tag{5.43}$$

where the Dark Matter fermion $\chi_{1/2}$ can be either of Dirac or Majorana type. The latter choice leads to some simplification of the basis. All needed matrix elements have been given in Eq. (5.2). Note that the matrix elements of the tensor operators vanish,

$$\langle 0 | \bar{b} \sigma^{\mu\nu} P_{L,R} q | B_q \rangle = 0. \tag{5.44}$$

For relevant D -meson decays one should substitute $m_b \rightarrow m_c$ and $b \rightarrow q$ currents with $c \rightarrow u$ currents.

Using the Hamiltonian of Eq. (5.43) we get for the branching ration of $B_q \rightarrow \bar{\chi}_{1/2}\chi_{1/2}$,

$$\begin{aligned} \mathcal{B}(B_q \rightarrow \bar{\chi}_{1/2}\chi_{1/2}) &= \frac{f_{B_q}^2 M_{B_q}^3}{16\pi\Gamma_{B_q}\Lambda^2} \sqrt{1 - 4x_\chi^2} \times \\ &\left[C_{57}C_{68} \frac{4M_{B_q}^2 x_\chi^2}{(m_b + m_q)^2} - (C_{57}^2 + C_{68}^2) \frac{M_{B_q}^2 (2x_\chi^2 - 1)}{(m_b + m_q)^2} \right. \\ &\left. - 2\tilde{C}_{1-8} \frac{x_\chi M_{B_q}}{m_b + m_q} + 2(C_{13} + C_{24})^2 x_\chi^2 \right], \end{aligned} \quad (5.45)$$

where we employed short-hand notations for the combinations of Wilson coefficients $C_{ij} = C_i^{(f)} - C_j^{(f)}$, and $\tilde{C}_{1-8} = C_{13}C_{57} + C_{24}C_{57} + C_{13}C_{68} + C_{24}C_{68}$. Due to its larger mass chirality suppression for the GeV-scale Dark Matter is not as severe as for neutrinos, even for purely left-handed interactions. The result in Eq. 5.45 leads to model-independent constraints on the Wilson coefficients of Eq. (5.42), which are based on experimental data for missing energy decays of B_d meson (see, e.g. Eq. (5.19)). They are displayed in Table 5.1. The upper limits can be used to constrain parameters of particular models of fermionic Dark Matter considered below.

The technique which we use for the computation of $\Gamma(B_q(D) \rightarrow \chi_{1/2}\bar{\chi}_{1/2}\gamma)$ is very similar

x_χ	C_1/Λ^2 $\times 10^8$ GeV $^{-2}$	C_2/Λ^2 , $\times 10^8$ GeV $^{-2}$	C_3/Λ^2 , $\times 10^8$ GeV $^{-2}$	C_4/Λ^2 , $\times 10^8$ GeV $^{-2}$	C_5/Λ^2 , $\times 10^8$ GeV $^{-2}$	C_6/Λ^2 , $\times 10^8$ GeV $^{-2}$	C_7/Λ^2 , $\times 10^8$ GeV $^{-2}$	C_8/Λ^2 , $\times 10^8$ GeV $^{-2}$
0	–	–	–	–	2.3	2.3	2.3	2.3
0.1	19	19	19	19	2.3	2.3	2.3	2.3
0.2	9.7	9.7	9.7	9.7	2.5	2.5	2.5	2.5
0.3	6.9	6.9	6.9	6.9	2.8	2.8	2.8	2.8
0.4	6.0	6.0	6.0	6.0	3.6	3.6	3.6	3.6

Table 5.1: Constraints (upper limits) on the Wilson coefficients of operators of Eq. (5.43) from the $B_q \rightarrow \chi_{1/2}\bar{\chi}_{1/2}$ transition. Note that operators $Q_9 - Q_{12}$ give no contribution to this decay.

to the one used for the radiative decay of heavy meson into scalar DM particles discussed above. The hadronic part of the matrix element remains the same, we only modify the part that describes Dark Matter. These lead to

$$\frac{d\Gamma}{dE_\gamma} = \frac{d\Gamma_{1-8}}{dE_\gamma} + \frac{d\Gamma_{9-12}}{dE_\gamma}, \quad (5.46)$$

$$\begin{aligned} \frac{d\Gamma_{1-8}}{dE_\gamma} &= \frac{f_{B_q}^2 F_{B_q}^2 \alpha M_{B_q}^2 E_\gamma \sqrt{M_{B_q}(1-4x_\chi^2) - 2E_\gamma}}{24\pi^2 \Lambda^2 \sqrt{M_{B_q} - 2E_\gamma}} \\ &\times \left[(C_1^2 + C_2^2 + C_3^2 + C_4^2)(M_{B_q} - x_\chi^2 M_{B_q} - E_\gamma) - \right. \\ &\left. - (3C_1 C_2 + 3C_3 C_4) x_\chi^2 M_{B_q} \right], \end{aligned} \quad (5.47)$$

$$\begin{aligned} \frac{d\Gamma_{9-12}}{dE_\gamma} &= \frac{64\alpha}{3M_{B_q}^2 \pi^2 \Lambda^2} \left(\frac{E_\gamma^3}{M_{B_q} - 2E_\gamma} \right) \frac{\sqrt{M_{B_q}(1-4x_\chi^2) - 2E_\gamma}}{\sqrt{M_{B_q} - 2E_\gamma}} \\ &\times \left[2 \left((C_{10}^2 + 9C_{11}C_{10} - 3C_{12}C_{10} + C_{11}^2 - 3C_{12}C_{11} + 3C_9(C_{10} + C_{11} + C_{12})) f_1^2 \right. \right. \\ &\quad - g_1 f_1 (C_{10}^2 + 3C_{10}(C_{11} + C_{12}) + C_{11}(C_{11} + 3C_{12}) - 3C_9(C_{10} + C_{11} + C_{12})) \\ &\quad + 2g_1^2 (C_{10}^2 - 6C_{10}C_{11} + C_{11}^2) \left. \right) x_\chi^2 M_{B_q}^2 \\ &\quad \left. + (f_1^2 - g_1 f_1 + 2g_1^2) (C_{10}^2 + C_{11}^2) (M_{B_q}^2 - 2M_{B_q} E_\gamma) \right]. \end{aligned} \quad (5.48)$$

While there are many models of light fermionic DM that employ operators $Q_1 - Q_8$, we are not aware of the models with operators $Q_9 - Q_{12}$. Therefore, we chose not to provide a closed analytic expression for $\mathcal{B}_{9-12}(B_q \rightarrow \chi_{1/2} \bar{\chi}_{1/2} \gamma)$ here due to overall bulkiness of the resulting expression. The numerical integration of Eq. (5.48) can be performed for a particular model, if needed. Integrating Eq. (5.48) over the photon energy analytically we obtain

$$\begin{aligned} \mathcal{B}_{1-8}(B_q \rightarrow \chi_{1/2} \bar{\chi}_{1/2} \gamma) &= \frac{F_{B_q}^2 f_{B_q}^2 M_{B_q}^2 \alpha}{144\pi^2 \sqrt{1-4x_\chi^2} \Lambda^2} \times \\ &\left[(C_1^2 + C_2^2 + C_3^2 + C_4^2) Y(x_\chi) + \frac{9}{2} (C_1 C_2 + C_3 C_4) Z(x_\chi) \right], \end{aligned} \quad (5.49)$$

x_χ	$C_1/\Lambda^2, \text{ GeV}^{-2}$	$C_2/\Lambda^2, \text{ GeV}^{-2}$	$C_3/\Lambda^2, \text{ GeV}^{-2}$	$C_4/\Lambda^2, \text{ GeV}^{-2}$
0	6.3×10^{-7}	6.3×10^{-7}	6.3×10^{-7}	6.3×10^{-7}
0.1	7.0×10^{-7}	7.0×10^{-7}	7.0×10^{-7}	7.0×10^{-7}
0.2	9.2×10^{-7}	9.2×10^{-7}	9.2×10^{-7}	9.2×10^{-7}
0.3	1.5×10^{-6}	1.5×10^{-6}	1.5×10^{-6}	1.5×10^{-6}
0.4	3.4×10^{-6}	3.4×10^{-6}	3.4×10^{-6}	3.4×10^{-6}

Table 5.2: Constraints (upper limits) on the Wilson coefficients of operators of Eq. (5.43) from the $B_q \rightarrow \chi_{1/2} \bar{\chi}_{1/2} \gamma$ transition. Note that operators $Q_5 - Q_8$ give no contribution to this decay.

where the factors $Y(x_\chi)$ and $Z(x_\chi)$ are defined as

$$\begin{aligned}
Y(x_\chi) &= 1 - 2x_\chi^2 + 3x_\chi^2(3 - 6x_\chi^2 + 4x_\chi^4)\sqrt{1 - 4x_\chi^2} \log\left(\frac{2x_\chi}{1 + \sqrt{1 - 4x_\chi^2}}\right) - \\
&\quad - 11x_\chi^4 + 12x_\chi^6, \\
Z(x_\chi) &= x_\chi^2 \left(1 + 2x_\chi^2 + 8x_\chi^2(1 - x_\chi^2)\sqrt{1 - 4x_\chi^2} \log\left(\frac{2x_\chi}{1 + \sqrt{1 - 4x_\chi^2}}\right) + 8x_\chi^4\right). \quad (5.50)
\end{aligned}$$

This equation can be used to place constraints on the individual Wilson coefficients of Eq. (5.43). They are listed in Table 5.2. Both Eq. (5.45) and Eq. (5.49) can now be used to constrain the parameters of the particular models of fermionic DM.

5.4.2 Production rates in particular models with fermionic DM

Models with hidden valleys

It was pointed out in [103] that there could be light particles called v -quarks interacting with Standard Model sector via heavy mediator Z' . In the simplest v -Model, a $SU(n_v) \times U(1)$ gauge group with couplings g' and g_v is added to the Standard Model². The $U(1)$ symmetry

²The g' coupling constant introduced here is not to be confused with the SM hypercharge coupling constant.

is broken by vacuum expectation value of the scalar field $\langle\phi\rangle$, giving Z' a mass of about 1 – 6 TeV. The Z' can mix with Standard Model Z via kinetic mixing $kF^{\mu\nu}F'_{\mu\nu}$. In this model the role of Dark Matter is played by the v -quarks ($\chi_{1/2} \equiv v$).

The model corresponds to the following set of parameters for the decay of B_s meson (for decays of B_d and D^0 parameters will be similar):

$$C_1 = \frac{G_F k g' M_Z M_{Z'} \alpha}{2g_w \sqrt{2} \sin^2 \theta_W} V_{tb} V_{ts}^* X(x), \quad \text{and} \quad \Lambda = M_{Z'} \quad (5.51)$$

where k is the kinetic mixing parameter, g' is a gauge coupling of the Z' and v -quarks, and $M_{Z'}$ is the mass of the heavy mediator. The rest of the Wilson coefficients C_i are zero. Thus, from Eq. (5.45),

$$\mathcal{B}(B_s \rightarrow v\bar{v}) \approx (1.76 \text{ GeV}^2) x_v^2 \sqrt{1 - 4x_v^2} \left(\frac{g'k}{M_{Z'}} \right)^2 \quad (5.52)$$

where $x_v = m_v/M_{B_q}$. The corresponding results for B_d and D^0 decays are

$$\mathcal{B}(B_d \rightarrow v\bar{v}) \approx (4.68 \times 10^{-2} \text{ GeV}^2) x_v^2 \sqrt{1 - 4x_v^2} \left(\frac{g'k}{M_{Z'}} \right)^2, \quad (5.53)$$

and

$$\mathcal{B}(D^0 \rightarrow v\bar{v}) \approx (2.68 \times 10^{-8} \text{ GeV}^2) x_v^2 \sqrt{1 - 4x_v^2} \left(\frac{g'k}{M_{Z'}} \right)^2, \quad (5.54)$$

respectively. The corresponding expression for the decay into two v -quarks and photon can be obtained by defining

$$C_1 = \frac{G_F k g' \alpha M_Z M_{Z'}}{2g \sqrt{2} \sin^2 \theta_W} V_{tb} V_{tq}^* X(x) \frac{e}{3}, \quad \text{and} \quad \Lambda = M_{Z'}. \quad (5.55)$$

We present our results in Fig. 5.3(a) in order to extract the dependence on DM mass. The

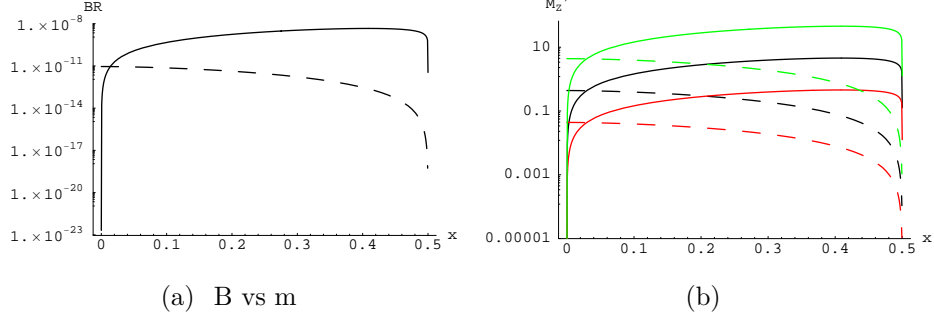


Figure 5.3: (a) $\mathcal{B}(B_d \rightarrow vv)$ as a function of $x = m_v/M_{B_d}$ evaluated at $g' = 1$, $k = 1$ and $M_{Z'} = 1 \text{ TeV}$; (b) Allowed values of the $M_{Z'}$ mass in GeV (above the curves) for $g_1 k = 1$ (black), 0.1 (red), and 10 (green) as a function of $x = m_v/M_{B_d}$. Solid lines represent the constraints from the 2-body decay, and the dashed ones – from the 3 body (radiative) decay. The constraints on the mass of Z' are very loose.

analytic results for the branching ratios can be well approximated by the following formulas,

$$\mathcal{B}(B_s \rightarrow v\bar{v}\gamma) \approx (2.76 \times 10^{-4} \text{ GeV}^2) \frac{g_1^2 k^2}{M_{Z'}^2} \times \frac{Y(x_v)}{\sqrt{1 - 4x_v^2}} \quad (5.56)$$

for the branching ratio of B_s radiative decay and

$$\mathcal{B}(B_d \rightarrow v\bar{v}\gamma) \approx (9.07 \times 10^{-6} \text{ GeV}^2) \frac{g_1^2 k^2}{M_{Z'}^2} \times \frac{Y(x_v)}{\sqrt{1 - 4x_v^2}}, \quad (5.57)$$

$$\mathcal{B}(D^0 \rightarrow v\bar{v}\gamma) \approx (3.68 \times 10^{-12} \text{ GeV}^2) \frac{g_1^2 k^2}{M_{Z'}^2} \times \frac{Y(x_v)}{\sqrt{1 - 4x_v^2}}, \quad (5.58)$$

for B_d and D^0 decays, respectively. The structure function $Y(x)$ appearing in this equation was defined in Eq. (5.50).

Right-handed massive neutrinos as a Fermionic Dark Matter

Massive right-handed neutrinos appear naturally in left-right symmetric models (see for example [105]). The see-saw mechanism is used to get light left-handed neutrinos and massive

right-handed ones. The coupling of the massive neutrino to the SM fields in this case is mediated by a right-handed gauge boson with mass in the TeV range. In this section $\chi_{1/2} \equiv \nu_R$.

$$\mathcal{H}_{eff} = \frac{4G_F^{(R)}}{\sqrt{2}} \frac{\alpha}{2\pi \sin^2 \theta_W} \sum_k \lambda_k X(x_k) (J_{Qq}^\mu) (\bar{\nu}_R \gamma_\mu \nu_R), \quad (5.59)$$

where $J_{Qq}^\mu = \bar{q}_R \gamma^\mu b_R$ for beauty and $J_{Qq}^\mu = \bar{u}_R \gamma^\mu c_R$ for charm transitions. The functions $\lambda_k X(x_k)$ are the combinations of the Cabbibo-Kobayashi-Maskawa (CKM) factors and Inami-Lim functions. $G_F^{(R)}$ is defined in analogy to the usual Fermi constant,

$$\frac{G_F^{(R)}}{\sqrt{2}} = \frac{g^2}{8M_{W_R}^2}, \quad (5.60)$$

which implies that

$$C_4 = \frac{g^2}{8} \frac{\alpha}{2\pi \sin^2 \theta_W}. \quad (5.61)$$

Following the procedure described above, we obtain the following results for decay branching ratios,

$$\mathcal{B}(B_s \rightarrow \nu_R \bar{\nu}_R) \approx \frac{3.6 \times 10^3 \text{ GeV}^4}{M_{W_R}^4} x_\nu^2 \sqrt{1 - 4x_\nu^2}, \quad (5.62)$$

$$\mathcal{B}(B_s \rightarrow \nu_R \bar{\nu}_R \gamma) \approx \frac{0.57 \text{ GeV}^4}{M_{W_R}^4} \times Y(x_\nu), \quad (5.63)$$

$$\mathcal{B}(B_d \rightarrow \nu_R \bar{\nu}_R) \approx \frac{10^2 \text{ GeV}^4}{M_{W_R}^4} x_\nu^2 \sqrt{1 - 4x_\nu^2}, \quad (5.64)$$

$$\mathcal{B}(B_d \rightarrow \nu_R \bar{\nu}_R \gamma) \approx \frac{1.9 \times 10^{-2} \text{ GeV}^4}{M_{W_R}^4} \times Y(x_\nu), \quad (5.65)$$

$$\mathcal{B}(D^0 \rightarrow \nu_R \bar{\nu}_R) \approx \frac{5.6 \times 10^{-5} \text{ GeV}^4}{M_{W_R}^4} x_\nu^2 \sqrt{1 - 4x_\nu^2}, \quad (5.66)$$

$$\mathcal{B}(D^0 \rightarrow \nu_R \bar{\nu}_R \gamma) \approx \frac{7.6 \times 10^{-9} \text{ GeV}^4}{M_{W_R}^4} \times Y(x_\nu), \quad (5.67)$$

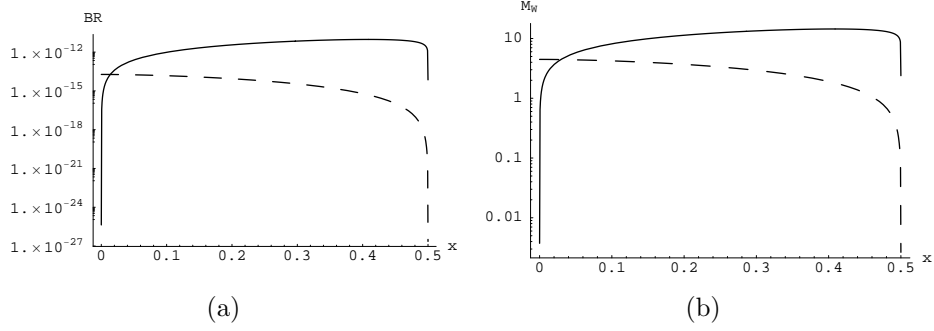


Figure 5.4: (a) $\mathcal{B}(B_d \rightarrow \nu_R \bar{\nu}_R)$ as a function of $x = m_{\nu_R}/M_{B_d}$ evaluated at $M_{W_R} = 1 \text{ TeV}$, (b) Allowed values of the M_{W_R} mass in GeV (above the curves) as a function of $x = m_{\nu_R}/M_{B_d}$. Solid lines represent the constraints from the 2-body, and the dashed ones – from the 3 body (radiative) decay. As one can see, the constraints on the mass of W_R are very loose.

where $Y(x)$ is defined in Eq. (5.50). These results are also presented in Fig. 5.4.

5.4.3 Majorana fermions

Majorana particles $\chi_{1/2} \equiv \chi$ often appear in many models of physics beyond the Standard Model. For generic studies of decays of heavy mesons to Majorana DM particles we can also use Lagrangian of Eq. (5.43). The resulting formulas, however, will be simplified due to the known properties of Majorana fermions [106],

$$\begin{aligned}\bar{\chi}\gamma_\mu\chi &= 0, \\ \bar{\chi}\sigma^{\mu\nu}\chi &= 0.\end{aligned}$$

Taking into account the conditions of Eq. (5.68), we can obtain the branching ratio for $B_q \rightarrow \chi\chi$ decay,

$$\mathcal{B}(B_q \rightarrow \chi\chi) = \frac{f_{B_q}^2 M_{B_q}^5}{16\pi\Gamma_{B_q}(m_b + m_q)\Lambda^2} \sqrt{1 - 4x^2} [C_{57}^2 + C_{68}^2 - 2x^2(C_{57} - C_{68})^2]. \quad (5.68)$$

The photon energy distribution in $B_q \rightarrow \chi\chi\gamma$ decay reads

$$\frac{d\Gamma}{dE_\gamma} = \frac{f_{B_q}^2 F_{B_q}^2 \alpha M_{B_q}^2 E_\gamma \sqrt{M_{B_q}(1 - 4x_\chi^2) - 2E_\gamma}}{48\pi^2 \Lambda^2 \sqrt{M_{B_q} - 2E_\gamma}} \times (C_{12}^2 + C_{34}^2)(M_{B_q}(1 + 2x_\chi^2) + E_\gamma), \quad (5.69)$$

which can be integrated over to obtain the branching fraction

$$\mathcal{B}(B_q \rightarrow \chi\chi\gamma) = \frac{f_{B_q}^2 F_{B_q}^2 \alpha M_{B_q}^5}{1152\pi^2 \Lambda^2} (C_{12}^2 + C_{34}^2) \times \left(36x_\chi^2 \log \frac{2x_\chi}{\sqrt{1 - 4x_\chi^2} + 1} + (4 + 17x_\chi^2 + 6x_\chi^4) \sqrt{1 - 4x_\chi^2} \right). \quad (5.70)$$

As an example, we consider a realization of the fermionic dark matter scenario proposed in [82]. In this model the Majorana fermion coupled to a higgs-higgsino pair is considered. It must be noted that by ‘‘higgsino’’ we mean a fermionic field with the same quantum numbers as a Higgs field. We, however, do not place any supersymmetric requirements on the coupling constants. With that,

$$-\mathcal{L}_f = \frac{M}{2} \bar{\psi}\psi + \mu \bar{\tilde{H}}_d \tilde{H}_u + \lambda_d \bar{\psi} \tilde{H}_d H_d + \lambda_u \bar{\psi} \tilde{H}_u H_u, \quad (5.71)$$

where $M \ll \mu$, $\lambda_u v_u$. The Dark Matter candidate is the lightest mass eigenstate, which we define as

$$\begin{aligned} \chi &= -\psi \cos \theta + \tilde{H}_d \sin \theta, & \sin^2 \theta &= \frac{\lambda_u^2 v_u^2}{\lambda_u^2 v_u^2 + \mu^2} \\ m_1 &= M \left(1 - \frac{\lambda_u^2 v_u^2}{\lambda_u^2 v_u^2 + \mu^2} \right). \end{aligned}$$

We are thus led to the following effective Lagrangian,

$$\mathcal{L}_{eff} = \frac{1}{2} \frac{V_{ts}V_{tb}^* \tan \beta}{32\pi^2 v_{sm}^3} \left(\frac{\lambda_d \lambda_u v_u \mu}{\lambda_u^2 v_u^2 + \mu^2} \right) \frac{m_b a_t \ln a_t}{(1 - a_t)} (\bar{b}_L s_R)(\bar{\chi} \chi), \quad (5.72)$$

where $a_t = m_t^2/M_h^2$ and $\tan \beta = v_u/v_d$. Matching this Lagrangian to Eqs. (5.42, 5.43), we observe that $C_5 = C_6$, and the remaining coefficients $C_i = 0$. In addition,

$$C_5 = C_6 = \frac{V_{ts}V_{tb}^* \tan b}{(16\pi)^2 v_{sm}^3} \left(\frac{\lambda_d \lambda_u v_u \mu}{\lambda_u^2 v_u^2 + \mu^2} \right) \frac{m_b m_t^2 \ln a_t}{(1 - a_t)}, \quad \text{and} \quad \Lambda = M_h. \quad (5.73)$$

The effective lagrangian and corresponding Wilson coefficients for decays of B_d and D^0 mesons can be obtained after suitable substitution of CKM matrix elements and quark masses.

Taking into account Eq. (5.70) we conclude that no decay into $\chi\bar{\chi}\gamma$ is possible in this particular model. However, a simpler decay into $\chi\chi$ is possible,

$$\mathcal{B}(B_s \rightarrow \chi\chi) \approx 1.47 \times 10^{-10} \sqrt{1 - 4x_\chi^2} \frac{\log^2(a_t)}{(1 - a_t)^2} \left(\frac{\tan(\beta)v_u \lambda_d \lambda_u \mu}{(v_u^2 \lambda_u^2 + \mu^2)} \right)^2, \quad (5.74)$$

$$\mathcal{B}(B_d \rightarrow \chi\chi) \approx 4.16 \times 10^{-12} \sqrt{1 - 4x_\chi^2} \frac{\log^2(a_t)}{(1 - a_t)^2} \left(\frac{\tan(\beta)v_u \lambda_d \lambda_u \mu}{(v_u^2 \lambda_u^2 + \mu^2)} \right)^2, \quad (5.75)$$

$$\mathcal{B}(D^0 \rightarrow \chi\chi) \approx 1.81 \times 10^{-11} \sqrt{1 - 4x_\chi^2} \left(\frac{\tan(\beta)v_u \lambda_d \lambda_u \mu}{(v_u^2 \lambda_u^2 + \mu^2)} \sum_{q=b, s, d} V_{cq} V_{uq}^* \frac{a_q \log(a_q)}{(1 - a_q)} \right)^2, \quad (5.76)$$

where $a_q = (m_q/M_H)^2$ and $x_\chi = m_\chi/M_{B_q}$. These results can be used to constrain the parameters of this model.

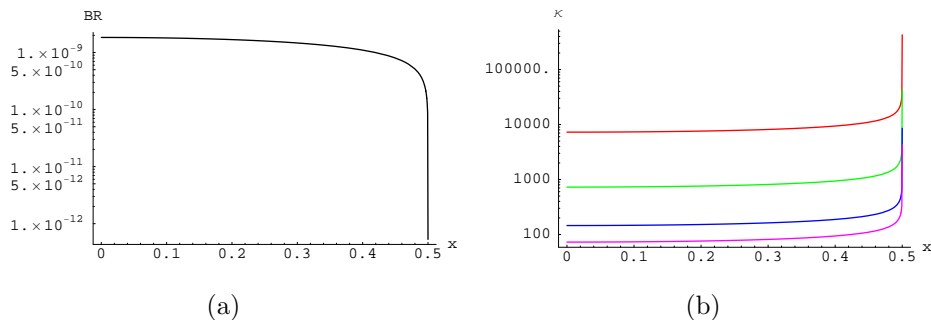


Figure 5.5: (a) $\mathcal{B}(B_d \rightarrow \chi\bar{\chi})$ as a function of $x = m_\chi/M_{B_d}$. The following numerical values were used: $\kappa = (\lambda_d\lambda_u v_u \mu)/(\lambda_u^2 v_u^2 + \mu^2) = 1$, $\tan \beta = 10$, $M_h = 102 \text{ GeV}$ (b) Allowed values of the κ (above the curves) for the values of $\tan \beta = 1$ (red), 10 (green), 100 (blue), and 1000 (purple) while mass of Higgs boson was fixed at $M_h = 120 \text{ GeV}$ as a function of $x = m_\chi/M_{B_d}$.

5.5 Vector Dark Matter production. Generic effective Hamiltonian and $B_q(D^0) \rightarrow \chi_1\chi_1$ decays

Vector DM is a quite popular concept in non-supersymmetric solutions of the hierarchy problem. In particular, it can be encountered in models with Universal Extra Dimensions (UED), little Higgs models with T-parity, and some variations of Randall-Sundrum models. All of the proposed models available in the literature involve weak-scale DM particles. This however, does not preclude the existence of the low mass vector DM.

Let us consider a generic case of a vector field χ_1^μ describing Dark Matter. This DM particle could be either a gauge boson, corresponding to some abelian or non-abelian gauge symmetry broken at some higher scale, or some composite state. The only assumption that we shall make is that χ_1 is odd under some Z_2 -type discrete symmetry, $\chi_1^\mu \rightarrow -\chi_1^\mu$. This condition results in the pair-production of DM particles.

We shall limit our discussion to the effective operators of the dimension no more than six. Since no gauge symmetry related to χ_1^μ is present at the scale m_Q , the most general

effective Hamiltonian is built out of the vector field χ_1^μ and its field strength tensor $\chi_1^{\mu\nu}$. In this case, an effective Hamiltonian has a very simple form,

$$\mathcal{H}_{eff}^{(v)} = \sum_i \frac{C_i^{(v)}}{\Lambda^2} O_i, \quad (5.77)$$

where Λ is the scale associated with the mass of the particle mediating interactions between the SM and DM fields, and $C_i^{(V)}$ are the Wilson coefficients. The effective operators are

$$\begin{aligned} O_1 &= m_b (\bar{b}_L q_R) \chi_{1\mu} \chi_1^\mu, & O_4 &= (\bar{b}_R \gamma_\mu q_R) \chi_1^{\mu\nu} \chi_{1\nu}, \\ O_2 &= m_b (\bar{b}_R q_L) \chi_{1\mu} \chi_1^\mu, & O_5 &= (\bar{b}_L \gamma_\mu q_L) \tilde{\chi}_1^{\mu\nu} \chi_{1\nu}, \\ O_3 &= (\bar{b}_L \gamma_\mu q_L) \chi_1^{\mu\nu} \chi_{1\nu}, & O_6 &= (\bar{b}_R \gamma_\mu q_R) \tilde{\chi}_1^{\mu\nu} \chi_{1\nu}, \end{aligned} \quad (5.78)$$

where $\tilde{\chi}_1^{\mu\nu} = (1/2)\epsilon^{\mu\nu\alpha\beta}\chi_{1\alpha\beta}$ and $q = s, d$. As before, the Hamiltonian relevant for charmed meson decays can be obtained by the proper substitution of $b \rightarrow q$ current with $c \rightarrow u$ current.

The $B_q(D) \rightarrow \chi_1 \chi_1$ transition rate can be computed using Eq. (5.78). Using the form-factors defined in Eq. (5.2), we obtain

$$\begin{aligned} \text{B}(B_q \rightarrow \chi_1 \chi_1) &= \frac{f_B^2 M m_b^2 \sqrt{M^4 (1 - 4x_\chi^2)}}{256(m_b + m_q)^2 \pi x_\chi^4 \Gamma_{B_q} \Lambda^4} [C_{12}^2 (1 - 4x_\chi^2 + 12x_\chi^4) \\ &+ (m_b + m_q)^2 (8C_{56}^2 (1 - 4x_\chi^2) + 3C_{34}^2) x_\chi^4 \\ &+ 2C_{12}C_{34}(m_b + m_q) (1 + 2x_\chi^2) x_\chi^2], \end{aligned} \quad (5.79)$$

where $C_{ik} = C_i^{(v)} - C_k^{(v)}$ and $x_{\text{DM}} = m_\chi/m_{B_q}$. It is necessary to point out that Eq. (5.79) is divergent at $m_\chi = 0$, which is related to the fact that operators in Eq. (5.78) contributing to the effective Lagrangian are not gauge invariant. Thus, for the case of massless DM the

x_χ	$C_1/\Lambda^2,$ GeV $^{-2}$	$C_2/\Lambda^2,$ GeV $^{-2}$	$C_3/\Lambda^2,$ GeV $^{-2}$	$C_4/\Lambda^2,$ GeV $^{-2}$	$C_5/\Lambda^2,$ GeV $^{-2}$	$C_6/\Lambda^2,$ GeV $^{-2}$
0	0	0	1.4×10^{-8}	1.4×10^{-8}	8.9×10^{-9}	8.9×10^{-9}
0.1	1.2×10^{-9}	1.2×10^{-9}	1.5×10^{-8}	1.5×10^{-8}	9.1×10^{-9}	9.1×10^{-9}
0.2	5.1×10^{-9}	5.1×10^{-9}	1.5×10^{-8}	1.5×10^{-8}	1.0×10^{-8}	1.0×10^{-8}
0.3	1.3×10^{-8}	1.3×10^{-8}	1.6×10^{-8}	1.6×10^{-8}	1.2×10^{-8}	1.2×10^{-8}
0.4	2.9×10^{-8}	2.9×10^{-8}	1.9×10^{-8}	1.9×10^{-8}	1.9×10^{-8}	1.9×10^{-8}

Table 5.3: Constraints (upper limits) on the Wilson coefficients of operators of Eq. (5.78) from the $B_q \rightarrow \chi_1 \chi_1$ transition.

upper limit on the Wilson coefficients $C_1^{(v)}$ and $C_2^{(v)}$ is zero (see Table 5.3).

Using Eq. (5.79), we can place general constraints on the Wilson coefficients of the effective Hamiltonian describing interactions of vector DM with quarks (see Eq. (5.77)). They are presented in Table 5.3.

We are not aware of particular models of light DM with spin-1 particles and masses $m_\chi < 3$ GeV. Thus we are unable to test particular models of vector DM.

5.6 Conclusions

We have argued that missing energy decays of the heavy mesons - B_d , B_s and D^0 - provide an important way to probe different properties of Dark Matter. Consideration of different decay modes - two body decays, radiative and light meson + DM decays - restricts different regions of the Dark Matter parameter space. Combined constraints obtained from different decay modes of various heavy mesons provide indispensable probe of physics beyond the Standard Model in general and the nature of the Dark Matter in particular. For instance, observation of $B_q(D^0) \rightarrow \gamma \cancel{E}$, but non-observation of $B_q(D^0) \rightarrow \cancel{E}$ transitions directly point to non-self-conjugated nature of scalar DM.

We reported general constraints on the Wilson coefficients of the effective operators de-

scribing interactions of DM with quarks (see Tables I-III). Restrictions obtained in our paper are much stricter than constraints from single decay modes. Our results combined with constraints from astrophysical observables (for example [96]), direct detection of Dark Matter and invisible decays of heavy hadrons [98] could provide a full set of tools needed to test (or rule out) the models of light Dark Matter [108].

Chapter 6

Future developments

There is only one fact that we know for sure about Dark Matter - it exists. However, it appears, that another semi-definite prediction can be made.

In theoretical studies the effective interaction of DM with Standard Model (SM) fields is often described in the form of:

$$\mathcal{L}_{int} = \frac{C}{\Lambda^n} (DM \dots DM)(SM \dots SM), \quad (6.1)$$

where ellipses stands for possible combinations of gamma matrices and/or derivatives (depending on type of interacting particles); C is a dimensionless coupling constant and Λ is a scale of the mediator between DM and SM sector; power n is picked in such a way that lagrangian would have the correct dimension. This interaction is represented in Fig. 6.1.

It is believed that for various types of SM particles such an interaction could be responsible for some of the experimental results (for example Fig.6.1(a) can explain the excess of positron flux in PAMELA data [31], while Fig.6.1(b) might be responsible for DAMA [6] observations)

It is well-known from nuclear physics that such a point-like interactions correspond to the δ -function interaction potential which in turn results in shallow bound state between interacting particles [109]. Properties of resulting resonance state can be determined based on experimental data for DM-SM annihilation and scattering . Schematically mechanism of

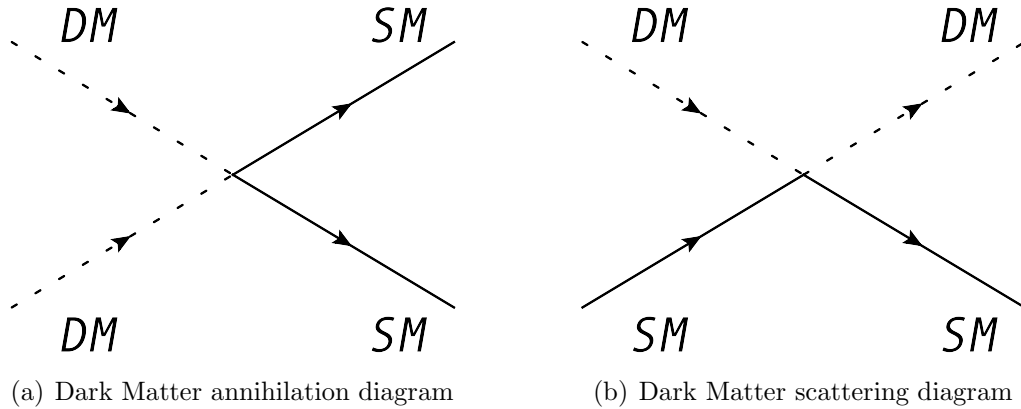


Figure 6.1: Generic DM-SM interaction vertices

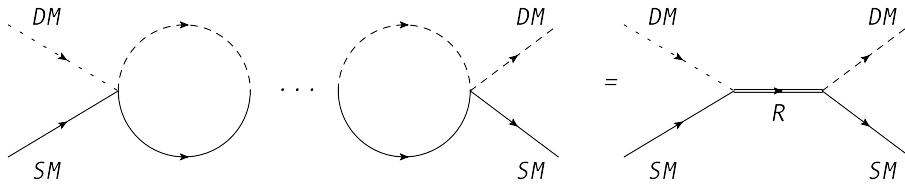


Figure 6.2: Dark Matter-SM resonance production

bound state creation is represented on Fig.6.2.

In what follows we consider the interaction of the Scalar DM with particles of spin $S = 0$ and $S = 1/2$. Such a choice of particles interacting with DM is motivated by following reasons. First of all, PAMELA data for positron excess might be explained by DM annihilation, thus it is natural to study the possibility of bound state between Dark Matter and electron (positron). Second of all, difference in results between DAMA and CDMS experiments can be explained by the fact that germanium (spin $S = 0$ or $S = 9/2$ depending on isotope) and iodine ($S = 5/2$) will interact with DM differently.

In what follows, we compute properties of bound state formed due to δ -function potential in the most general case [110]. Using general result we consider the possibility of bound state between DM and a scalar particle, and DM and a fermion.

As it was mentioned earlier in this chapter, the point-like interaction results in the δ -

function interaction potential:

$$\mathcal{H} = H_0 + V = H_0 + \lambda\delta(\mathbf{x}). \quad (6.2)$$

Later in this section we shall find the correspondence between potential strength λ and parameters of Lagrangian describing DM-SM interaction.

Interaction between the Dark Matter and a scalar particle can be presented in the following way:

$$\mathcal{L} = C^{(s)}(\phi^*\phi)(\Phi^*\Phi), \quad (6.3)$$

where ϕ stands for the scalar DM field. This is the most general lagrangian that can be written at this order. Here and further in text Φ describes a SM particle (nucleus) with spin $S = 0$.

Computing transition matrix elements for DM-nucleus scattering and comparing it with Born approximation one can get the direct correspondence between strength of the δ -function potential λ and parameters of the lagrangian (Eq.6.3):

$$\begin{aligned} \langle f|iT|i\rangle &= -iV(\mathbf{q})(2\pi)\delta(E_f - E_i) \rightarrow V(\mathbf{x}, \mathbf{y}) = \lambda\delta(\mathbf{x} - \mathbf{y}) \\ \lambda &\rightarrow \lambda^{(s)} = \frac{C^{(s)}}{4} \frac{1}{mM} \end{aligned} \quad (6.4)$$

here M and m stand for DM and scalar particle (nuclei) masses respectively.

In a similar way we consider the interaction of Dark Matter with a SM fermion field.

$$\mathcal{L}_{int} = \frac{C_1}{\Lambda^2} m(\phi^*\phi)(\bar{f}f) + \frac{C_2}{\Lambda^2} m(\phi^*\phi)(\bar{f}\gamma_5 f). \quad (6.5)$$

Here ϕ represents scalar Dark Matter field, $f(\bar{f})$ is a Standard Model fermion particle (an-

tiparticle), and m stands for the mass of the SM field. It leads to the following result:

$$\begin{aligned}
 \langle f|iT|i\rangle &= -iV(\mathbf{q})(2\pi)\delta(E_f - E_i) \\
 V(\mathbf{x}, \mathbf{y}) &= \frac{2\pi C_1}{\Lambda^2}\delta(\mathbf{x} - \mathbf{y}) \\
 \lambda \rightarrow \lambda^{(f)} &= \frac{2\pi C_1}{\Lambda^2}
 \end{aligned} \tag{6.6}$$

As one can see, regardless of spin assignment, form of potential obtained here is very similar. In the next chapter we shall consider creation of the bound state in the generic case of δ -function potential and then match the general result with one obtained in Eq.6.4 and Eq.6.6.

6.1 Delta-function potential

From a theoretical point of view, determination of the properties of the resonance means finding a pole in Green function. The Green function associated with Hamiltonian \mathbf{H} and corresponding to the energy E is defined in the following way:

$$\begin{aligned}
 (E - \mathbf{H})G(E, \mathbf{x}, \mathbf{y}) &= \delta(\mathbf{x} - \mathbf{y}) \\
 \lim_{|\mathbf{x}-\mathbf{y}|\rightarrow\infty} G(E, \mathbf{x}, \mathbf{y}) &= 0
 \end{aligned} \tag{6.7}$$

Separating the Hamiltonian into two parts:

$$\mathbf{H} = \mathbf{H}_0 + \lambda\delta(\mathbf{x})$$

we can express Green function for system with interaction ($G(\mathbf{x}, \mathbf{y})$) in terms of Green function of free particles($G_0(\mathbf{x}, \mathbf{y})$) :

$$G(\mathbf{x}, \mathbf{y}) = G_0(\mathbf{x}, \mathbf{y}) + \lambda \frac{G_0(\mathbf{x}, \mathbf{0})G_0(\mathbf{0}, \mathbf{y})}{1 - \lambda G_0(\mathbf{x}, \mathbf{y})} \quad (6.8)$$

There are no poles in the free particles' Green function, thus poles (if any) appear in the second term on the right hand side of Eq.6.8. Therefore in order to find properties of bound state we must solve the following equation:

$$1 - \lambda G_0(\mathbf{x}, \mathbf{y}) = 0 \quad (6.9)$$

Computing free Green function using Eq.6.7 we obtain the following equation:

$$1 - \lambda \int \frac{d^3k}{(2\pi)^3} \frac{1}{E - \mathbf{k}^2/2\mu} = 0, \quad (6.10)$$

where $\mu = m_1 m_2 / (m_1 + m_2)$ is reduced mass of two-body system. Integral is divergent and needs to be regularized and coupling constant λ needs to be renormalized.

It can be done in several ways. The naive cut-off regularization provides a result that depends on the cut-off scale $\Lambda^{(R)}$:

$$\int \frac{d^3k}{(2\pi)^3} \frac{1}{E - \mathbf{k}^2/2\mu} = \Lambda^{(R)} - \sqrt{-2\mu E} \tan^{-1} \frac{\Lambda^{(R)}}{\sqrt{-2\mu E}} \quad (6.11)$$

The cut-off scale needs to be fixed based on experimental data, thus we cannot provide a prediction for the value of the binding energy in this approach.

Using the dimensional regularization scheme we obtain [111]:

$$\int \frac{d^3k}{(2\pi)^3} \frac{1}{E - \mathbf{k}^2/2\mu} = -\frac{\mu}{2\pi} K \quad (6.12)$$

where $K \equiv \sqrt{-2\mu E}$ is the value of momentum corresponding to the binding energy E . As one can see, this result is not scale dependent. However, one might notice that this result is finite, while integral in the Eq.6.10 is divergent. Such a situation occurs because dimensional regularization does not regularize power divergent integrals. This result immediately leads to the following prediction for the binding energy of the resonant state:

$$E = \frac{2\pi^2}{\lambda^2 \mu^3} \quad (6.13)$$

One can estimate numerical value of the binding energy obtained in this approach using constraints onto $C_{1,2}$ from PAMELA positron flux data [31].

Instead of fitting experimental data using our lagrangian Eq.(6.5) we will use results already available in the literature. It was reported in [112] that PAMELA positron excess can be explained by DM annihilation into positrons, and numerical results for thermally averaged cross-section $\langle\sigma v\rangle$ and boost factors were provided. The value of the annihilation cross-section directly depends on parameters of the lagrangian. Thus after direct computation of thermally averaged cross-section we can conclude that values of $C_{1,2}$ are restricted by the following region:

$$\frac{m^2}{\Lambda^4}(C_1^2 + C_2^2) \approx 170 \text{ GeV}^{-2} \quad (6.14)$$

Since pseudoscalar coupling in lagrangian does not contribute to the creation of bound

state, in further discussion we will assume that $C_2 = 0$. Thus,

$$\frac{m_e}{\Lambda^2} C_1 \leq 13 \text{ GeV}^{-1} \quad (6.15)$$

Using results from Eqs. (6.14, 6.15, 6.13) one immediately can conclude that DM-electron bound state should have the following binding energy:

$$B \geq 1.1 \times 10^4 \text{ GeV} \times \left(\frac{m_e + M}{M} \right)^3 \quad (6.16)$$

One can notice, that dimensionless factor $\left(\frac{m_e + M}{M} \right)^3$ is always greater or equal to 1. It means that electron-DM bound state should have the binding energy of the order of TeV. Obviously this result is non physical. Such an unphysical value for two-body system binding energy is not a new result [109]. This problem can be solved by construction of an effective DM-SM interaction theory and subsequent introduction of renormalization scheme to regularize the integral in Eq. 6.10. Similar formalism was developed for the nucleon-nucleon interaction [111] and in principle can be applied to the computation of the resonant state in our case.

The only definite prediction that can be made at this moment is that DM-SM bound state should exist. It will explain the various experimental results in a way similar to the resonant and inelastic Dark Matter models (see for example [43] and [44]) without expansion of the Dark Matter particle content. Work on this project is in progress, and results are not available at the moment.

Chapter 7

Conclusions

Now is an extremely exciting period of time to work in particle physics. New data from LHC is literally around the corner. Thus all questions about electroweak symmetry breaking and mass generation can be answered in the nearest future. We are looking forward for the physics above the TeV scale. What will be there? Supersymmetry? Strings? Extra dimensions? Answer to this question depends on who you are asking. In fact, all of the mentioned scenarios are plausible, but none of them is guaranteed.

In the Chapters 4 and 5 I argued that it is possible to indirectly probe the Physics Beyond the Standard Model using currently available low-energy experimental data. The most precise available today theoretical prediction for the lifetime difference of $B_s - \bar{B}_s$ mesons was obtained. The possibility of the New Physics contribution to the lifetime difference was considered and shown that it can be dominating in certain NP scenarios. Three years after this prediction was made, the D0 collaboration detected signs of the New Physics in the mixing of B mesons [113] which resulted in the spark of interest to this phenomenon from theorists [114].

Dark Matter phenomenology is a somewhat special case in the particle physics. In some sense it is a *tabula rasa*. One can build as many models as wants that would describe available experimental data to some extent. In this situation, model independent predictions are of extreme importance. Results obtained in the Chapter 5 allow us to discriminate between various DM models before making any additional analysis.

I think present time can be compared to the beginning of the 20-th century. People believed that quantum mechanics can explain everything and physics can explain everything. It turned out that there were new questions that could not be answered in the framework of quantum mechanics. That's how development of the quantum field theory started. Somewhat similar situation is observed nowadays. Is it enough to simply extend the Standard Model or maybe we need to reconsider the quantum field theory approach? I do not think anyone has definite answer to these questions. I think the research I did during my graduate studies helped us to approach the answer. I am definitely looking forward to continuing the research in the particle physics and contributing to our understanding of the Universe.

REFERENCES

- [1] C. Amsler et al. (Particle Data Group), Physics Letters B667, 1 (2008)
- [2] WMAP collaboration website <http://map.gsfc.nasa.gov/>
- [3] ATLAS collaboration website <http://atlas.ch/>;
ALICE collaboration website <http://aliceinfo.cern.ch/Public/Welcome.html>;
CMS collaboration website <http://cms.web.cern.ch/cms/index.html>;
LHCb collaboration website <http://lhcb-public.web.cern.ch/lhcb-public/>;
TOTEM collaboration website <http://totem-experiment.web.cern.ch/totem-experiment/>
- [4] CDF collaboration website <http://www-cdf.fnal.gov/> D0 collaboration website <http://www-d0.fnal.gov/>
- [5] CDMS collaboration website: <http://cdms.berkeley.edu/>
- [6] DAMA collaboration website: <http://people.roma2.infn.it/dama/web/home.html>;
- [7] XENON collaboration website: <http://xenon.physics.rice.edu/xenon100.html>
- [8] C. Quigg, Gauge Theories of the Strong, Weak, and Electromagnetic Interactions (Addison-Wesley Pub. Co., Menlo Park, 1983).
- [9] J. F. Donoghue, E. Golowich and B. R. Holstein, Camb. Monogr. Part. Phys. Nucl. Phys. Cosmol. **2**, 1 (1992).
- [10] W. B. Rolnick, *Reading, USA: Addison-Wesley (1994) 466 p*

- [11] P. W. Higgs, Phys. Lett. 12, 132 (1964); F. Englert and R. Brout, Phys. Rev. Lett. 13, 321 (1964); G. S. Guralnik, C. R. Hagen, and T. W. B. Kibble, Phys. Rev. Lett. 13, 585 (1964).
- [12] Lev Borisovich Okun (1982). Leptons and Quarks. Amsterdam, Netherlands: North-Holland Physics Publishing ISBN 0-444-86924-7.
- [13] K. S. Babu and E. Ma, Phys. Rev. D **31**, 2861 (1985) [Erratum-ibid. D **33**, 3471 (1986)].
- [14] T. Kobayashi, Lett. Nuovo Cim. **44**, 417 (1985).
- [15] D. B. Kaplan, H. Georgi and S. Dimopoulos, Phys. Lett. B **136**, 187 (1984).
- [16] K. Agashe, R. Contino and A. Pomarol, Nucl. Phys. B **719**, 165 (2005) [arXiv:hep-ph/0412089].
- [17] N. Cabibbo, Phys. Rev. Lett. 10, 531 (1963). M. Kobayashi and T. Maskawa, Prog. Theor. Phys. 49, 652 (1973).
- [18] L. Wolfenstein, Phys. Rev. Lett. 51 (1983) 1945.
- [19] K. Lande, L. M. Lederman and W. Chinowsky, Phys. Rev. **105**, 1925 (1957).
- [20] N. Ellis, *In the Proceedings of 23rd International Conference on High-Energy Physics, Berkeley, California, 16-23 Jul 1986, pp 801-805.* H. R. Band *et al.* [MAC COLLABORATION Collaboration], *Preprint - BAND, H.R. (87,REC.AUG.) 13p*
- [21] B. Aubert *et al.* [BABAR Collaboration], Phys. Rev. Lett. **98**, 211802 (2007) [arXiv:hep-ex/0703020].

- [22] A. Abulencia *et al.* [CDF Collaboration], Phys. Rev. Lett. **97**, 242003 (2006) [arXiv:hep-ex/0609040].
- [23] V. M. Abazov *et al.* [D0 Collaboration], Phys. Rev. Lett. **97**, 021802 (2006) [arXiv:hep-ex/0603029].
- [24] F. Zwicky, Helv. Phys. Acta **6**, 110 (1933).
- [25] Milgrom, M. Astroph. Jour. 270, 365, Milgrom, M. Astroph. Jour. 270, 371, Milgrom, M. Astroph. Jour. 270, 384.
- [26] J. D. Bekenstein, arXiv:1001.3876 [astro-ph.CO]. Published in Particle Dark Matter: Observations, Models and Searches, G. Bertone, Ed. Cambridge U. Press, 2010, 95-114
- [27] Clowe, Douglas, et al.; Brada, Marua; Gonzalez, Anthony H.; Markevitch, Maxim; Randall, Scott W.; Jones, Christine; Zaritsky, Dennis (2006). "A Direct Empirical Proof of the Existence of Dark Matter". The Astrophysical Journal **648**: L109L113. doi:10.1086/508162. [arXiv:astro-ph/0608407]
- [28] M. S. Turner, arXiv:astro-ph/9904051; Published in "Asilomar 1998, Particle physics and the early universe" 113-128
- [29] G. Bertone, D. Hooper and J. Silk, Phys. Rept. **405**, 279 (2005) [arXiv:hep-ph/0404175].
- [30] X. D. Shi and G. M. Fuller, Phys. Rev. Lett. **82**, 2832 (1999) [arXiv:astro-ph/9810076].
- [31] PAMELA collaboration website: <http://pamela.roma2.infn.it/index.php>;
- [32] A. W. Strong and I. V. Moskalenko, Astrophys. J. **509**, 212 (1998) [arXiv:astro-ph/9807150].

- I. V. Moskalenko and A. W. Strong, *Astrophys. J.* **493**, 694 (1998) [arXiv:astro-ph/9710124].
- [33] A. Sommerfeld, *Annalen der Physik* **403**, 257 (1931)
- J. Hisano, S. Matsumoto and M. M. Nojiri, *Phys. Rev. Lett.* **92**, 031303 (2004) [arXiv:hep-ph/0307216].
- [34] R. Dave, D. N. Spergel, P. J. Steinhardt and B. D. Wandelt, *Astrophys. J.* **547**, 574 (2001) [arXiv:astro-ph/0006218].
- [35] Talk given by Jonathan Feng at Inaugural Workshop, Center for Particle Cosmology, University of Pennsylvania, 11 December 2009
- [36] B. W. Lee and S. Weinberg, *Phys. Rev. Lett.* **39**, 165 (1977); M. I. Vysotsky, A. D. Dolgov and Y. B. Zeldovich, *JETP Lett.* **26**, 188 (1977) [*Pisma Zh. Eksp. Teor. Fiz.* **26**, 200 (1977)].
- [37] INTEGRAL collaboration website <http://www.esa.int/esaMI/Integral/>
- [38] M. Kamionkowski, arXiv:hep-ph/9710467.
- [39] R.D. Peccei and H.R. Quinn, *Phys. Rev. Lett.* **38**, 1440 (1977); F. Wilczek, *Phys. Rev. Lett.* **40**, 279 (1978); S. Weinberg, *Phys. Rev. Lett.* **40**, 223 (1978).
- [40] M.A. Bershadsky, M.T. Ressell, and M.S. Turner, *Phys. Rev. Lett.* **66**, 1398 (1991).
- [41] P. Sikivie, *Phys. Rev. Lett.* **51**, 1415 (1983). K. van Bibber et al., *Int. J. Mod. Phys. Suppl. D* **3**, 33 (1994); C. Hagmann et al., *Nucl. Phys. (Proc. Suppl.) B* **51**, 209 (1996). I. Ogawa, S. Matsuki, and K. Yamamoto, *Phys. Rev. D* **53**, 1740 (1996); S. Matsuki, I. Ogawa, and K. Yamamoto, *Phys.Lett. B* **336**, 573 (1994).

- [42] M. Y. Khlopov, “Physical Arguments, Favouring Multicomponent Dark Matter,”
Prepared for 30th Rencontres de Moriond: Perspectives in Particle Physics, Atomic Physics and Gravitation, Villars-sur-Ollon, Switzerland, 21-28 Jan 1995
- D. Feldman, Z. Liu, P. Nath and G. Peim, Phys. Rev. D **81**, 095017 (2010)
[arXiv:1004.0649 [hep-ph]].
- [43] Y. Bai and P. J. Fox, JHEP **0911**, 052 (2009) [arXiv:0909.2900 [hep-ph]].
- [44] D. Tucker-Smith and N. Weiner, Phys. Rev. D **64**, 043502 (2001) [arXiv:hep-ph/0101138].
- D. Tucker-Smith and N. Weiner, Phys. Rev. D **72**, 063509 (2005) [arXiv:hep-ph/0402065].
- [45] A. Badin, F. Gabbiani and A. A. Petrov, Phys. Lett. B **653**, 230 (2007)
[arXiv:0707.0294 [hep-ph]].
- [46] J. G. Korner, A. I. Onishchenko, A. A. Petrov and A. A. Pivovarov, Phys. Rev. Lett. **91**, 192002 (2003) [arXiv:hep-ph/0306032]; S. Narison and A. A. Pivovarov, Phys. Lett. B **327**, 341 (1994) [hep-ph/9403225].
- [47] E. Dalgic *et al.*, Phys. Rev. D **76**, 011501 (2007) [arXiv:hep-lat/0610104].
- [48] D. Becirevic, V. Gimenez, G. Martinelli, M. Papinutto, and J. Reyes, JHEP **0204**, 025 (2002) [hep-lat/0110091].
- [49] V. Gimenez and J. Reyes, Nucl. Phys. Proc. Suppl. **94** (2001) 350 [hep-lat/0010048].
- [50] S. Aoki *et al.* [JLQCD Collaboration], arXiv:hep-ph/0307039; S. Aoki *et al.* [JLQCD Collaboration], Phys. Rev. D **67** (2003) 014506 [hep-lat/0208038].

- [51] V. M. Abazov *et al.* [D0 Collaboration], Phys. Rev. Lett. **98**, 121801 (2007) [arXiv:hep-ex/0701012].
- [52] D. Acosta *et al.* [CDF Collaboration], Phys. Rev. Lett. **94**, 101803 (2005) [arXiv:hep-ex/0412057].
- [53] R. Barate *et al.* [ALEPH Collaboration], Phys. Lett. B **486**, 286 (2000).
- [54] E. Barberio *et al.* [Heavy Flavor Averaging Group (HFAG) Collaboration], arXiv:0704.3575 [hep-ex].
- [55] M. Beneke, G. Buchalla, and I. Dunietz, Phys. Rev. D **54**, 4419 (1996). M. Beneke, G. Buchalla, A. Lenz, and U. Nierste, Phys. Lett. B **576**, 173 (2003).
- [56] M. Beneke, G. Buchalla, C. Greub, A. Lenz, and U. Nierste, Phys. Lett. B **459**, 631 (1999) [arXiv:hep-ph/9808385].
- [57] M. Ciuchini, E. Franco, V. Lubicz, F. Mescia, and C. Tarantino, JHEP **0308**, 031 (2003) [arXiv:hep-ph/0308029].
- [58] A. Lenz and U. Nierste, arXiv:hep-ph/0612167.
- [59] Y. Grossman, Y. Nir and G. Paz, Phys. Rev. Lett. **97**, 151801 (2006) [arXiv:hep-ph/0605028].
- [60] Z. Ligeti, M. Papucci and G. Perez, Phys. Rev. Lett. **97**, 101801 (2006) [arXiv:hep-ph/0604112].
- [61] Y. Grossman, Phys. Lett. B **380**, 99 (1996) [arXiv:hep-ph/9603244].

- [62] I. Dunietz, R. Fleischer and U. Nierste, *Phys. Rev. D* **63**, 114015 (2001) [arXiv:hep-ph/0012219].
- [63] G. Buchalla, A. J. Buras, Asia 7750 vs ETA 7750 and M. E. Lautenbacher, *Rev. Mod. Phys.* **68**, 1125 (1996) [arXiv:hep-ph/9512380].
- [64] M. A. Shifman and M. B. Voloshin, *Sov. J. Nucl. Phys.* **41**, 120 (1985) [*Yad. Fiz.* **41**, 187 (1985)].
- [65] F. Gabbiani, A. I. Onishchenko, and A. A. Petrov, *Phys. Rev. D* **70**, 094031 (2004) [arXiv:hep-ph/0407004]. F. Gabbiani, A. I. Onishchenko, and A. A. Petrov, *Phys. Rev. D* **68**, 114006 (2003).
- [66] “Lifetimes and lifetime differences in heavy mesons,” talk given by A. A. Petrov at 33rd International Conference on High Energy Physics (ICHEP 06), Moscow, Russia, 26 Jul - 2 Aug 2006.
- [67] M. Beneke, G. Buchalla, M. Neubert and C. T. Sachrajda, *Phys. Rev. Lett.* **83**, 1914 (1999) [arXiv:hep-ph/9905312]; C. W. Bauer, S. Fleming, D. Pirjol and I. W. Stewart, *Phys. Rev. D* **63**, 114020 (2001) [arXiv:hep-ph/0011336].
- [68] E. Golowich, S. Pakvasa and A. A. Petrov, *Phys. Rev. Lett.* **98**, 181801 (2007) [arXiv:hep-ph/0610039].
- [69] S. L. Glashow and S. Weinberg, *Phys. Rev. D* **15**, 1958 (1977).
- [70] V. D. Barger, J. L. Hewett and R. J. N. Phillips, *Phys. Rev. D* **41**, 3421 (1990).
- [71] D. Atwood, L. Reina and A. Soni, *Phys. Rev. D* **55**, 3156 (1997) [arXiv:hep-ph/9609279].

- [72] E. Golowich and T. Yang, Phys. Lett B **80**, 245 (1979)
- [73] R. N. Mohapatra and J. C. Pati, Phys. Rev. D **11**, 2558 (1975); For a review and complete set of original references, see R. N. Mohapatra, “UNIFICATION AND SUPERSYMMETRY. THE FRONTIERS OF QUARK - LEPTON PHYSICS,” *Berlin, Germany: Springer (1986) 309 p. (Contemporary Physics)*
- [74] K. Kiers, M. Assis and A. A. Petrov, Phys. Rev. D **71**, 115015 (2005) [arXiv:hep-ph/0503115].
- [75] G. Beall, M. Bander and A. Soni, Phys. Rev. Lett. **48**, 848 (1982).
- [76] F. I. Olness and M. E. Ebel, Phys. Rev. D **30**, 1034 (1984).
- [77] D. Chang, R. N. Mohapatra and M. K. Parida, Phys. Rev. D **30**, 1052 (1984).
- [78] E. Golowich, J. Hewett, S. Pakvasa and A. A. Petrov, Phys. Rev. D **76**, 095009 (2007) [arXiv:0705.3650 [hep-ph]].
- [79] D. Clowe, M. Bradac, A. H. Gonzalez, M. Markevitch, S. W. Randall, C. Jones and D. Zaritsky, Astrophys. J. **648**, L109 (2006) [arXiv:astro-ph/0608407].
- [80] While no elementary particle with appropriate for DM properties exist in the SM, it does not mean that New Physics is required to explain DM. For example, DM could exist in the form of small primordial black holes. For more details see C. Bambi, A. D. Dolgov and A. A. Petrov, Phys. Lett. B **670**, 174 (2008) [Erratum-ibid. **681**, 504 (2009)] [arXiv:0801.2786 [astro-ph]]; P. H. Frampton, M. Kawasaki, F. Takahashi and T. T. Yanagida, JCAP **1004**, 023 (2010) [arXiv:1001.2308 [hep-ph]]; A. D. Dolgov, P. D. Naselsky and I. D. Novikov, arXiv:astro-ph/0009407.

- [81] D. N. Spergel *et al.* [WMAP Collaboration], *Astrophys. J. Suppl.* **148**, 175 (2003) [arXiv:astro-ph/0302209].
- [82] C. Bird, R. Kowalewski and M. Pospelov, *Mod. Phys. Lett. A* **21**, 457 (2006).
- [83] C. P. Burgess, M. Pospelov and T. ter Veldhuis, *Nucl. Phys. B* **619**, 709 (2001) [arXiv:hep-ph/0011335].
- [84] J. L. Feng and J. Kumar, *Phys. Rev. Lett.* **101**, 231301 (2008) [arXiv:0803.4196 [hep-ph]].
- [85] M. Pospelov, A. Ritz and M. B. Voloshin, *Phys. Lett. B* **662**, 53 (2008) [arXiv:0711.4866 [hep-ph]].
- [86] F. Petriello and K. M. Zurek, *JHEP* **0809**, 047 (2008) [arXiv:0806.3989 [hep-ph]].
- [87] HESS collaboration website: <http://www.mpi-hd.mpg.de/hfm/HESS/> see also S. W. Barwick *et al.* [HEAT Collaboration], *Astrophys. J.* **482**, L191 (1997) [arXiv:astro-ph/9703192]; S. Coutu *et al.*, *Astropart. Phys.* **11**, 429 (1999), [arXiv:astro-ph/9902162].
- [88] M. Antonelli *et al.*, arXiv:0907.5386 [hep-ph]; for charm physics observables see D. Atwood and A. A. Petrov, *Phys. Rev. D* **71**, 054032 (2005) [arXiv:hep-ph/0207165].
- [89] For a recent review and references see, for example, M. H. G. Tytgat, arXiv:0906.1100 [hep-ph] Asia 7750 vs ETA 7750.
- [90] G. Buchalla and A. J. Buras, *Nucl. Phys. B* **400**, 225 (1993).
- [91] T. Inami and C. S. Lim, *Prog. Theor. Phys.* **65**, 297 (1981) [Erratum-*ibid.* **65**, 1772 (1981)].

- [92] T. M. Aliev and C. S. Kim, Phys. Rev. D **58**, 013003 (1998) [arXiv:hep-ph/9710428].
- [93] T. M. Aliev, A. Özpineci and M. Savci Phys.Lett.B520:69-77,2001 [arXiv:hep-ph/0105279].
- [94] A. Goobar, S. Hannestad, E. Mortsell and H. Tu, JCAP **0606**, 019 (2006) [arXiv:astro-ph/0602155].
- [95] T. M. Aliev, A. Ozpineci and M. Savci, Phys. Lett. B **393**, 143 (1997) [arXiv:hep-ph/9610255]; C. D. Lu and D. X. Zhang, Phys. Lett. B **381**, 348 (1996) [arXiv:hep-ph/9604378].
- [96] A. Badin, G. K. Yeghiyan and A. A. Petrov, arXiv:0909.5219 [hep-ph].
- [97] BABAR Collaboration, Bernard Aubert et al., Phys.Rev.Lett.93:091802,2004. [arXiv:hep-ex/0405071]
- [98] G. K. Yeghiyan, Phys. Rev. D **80**, 115019 (2009) [arXiv:0909.4919 [hep-ph]].
- [99] M. Bauer, B. Stech, M. Wirbel, Z. Phys.C 34, 103-115 (1987), *ibid*, Z. Phys.C 29, 637-642 (1985).
- [100] G. P. Korchemsky, D. Pirjol and T. M. Yan, Phys. Rev. D **61**, 114510 (2000) [arXiv:hep-ph/9911427].
- [101] Y. Dincer and L. M. Sehgal, Phys. Lett. B **521**, 7 (2001) [arXiv:hep-ph/0108144].
- [102] E. Lunghi, D. Pirjol, and D. Wyler, Nucl. Phys. B 649 (2003) 349-364; C.W. Bauer, S. Fleming, M. Luke, Phys. Rev. D 63 (2001) 014006; C.W. Bauer, S. Fleming, D. Pirjol, I.W. Stewart, Phys. Rev. D 63 (2001) 114020; C.W. Bauer, I.W. Stewart, Phys.

- Lett. B 516 (2001) 134; C.W. Bauer, D. Pirjol, I.W. Stewart, Phys. Rev. D 65 (2002) 054022.
- [103] M. J. Strassler and K. M. Zurek, Phys. Lett. B **651**, 374 (2007) [arXiv:hep-ph/0604261].
- [104] Y. G. Kim, K. Y. Lee and S. Shin JHEP 0805:100, 2008 [arxiv:0803.2932v2]
- [105] J.-M. Frère et al., Phys.Rev.D75:085017, 2007 [arxiv:hep-ph/0610240v2]
- [106] H. E. Haber and G. L. Kane Phys. Rept. 117 (1985) 75-263.
- [107] V. Silveira and A. Zee, Phys. Let. B161, 136(1985); J. McDonald Phys. Rev. D50, 3637 (1994)
- [108] A. Badin and A. A. Petrov, arXiv:1005.1277 [hep-ph]. Accepted for publication in PRD.
- [109] S. Weinberg, Phys. Lett. B **251**, 288 (1990). S. Weinberg, Nucl. Phys. B **363**, 3 (1991).
- [110] Andriy Badin and Alexey A. Petrov *Sticky Dark Matter - to be published*
- [111] D. B. Kaplan, M. J. Savage and M. B. Wise, Nucl. Phys. B **478**, 629 (1996) [arXiv:nucl-th/9605002].
- D. B. Kaplan, M. J. Savage and M. B. Wise, Nucl. Phys. B **534**, 329 (1998) [arXiv:nucl-th/9802075].
- D. B. Kaplan, M. J. Savage and M. B. Wise, Phys. Lett. B **424**, 390 (1998) [arXiv:nucl-th/9801034].
- [112] T. Delahaye, R. Lineros, F. Donato, N. Fornengo and P. Salati, Phys. Rev. D **77**, 063527 (2008) [arXiv:0712.2312 [astro-ph]].

[113] V. M. Abazov *et al.* [The D0 Collaboration], arXiv:1005.2757 [hep-ex].

[114] N. G. Deshpande, X. G. He and G. Valencia, arXiv:1006.1682 [hep-ph].

C. W. Bauer and N. D. Dunn, arXiv:1006.1629 [hep-ph].

B. A. Dobrescu, P. J. Fox and A. Martin, arXiv:1005.4238 [hep-ph].

ABSTRACT

LOW ENERGY SEARCH FOR PHYSICS BEYOND THE STANDARD MODEL

by

ANDRIY BADIN

August 2010

Advisor: Alexey A. Petrov

Major: Physics

Degree: Doctor of Philosophy

Various approaches to the detection of the physics Beyond the Standard Model were considered. After discussion of the theoretical aspects of the Standard Model we point out experimental observations that can not be answered within its framework. Methods for the indirect detection of the heavy (electroweak scale and above) and light New Physics particles are discussed. Study of the meson mixing in the B_s system is proposed as the way to indirectly probe NP. We predict that New Physics contribution to the lifetime difference of B_s - \bar{B}_s system can be dominant in certain scenarios. As an example of the way to detect the light New Physics we considered the Dark Matter production in the heavy meson decays. A comprehensive study of light Dark Matter production in heavy meson decays with missing energy \cancel{E} in the final state, such as $B_q(D^0) \rightarrow \cancel{E}$ and $B_q(D^0) \rightarrow \gamma\cancel{E}$ was provided. It was argued that such transitions can be studied at the current flavor factories (and future super-flavor factories) by tagging the missing-energy decays with $B(D^0)$ decays “on the other side.”

AUTOBIOGRAPHICAL STATEMENT

Education

2005 - 2010

Wayne State University, Detroit
Ph.D. in Physics

2003 - 2005

Kharkov National University, Ukraine,
M.S. in Physics with Honor

1999 - 2003

Kharkov National University, Ukraine,
B.S. in Physics with Honor

Professional training

2008

2008 Joint CERN-FERMILAB
Hadron Collider Physics Summer school,
Fermilab, Batavia, IL

2004

42-nd Summer school on Subnuclear Physics
Erice, Italy

Publications

1. *Light Dark matter production in heavy mesons decays*
Andriy Badin, Alexey A. Petrov. Accepted Phys. Rev. D (e-print archive - arXiv:1005.1277)
2. *Lifetime Difference in B_s mixing: Standard Model and Beyond*
Proceedings of APS DPF meeting 2009, Detroit [arXiv:0909.4897]
3. *Light Dark matter annihilation in model independent approach*
Proceedings of APS DPF meeting 2009, Detroit [arXiv:0909.5219]
4. *Lifetime Difference in B_s mixing: Standard Model and Beyond*
Andriy Badin, Fabrizio Gabbiani, Alexey A. Petrov Phys.Lett.B653:230-240,2007
(e-print archive - arXiv:0707.0294) [hep-ph]
5. A. Badin, A. Molev "Analysis of refractive structure in $O^{16} - C^{12}$ scattering cross-section". Contribution to "LIII INTERNATIONAL MEETING ON NUCLEAR SPECTROSCOPY AND NUCLEAR STRUCTURE "NUCLEUS 2003"" book of abstracts, October 7-10, 2003, Moscow, p.216